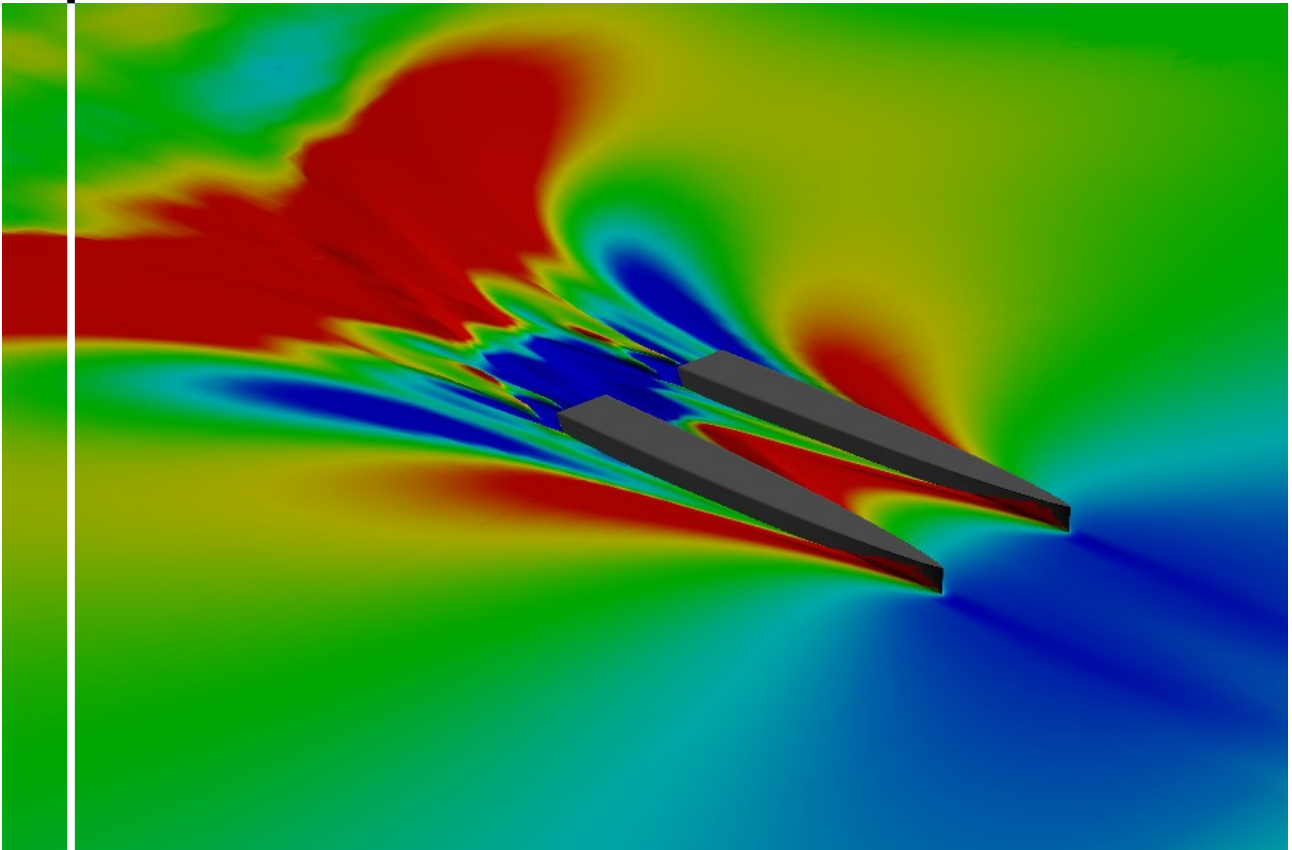


Resistance Prediction for Cruising Motor Catamarans

***Bare Hull Resistance, Form Factor
and Interference Resistance
of a Systematic Series
of Slender Catamaran Hulls***



Koen Geurts
1010646
Geurts.Koen@gmail.com

Ship Hydromechanics
Graduation Thesis
June 2009

Resistance Prediction for Cruising Motor Catamarans

***Bare Hull Resistance, Form Factor
and Interference Resistance
of a Systematic Series
of Slender Catamaran Hulls***



Dr. Ir. J.A. Keuning

Prof. Dr. Ir. R.H.M. Huijsmans



Marc Van Peteghem

Ir. Charles Simonin

Koen Geurts

1010646

Geurts.Koen@gmail.com

Ship Hydromechanics

Graduation Thesis

June 2009

Preface

The final assignment of a Master student at the Delft University of Technology, is to complete a graduation thesis. This graduation thesis covers a period of at least nine months and can be carried out in co-operation with the industry, research institutes or in-house, depending on the student's preference and availability of positions in the industry. Due to the emerging market of the motor catamarans at the Van Peteghem Lauriot Prévost Yacht Design office, they offered me an interesting and challenging research position at their office in Paris. The design office existing of a young team of talented designers and engineers is located in the city centre, next to the only marina in Paris in the close proximity of Bastille, which makes it a historical and attractive location to work and live.

Readers who are not familiar with the subject of resistance of motor catamarans can find extensive background information in chapter 2 . Readers who are only interested in a regression formula for the estimation of the catamaran resistance can turn to chapter 3 , where a regression formula is defined from the data of existing researches.

Chapter 4 can be seen as an extensive introduction to the rest of the project and report as from this point on, the CFD tests and towing tank tests for this research are used. Several research subjects will be discussed in the subsequent chapters. For people that are only interested in the result from the towing tank tests and the CFD calculations are directed to chapter 5 , where they can find the results and a comparison of the trim and sinkage results of both methods. The main subject of the research concerns the form factor determination and its use for scaling results to the correct waterline length of the vessel. Both subjects are studied in chapter 6 and 7 respectively. An important factor in the resistance of catamarans is the interference due to the presence of the two hulls, therefore, the entire chapter 8 is dedicated to this resistance component. Finally, in chapter 9 , the transom stern resistance is discussed as this component plays an important role during the towing tank tests for the form factor determination.

Engineers or technicians who want to build further on the acquired information can read the conclusions and the recommendations at the end of the report. The appendices contain all additional information and referenced data in order to give a thorough collection of all information required for a good understanding of the project.

Without help from different people, I could not have completed this research and the preceding education. These people I want to thank for their help and understanding during the time span of this research and my education. I would like to express my gratitude towards the entire VPLP Design Team for sharing their knowledge and friendship to help me succeed, especially towards Marc and Charles as they followed up the project and at the same time gave me a lot of liberty in my work. It is a pleasure to be part of this team of talented and motivated designers and engineers. Furthermore, I would like to thank Michiel for his help with the towing tank tests.

I would like to thank my parents for all the opportunities they have given me in life. They have been there to support me and have given me the freedom to develop my personality and chase my own dreams. Furthermore, thanks goes out to Marika for her love, care and support for the past seven years. Last but not least my appreciation goes out to other friends and family and everybody who I can't possibly mention here by name.

Table of Contents

Preface.....	iii
Table of Contents.....	v
Summary.....	ix
List of Figures.....	xi
List of Tables.....	xiii
Nomenclature.....	xv
Geometry.....	xv
Resistance.....	xvi
Fluid Properties.....	xvii
Subscripts.....	xvii
1 Introduction.....	1
2 Resistance of Catamarans.....	3
2.1 Total Catamaran Resistance.....	3
2.1.1 Total Catamaran Resistance Components.....	3
2.1.2 Speed Dependence.....	3
2.1 Bare Hull Resistance.....	4
2.1.1 Residuary Resistance + Skin Friction.....	6
2.1.2 Pressure Resistance + Friction Resistance.....	7
2.1.3 Wave Resistance + Transom Resistance + Friction Resistance.....	7
2.2 Interference Resistance.....	8
2.3 Windage or Wind Resistance.....	8
2.4 Appendage Resistance.....	9
2.4.1 As function of Hull Skin Friction.....	9
2.4.2 As function of Appendage Skin Friction.....	10
2.1 Resistance due to Lift.....	11
2.1.1 Induced drag due to hull lift.....	11
2.1.2 Induced drag due to foil lift.....	12
2.2 Resistance due to sea-way.....	12

3	Preliminary Project.....	13
3.1	Available Information.....	13
3.1.1	Müller-Graf Data.....	13
3.1.1	NPL-Molland Data.....	15
3.1.2	Schwetz-Sahoo Data [2002].....	17
3.1.3	Sahoo Data [2004].....	18
3.2	Regression Analysis.....	19
3.2.1	Regression Method.....	19
3.2.2	Matlab.....	20
3.2.3	Regression Parameters.....	20
3.2.4	Final Regression.....	21
3.3	Validation and Accuracy.....	22
3.3.1	Monohull Resistance.....	22
3.3.2	Catamaran Resistance.....	24
3.4	Conclusion.....	24
4	Final Project.....	25
4.1	Project Lay-out.....	25
4.1.1	Project Goals.....	25
4.1.2	Working Method.....	25
4.1.3	Boundary Conditions.....	25
4.2	Research Topics.....	26
4.2.1	Bare Hull Resistance.....	26
4.2.2	Form Factor.....	27
4.2.3	Scaling Methods.....	27
4.2.4	Interference Resistance.....	27
4.2.5	Transom Stern Resistance.....	27
4.3	VPLP Catamaran.....	28
4.3.1	Hull Form.....	28
4.3.2	Parameter Range.....	28
4.4	Facilities / Programme.....	29
4.4.1	Computational Fluid Dynamics.....	29
4.4.1	Towing Tank Tests.....	30
4.4.2	Test Results.....	30
4.5	Test Data.....	31
4.5.1	Test Configurations.....	31
4.5.2	Test Speeds.....	32
4.5.3	Nomenclature.....	33
5	Bare Hull Resistance.....	35
5.1	Bare Hull Resistance Determination.....	35
5.1.1	Towing Tank Tests.....	35
5.1.2	CFD Calculations.....	38
5.2	Comparison.....	39
5.3	Conclusion.....	40

6	Form Factor.....	41
6.1	Definition.....	41
6.2	Form Factor Determination.....	41
6.2.1	Slow Speed Tests.....	41
6.2.2	Computational Fluid Dynamics.....	42
6.2.3	Wind tunnel measurements.....	42
6.2.4	No free surface.....	42
6.2.5	Full scale tests.....	43
6.3	Form Factor Estimation.....	43
6.3.1	Monohull.....	43
6.3.2	Catamaran.....	45
6.4	Data Analysis.....	46
6.4.1	Computational Fluid Dynamics.....	46
6.4.2	Towing Tank Tests.....	48
6.4.3	Comparison.....	50
6.5	Conclusion.....	50
7	Scaling Results.....	51
7.1	Scaling Methods.....	51
7.1.1	Without Form Factor.....	51
7.1.2	With Form Factor.....	52
7.2	Skin Friction.....	53
7.3	Friction Resistance with Transom Resistance.....	53
7.4	Friction Resistance.....	54
7.5	Comparison.....	55
7.6	Conclusions.....	57
8	Interference Resistance.....	59
8.1	Definition.....	59
8.1.1	Total Interference Resistance.....	59
8.1.2	Total Interference Factor.....	59
8.2	Components.....	59
8.3	Existing Research.....	60
8.4	Data Analysis.....	61
8.4.1	Total Interference Factor.....	61
8.4.2	Viscous Interference Factor.....	62
8.4.3	Wave Interference Factor.....	64
8.5	Conclusion.....	66

9 Hydrostatic Transom Resistance.....	67
9.1 Definition.....	67
9.2 Regression Doctors	68
9.3 Regression VPLP.....	68
9.4 Comparison VPLP - Doctors.....	69
Conclusions.....	71
Recommendations.....	73
References.....	75
Appendices.....	79
Appendix A Project Flow Chart.....	I
Appendix B Aerodynamic drag and lift of catamarans.....	III
B.1 Model.....	III
B.2 Narrow: $B/L = 0.4$ $s/L = 0.28$	IV
B.3 Large: $B/L = 0.5$ $s/L = 0.38$	VI
Appendix C Summary of Regression Formulae.....	VII
C.1 DSYHS.....	VII
C.2 NPL-Molland Regression.....	IX
C.3 Schwetz-Sahoo Resistance Regression.....	XII
C.4 Sahoo Resistance Regression.....	XIII
C.5 Doctors Transom Wetted Surface Area.....	XV
C.6 VPLP Transom Wetted Surface Area.....	XV
Appendix D Design of the VPLP Hull Form.....	XVII
D.1 Hull Form Concepts.....	XVII
D.2 Choice of VPLP Hull Form.....	XVIII
D.3 Final Design VPLP Hull Form.....	XVIII
Appendix E Test Matrices.....	XXI
E.1 Form Factor Test Matrix.....	XXI
E.2 Validation Resistance Matrix.....	XXI
E.3 Proposed Total Resistance Matrix.....	XXII
Appendix F Van Peteghem Lauriot Prévost Yacht Design.....	XXIII

Summary

In the early design stages of motor catamarans, an estimation of the weight and the resistance is important. Both estimations depend on each other, so accurate estimation methods are required. From the design process of racing trimarans, one of the specializations of VPLP Yacht Design is accurate weight estimations. For the determination of the catamaran resistance however, the estimation methods for the resistance of racing and cruising sailing multihulls is not valid. The amount of available information on the resistance of cruising motor catamarans is limited, and for this reason, VPLP Yacht Design started an extensive research programme. This report describes the research on the resistance of catamarans. The results attained here will be used to create an accurate velocity prediction programme (VPP) for cruising motor catamarans, in order to estimate the required propulsion power.

The main questions to be answered in this research are which are the important resistance components of cruising motor catamarans, and how can these different resistance components accurately be estimated?

With the available literature, a regression formula is created to estimate the resistance in an early stage of the design process, when only a few geometrical characteristics of the yacht are known. The solutions of this regression will be compared to CFD calculations that are performed on a generic designed hull for motor catamarans. A full set of towing tank tests and CFD calculations using two different software packages, are used to collect a large database of resistance, trim and sinkage results for the study of different important topics in the resistance estimation of motor catamarans.

From the available data from previous researches, a regression formula is built in order to give a first estimation of the resistance of catamarans. In the second step of the project, CFD calculations and towing tank tests are performed on a hull form designed especially for this project. Comparisons are made between the two CFD tools, ISIS and ICARE, and the towing tank test results. Further comparison between these test results and the Molland test data shows a significant difference in the behaviour of the monohull and catamaran resistance. It becomes obvious that more profound analysis of the test data is required for the following fields of interest:

- The determination of the form factor, required for accurate scaling of test results
- Different methods of scaling of test and calculation results
- The interference resistance components for catamarans with different separation ratios
- The transom resistance of the immersed transom

Studying these different topics results in several important conclusions. It is found that the regression analysis of the Molland results gives a good representation of the data, but it is very sensitive to changes in position of the longitudinal centre of buoyancy.

There are large differences between the results of the two CFD codes. When comparing the CFD results to the towing tank test results, it can be seen that the ISIS results are the closest to the towing tank test data. From this, it can be assumed that ISIS is more accurate than ICARE for this type of calculations.

Furthermore, it is shown that the monohull and catamaran resistance results at high speeds converge to same value. Molland showed an offset between the converging resistance of catamarans of different separation ratio and the resistance of monohulls. This difference indicates some incorrectness of the resistance tests of the monohull and catamaran configurations performed by Molland.

From the CFD calculations, it is shown that the form factor can be determined from towing tank tests with the hull trimmed bow down so that the transom runs clear. This is valid for slender hull forms with U-sections at the bow, so that the changes of the waterlines of the trimmed hull form stay acceptable.

The ISIS results give a good approximation with respect to the towing tank results, while ICARE overestimates the form factor.

The form factors from Molland and corrected for transom effects by Couser remain too high. This can indicate that the hydrostatic transom resistance used by Couser, to correct the Molland data, still underestimates the total transom resistance and therefore overestimates the form factor.

The two scaling methods, one without the use of the form factor, the other with its use, and the ISIS calculations are within 2 - 3 % of each other, which can be defined as very accurate, implying that both scaling methods can be used for slender hull forms.

The total interference factor is difficult to predict at low speeds due to the oscillating nature of the wave interference between the hulls. However, at higher speeds clear trends are shown. The CFD calculations give negative values for the viscous interference factor, while existing results and the towing tank tests give positive values that change with the length-displacement ratio, the separation ratio and hull shape. It can be concluded that this viscous interference factor is specific to each case. With respect to the form factors, the existing results of Couser show an increase of 10% due to the viscous effects while in this research an increase of 3 – 6 % is found. The wave interference factor shows the same overall behaviour as the total interference factor.

The VPLP regression underestimates the unwetted surface with respect to the Doctors regression. This results in a small overestimation of the transom resistance. More towing tank test data for the dynamic wetted surface area of the transom is required to build a more accurate regression. However, the question remains if the method of the missing hydrostatic transom pressure is a good simulation of the transom resistance.

List of Figures

Figure 2.1: Resistance components.....	5
Figure 3.1: VWS series '89 catamaran hull form [Müller-Graf, 1993].....	13
Figure 3.2: The NPL parent hull form.....	15
Figure 3.3: Residuary resistance of model 5a at scale of 1 metre.....	16
Figure 3.4: Schwetz systematic series of hull forms.....	17
Figure 3.5: Sahoo systematic series of hull forms.....	18
Figure 3.6: Regression results in comparison with CFD for the design displacement case.....	22
Figure 3.7: Regression results in comparison with CFD for the heavy displacement case.....	23
Figure 3.8: Influence of out-of-range LCB position on the regression results.....	23
Figure 3.9: Catamaran regression results in comparison to CFD results.....	24
Figure 4.1: VPLP V-shape parent hull form.....	28
Figure 5.1: Friction resistance of the turbulence strips.....	35
Figure 5.2: Example of the gathered towing tank test resistance data.....	36
Figure 5.3: Example of the gathered towing tank test trim data.....	37
Figure 5.4: Example of the gathered towing tank test sinkage data.....	37
Figure 5.5: ISIS and ICARE results for friction and total resistance.....	38
Figure 5.6: ISIS and ICARE trim angle for monohull and catamaran.....	38
Figure 5.7: Comparison of trim angle between CFD and towing tank tests.....	39
Figure 5.8: Comparison of sinkage between CFD and towing tank tests.....	39
Figure 6.1: Hughes method of determining the form factor.....	42
Figure 6.2: Form factor results from CFD.....	47
Figure 6.3: Form factor results from ISIS for different configurations.....	48
Figure 6.4: Form factor comparison.....	50
Figure 7.1: Scaling of towing tank results without the form factor.....	53
Figure 7.2: Scaling of towing tank results with the form factor determined with immersed transom.....	54
Figure 7.3: Scaling of towing tank results with the form factor.....	54
Figure 7.4: Friction resistance scaling.....	55
Figure 7.5: Pressure resistance scaling.....	55
Figure 7.6: Scaled bare hull resistance of the monohull configuration.....	56
Figure 7.7: Scaled bare hull resistance of the catamaran configuration.....	56
Figure 8.1: The total interference resistance factor as a function of the separation ratio.....	61
Figure 8.2: Total interference factor.....	61
Figure 8.3: Form factor with viscous interference factor	64

Figure 8.4: Viscous interference factor	64
Figure 8.5: Total interference factor	65
Figure 9.1: Definition of the geometry of transom unwetting [Doctors, 2007].....	67
Figure 9.2: Ratio of dynamic WSA of the transom and the static WSA of the transom.....	69
Figure 9.3: VPLP regression and Doctors regression for transom unwetting.....	70
Fig.App 1: Model set-up in the Southampton windtunnel.....	III
Fig.App 2: Drag and lift coefficients of catamaran superstructures with narrow hull spacing.....	V
Fig.App 3: Drag and lift coefficients of catamaran superstructures with large hull spacing.....	VI
Fig.App 4: The 4 hull concepts.....	XVII
Fig.App 5: VPLP V-shape parent hull form sections.....	XIX
Fig.App 6: VPLP V-shape parent hull form lines.....	XX
Fig.App 7: VPLP's first realisation: The foiling trimaran Gerard Lambert (1984).....	XXIII
Fig.App 8: Noah 86' trawler catamaran.....	XXIV

List of Tables

Table 2.1: Appendage form factors.....	10
Table 3.1: Parameter range of the VWS series '89 [Müller-Graf, 1993].....	14
Table 3.2: Parameter range of the Molland catamaran series [1994].....	16
Table 3.3: Parameter range of the Schwetz and Sahoo research [2002].....	17
Table 3.4: Parameter range of the Sahoo research [2004].....	19
Table 4.1: Parameter range of the VPLP research.....	28
Table 4.2: Delft towing tank characteristics.....	30
Table 4.3: Main hydrostatic values of the model.....	30
Table 4.4: Output from CFD and towing tank tests.....	31
Table 4.5: Form factor test matrix.....	31
Table 4.6: Resistance test matrix (CFD).....	32
Table 4.7: Resistance test matrix (towing tank).....	32
Table 4.8: Model Test speeds for form factor determination.....	33
Table 4.9: Model and full scale resistance test speeds.....	33
Table 5.1: Friction resistance of the turbulence strips.....	36
Table 6.1: Constants for Holtrop form factor determination.....	44
Table 6.2: Parameter range for Holtrop form factor determination.....	44
Table 6.3: Suggested form factors according to Couser [1997].....	45
Table 6.4: CFD form factor for monohull.....	46
Table 6.5: CFD form factor for catamaran.....	47
Table 6.6: Measured values for the hull with tunnel:.....	49
Table 6.7: Measured values for the hull without tunnel:.....	49
Table 6.8: Form factor without transom resistance component:.....	49
Table 8.1: Suggested form factors and corresponding viscous interference factor from Couser [1997].....	60
Table 8.2: Form factors and corresponding viscous interference factor from ICARE.....	62
Table 8.3: Form factors and corresponding viscous interference factor from ISIS.....	63
Table 8.4: Viscous interference factor.....	63
Table.App 1: Parameter range of the DSYHS [Keuning, 1998].....	VII
Table.App 2: DSYHS regression constants 1998.....	VIII
Table.App 3: Parameter range of the DSYHS [Keuning, 2008].....	VIII
Table.App 4: DSYHS regression constants 2008.....	IX

Table.App 5: Parameter range of the NPL-Molland Series [Molland, 1994].....	X
Table.App 6: Catamaran residuary resistance regression constants.....	X
Table.App 7: Monohull residuary resistance regression constants.....	XI
Table.App 8: Catamaran trim regression constants.....	XI
Table.App 9: Monohull trim regression constants.....	XII
Table.App 10: Parameter range of the Schwetz-Sahoo regression [Schwetz, 2002].....	XII
Table.App 11: Monohull wave resistance regression constants.....	XIII
Table.App 12: Catamaran wave resistance regression constants	XIII
Table.App 13: Parameter range of the Sahoo Regression [Sahoo, 2004].....	XIV
Table.App 14: Monohull wave resistance regression constants.....	XIV
Table.App 15: Catamaran wave resistance regression constants.....	XIV
Table.App 16: Monohull transom wetted surface area regression constants.....	XV
Table.App 17: Overview of hull concepts.....	XVIII
Table.App 18: Form factor test matrix.....	XXI
Table.App 19: Test matrix of CFD tests for the validation.....	XXI
Table.App 20: Test matrix for towing tank tests for validation CFD.....	XXII
Table.App 21: Total proposed matrix.....	XXII

Nomenclature

Geometry

Symbol	Definition	SI Unit
A_p	Projected Planning Bottom Area	m^2
A_v	Area of Superstructure exposed to the wind	
A_w	Water Plane Area	m^2
A_x	Area of Maximum Section	
B	Beam or Breadth of the ship	mm
B_{px}	Maximum Beam over chines	mm
B_{WL}	Maximum Beam at DWL (design waterline) of one hull	mm
C_B	Block Coefficient	-
C_M	Mid-Ship Section Coefficient	-
C_P	Longitudinal Prismatic Coefficient	-
g	Gravitational Acceleration	m/s^2
i_E	Half Waterline Entry Angle	
$1 + k$	Form Factor	
k_s	Surface Roughness	mm
L	Length	mm
LCB	Longitudinal Centre of Buoyancy	
LCB_{fpp}	Longitudinal Centre of Buoyancy measured from fore perpendicular	mm
LCB_{mid}	Longitudinal Centre of Buoyancy measured from midship	mm
LCF	Longitudinal Centre of Flotation	mm
LCP_{fpp}	Longitudinal Centre of Buoyancy measured from fore perpendicular	mm
L_F	Foil Lift	N
L_{OA}	Length overall	mm
L_p	Projected length of the planning bottom area	mm
L_{wl}	Length of Waterline	mm
s	Hull Separation	mm
S	Surface	m^2
S_c	Wetted Surface Area of canoe body hull	m^2
S_0	Static Wetted Surface Area	m^2
S_{AP}	Appendage Wetted Surface Area	m^2
S_{TR}	Wetted Surface Area of Transom	
T_c	Draft of the canoe body	M
T_{TR}	Draft of Transom	
β	Averaged deadrise angle	degrees
τ	Running Trim Angle	degrees
Δ	Displacement Force / Mass	N / Tonnes
∇	Displacement Volume	m^3
∇_c	Displacement Volume of canoe body hull	m^3

Resistance

Symbol	Definition	SI Unit
C_{AA}	Air or Wind Resistance Coefficient	-
C_{BH}	Bare Hull Resistance Coefficient	-
C_D	Drag Coefficient	-
C_F	Frictional Resistance Coefficient of a body	-
C_{F0}	Frictional Resistance Coefficient of a corresponding flat plate	-
C_L	Lift Coefficient	-
C_P	Pressure Resistance Coefficient	-
C_R	Residuary Resistance Coefficient	-
C_T	Total Resistance Coefficient	-
C_V	Viscous Resistance Coefficient	-
C_W	Wave making Resistance Coefficient	-
C_{Wcat}	Wave making Resistance Coefficient for the catamaran	-
C_{Wmon}	Wave making Resistance Coefficient for a demi-hull	-
F_{Icat}	Interference Factor	-
R_{AA}	Aerodynamic Resistance, Windage or Wind Resistance	N
R_{AP}	Appendage Resistance	N
R_F	Frictional Resistance of a body	N
R_{F0}	Frictional Resistance of a flat plate	N
R_{Icat}	Hull Interference Resistance of a catamaran	N
R_{PV}	Viscous pressure Resistance	-
R_R	Residuary Resistance	N
R_{Rcat}	Residuary Resistance of the catamaran	N
R_{Rmon}	Residuary Resistance of one demi-hull	N
R_T	Total Resistance	N
R_{TR}	Transom Resistance	-
R_V	Viscous Resistance	N
R_W	Wave making Resistance	N
R_{WP}	Wave Pattern Resistance	N
V	Speed	m/s
V_{kts}	Speed in knots	kts
V_R	Apparent Wind Speed	m/s
ΔR_{AW}	Added Resistance due to rippling seas	N
β	Viscous Interference Factor	-
τ	Hull Interference Factor	-

Fluid Properties

Symbol	Definition	SI Unit
μ	Viscosity	kg / m s
ν	Kinematic Viscosity	m ² / s
ρ	Density	kg / m ³
F _n	Froude Number	-
F _{n_{TR}}	Froude Number based on Transom Depth	-
Re	Reynolds Number	-
Re _{TR}	Reynolds number based on Transom Depth	-

Subscripts

Symbol	Definition
A	Air
cat	Catamaran
dyn	Dynamic
mon	Demi-hull
FW	Fresh Water
M	Ship at model scale
S	Ship at real scale
SW	Sea Water

1 Introduction

In order to stay at the top of their game, Van Peteghem Lauriot Prévost Yacht Design (VPLP) is always looking towards challenging new projects. One of these challenges is the design of high quality luxurious cruising catamarans to be propelled by engine power. Up to now, they only specialised on the design of racing and cruising sailing multihulls. While exploring the world of motor catamarans, it was found that an extensive knowledge is required in different fields with respect to sailing vessels. For motor catamarans, the most important knowledge requirements at the begin stage of the design process are a precise weight estimate and an accurate method to estimate the catamarans resistance. Estimating the weight with high precision is one of the specialities of VPLP with their experience in designing high speed racing trimarans, however, resistance estimation for motor catamarans is a lot different to the resistance estimation of cruising and racing multihulls propelled by sails. The research elaborated in this report is part of the RCM project in which a large scale research programme is started that specializes in the accurate estimation of the resistance of catamarans for the luxury market, ranging from 15 to 30 meters.

The purpose of this report is to document the search for an accurately estimation method for the different resistance components of a motor catamaran. This search is part of the RCM project at VPLP Yacht Design to find an accurate and robust resistance prediction method in the early stages of the design process of luxurious cruising catamarans. This report is build up out of two parts, as the goal of the RCM project is twofold: firstly, an attempt to increase the accuracy of the resistance and motor power determination in the early stages of the design based on current knowledge, and secondly, to develop a specialized resistance and power estimation method more suited for the hull types designed at VPLP Yacht Design. Therefore, the first part, named the preliminary project, uses the available literature for the resistance estimation, so that it could be integrated rapidly in the existing VPP for motor catamarans. The final project is more extensive and is based on the data gathered from computational fluid dynamics and towing tank tests performed specifically for this research. A systematic series of catamaran hull forms is set up in order to study the important resistance components in more detail. The goal of the entire VPLP project is to implement this new acquired information in the existing VPP mentioned before to reach an even higher degree of accuracy. The research presented in this report is dedicated to the specific case of luxurious motor catamaran that can be used by the design offices in the early stage of the design process. Therefore, it is important to note that the hull form designed for this research is a specific example of the hull forms used in this industry, and its parameters are based on existing designs.

The report starts with a chapter, dedicated to the resistance of a motor catamaran and its components and a summary of available information concerning these components is given. In chapter 3, the existing researches with catamarans as subject are studied in order to use their data to build a resistance estimation regression to implement in the existing VPP at VPLP. From there on, the final project is started with chapter 4, where an extensive introduction is given for the rest of the report and the research.

The bare hull resistance is determined with computational fluid dynamics and towing tank tests and the results are presented in chapter 5, where also some results of the tests are compared. In order to scale the results from model scale towing tank tests towards a full scale vessel as studied in chapter 7, first the form factor needs to be determined, which is done extensively in chapter 6. For a multihull, the interference resistance plays an important role as could be expected, so also this subject will be researched thoroughly in chapter 8. As the hull form features a transom stern, the transom resistance is studied in chapter 9 and a regression for the estimation of the hydrostatic transom resistance is presented. Finally the report is rounded off with a summary of the conclusions and the recommendations. All additional and referenced information is summarized in the appendices.

2 Resistance of Catamarans

The total resistance of a catamaran is complicated to estimate. As an aid to estimate or calculate the total resistance, it is divided into different components depending on the resistance sources. In the first section, the total catamaran resistance and the division into components will be discussed, after which these different resistance components will be discussed elaborately.

2.1 Total Catamaran Resistance

The total catamaran resistance is the sum of all different forces working on the catamaran against the sailing direction. The total catamaran resistance will be divided into components depending on the different drag forces as such that they can be estimated or calculated more easily. Furthermore, the total resistance is depending on the speed the ship is sailing, which will be discussed too.

2.1.1 Total Catamaran Resistance Components

The components of the total catamaran resistance will be based on the different components of the catamaran, such as the bare hull, the appendages, the superstructure... The lower part of the hull and appendages move through the water, while the upper part of the hulls and the superstructure move through the air, creating hydrodynamic resistance and aerodynamic drag. [Müller-Graf, 1997] Furthermore, also the sailing conditions, as wind strength and direction and sea-state, have an influence on the total resistance and will be taken into account by the appropriate components. The total resistance can be written as the sum of the resistance components as given in [Müller-Graf, 1997] and applied to the catamaran in this research, this becomes:

$$R_{Tcat} = 2 * R_{BH} + R_{Icat} + R_L + R_{AP} + R_{AA} + R_{AW} \quad [2.1]$$

Where:

- R_{BH} is the bare hull resistance of one demi-hull
- R_{Icat} is the hull interference resistance of a catamaran
- R_L is the resistance due to hydrodynamic lift
- R_{AP} is the appendage resistance
- R_{AA} is the aerodynamic drag, windage or wind resistance
- R_{AW} is the added resistance due to rippling seas

The magnitude of each resistance component is depending on different parameters describing the catamaran geometry, the wind speed and direction, the sailing speed, the sea-state and currents. The different components summarized above will be elaborated in the following paragraphs and information about their determination and estimation will be given.

2.1.2 Speed Dependence

As speed increases, also the total resistance of a vessel increases. However, not all resistance components will increase at the same rate. Therefore, dividing the total speed range into several regimes is a common used way to explain physically what is happening to the different resistance components. An actual stepwise division is arbitrary as in real life there is no stepwise change in behaviour of a vessel or its resistance components. In this section three speed regimes will be elaborated in order to better understand some hull designs. Remember however that the limits of each regime are not visible and the vessel will experience a continuous change from one regime to the other. Hull shapes are most often optimized for a certain speed regime, or are a compromise between two speed regimes. These different speed regimes will result in different hull forms that minimize the major resistance components in that speed regime.

Displacement Range: $0.1 < F_n < 0.6$

In the displacement range, the vessel is supported by hydrostatic forces or Archimedean forces. In the displacement range, the wave resistance component is the largest. It can be up to 70% of the total resistance of the catamaran at about $F_n = 0.45$. For monohulls, the friction resistance component is small as it is dependant on the Reynolds number and thus the speed of the vessel.

For catamarans, the wave interference resistance is depending on the wave resistance, and as the wave resistance component is large, also the wave interference resistance for the catamaran will be large. Furthermore, [Müller-Graf, 1997] made some conclusions concerning the resistance of differently shaped catamarans in the displacement regime:

- For $F_n < 0.6$, a catamaran with symmetrical hulls has the largest interference resistance over catamarans with asymmetrical hull forms. The maximum of this interference resistance occurs at $F_n = 0.48$.
- For $0.3 < F_n < 0.6$ the asymmetrical hull has the largest wave resistance and this can be explained by the magnitude of the angle of entrance, which is doubled with respect to the angle of entrance of the symmetrical hull.

When talking about slender catamaran hulls, it should be noted that their relatively large wetted surface area to displacement ratio, the friction resistance in the lower speed regime is already a major contributing factor to the total resistance.

Semi-Displacement Range: $0.6 < F_n < 1.2$

In the semi-displacement range, the hull is supported by both hydrostatic and hydrodynamic forces. The hydrodynamic forces are also called hydrodynamic lift, as they result from the pressure distribution on the hull due to the accelerations and decelerations of the flow around the hull form. The wave resistance decreases with speed as the displaced water volume decreases and the frictional resistance increases with the second power of speed.

- For speed higher than $F_n = 0.6$, the viscous pressure resistance disappears.
- Appendage drag in this speed range is of the order of 8% – 15% of the total resistance, depending on their size, number and design.

For catamarans at this speed, resistance components due to the presence of the two hulls are increasing rapidly. The resistance components include the extra friction resistance due to the higher flow velocity between the hulls and extra spray resistance due to spray wetting on the tunnel roof and inner sides of the demi-hulls.

Planing Range: $1.2 < F_n$

In the planning speed range, the frictional resistance is the largest contribution to the total resistance, while the wave resistance becomes negligible. For catamarans, also the friction resistance components due to wetting, which are important in the semi-displacement regime, are decreasing. The resistance due to aerodynamic lift of the catamaran due to its tunnel and superstructure shape will become very important.

These effects are mainly applicable for planing hulls. When looking at slender or super slender hulls, this planing range will not exist at $Froude = 1.2$ due to the combination of their high displacement to water plane area ratio and their wave piercing hull shape. A good example of this are the floats of the ORMA 60 foot trimarans when flying one float and their central hull. These hulls remain much longer in the semi-displacement range, and are lifted out of the water by foils to decrease their resistance.

Knowing that the largest part of the appendage resistance comes from the friction component, the appendage resistance will increase quadratic as the speed increases, delivering 20% - 25% of the total drag in the planning speed range. [Müller-Graf, 1997]

2.1 Bare Hull Resistance

The bare hull resistance is the resistance of the bare hull in the upright position in calm water. The bare hull is a single hull without any appendages. The bare hull resistance can be divided into different components depending on some hull characteristics and the physical characteristics of the flow. In its

simplest form, the bare hull resistance is equal to the hydrodynamic resistance of a displacement monohull without appendages in upright position in calm water.

$$R_{BH} = R_W + R_S + R_V + R_{SR} + R_{TR} \quad [2.2]$$

Where:

- R_W is the wave resistance
- R_S is the spray resistance
- R_V is the viscous resistance
- R_{SR} is the spray rail resistance
- R_{TR} is the transom resistance

Introducing heel and leeway, introduces changes in most of these resistance components. While heel and leeway are common for sailing monohulls, they are not for motor catamarans, and therefore these changes will not be discussed during this research.

More elaborate, the division into different components according to [Sahoo, 1997] is visualized in the following figure. This figure explains the different components and their relation to one and another. This is important to understand, as the different terms found here will be used repetitively throughout this report.

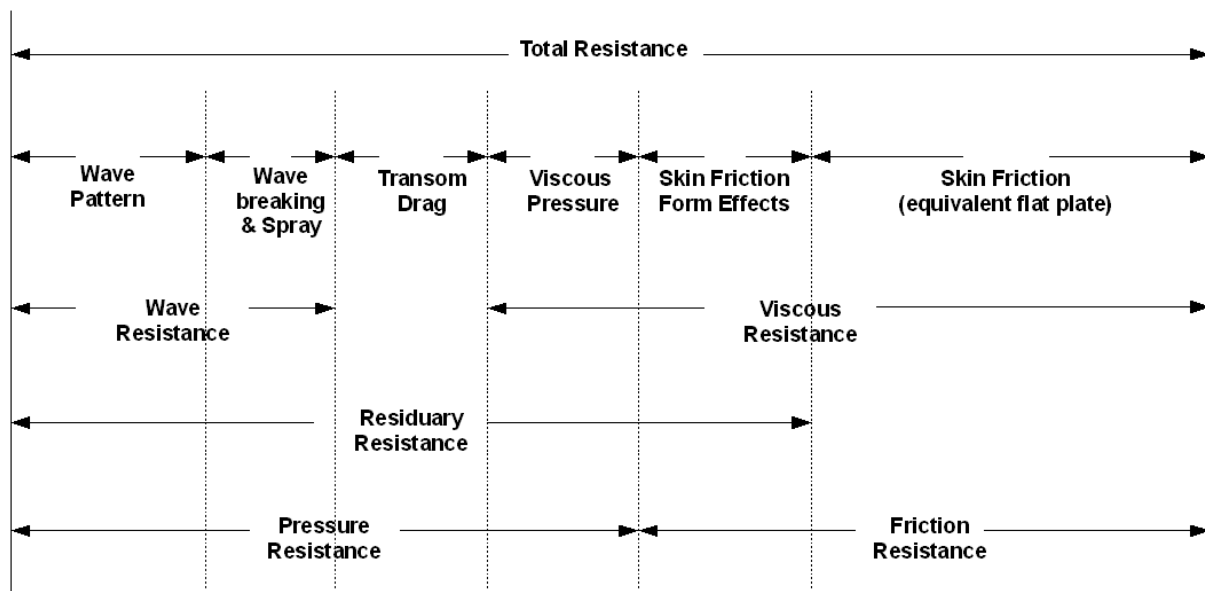


Figure 2.1: Resistance components

- Wave Pattern R_{WP} Resistance due to the generation of free wave systems of transverse and divergent waves.
- Wave Breaking R_{WB} Resistance is caused by the energy losses due to the breaking of the bow wave.
- Transom Drag R_{TR} Resistance component induced by the lower pressure on the transom when the transom is dry.
- Viscous Pressure Resistance R_{PV} Resistance caused by viscous effects of the hull shape and flow separation and eddymaking (for high speed ($Fn > 0.6$) this components disappears)

Form Effects	Difference in Resistance between friction resistance and skin friction which will be explained more elaborate in the following section
Friction Resistance R_F	Resistance cause by the shear forces of the water within the boundary layer of the hull (3D)
Skin Friction R_{F0}	Defined by the ITTC as the friction resistance of an equivalent flat plate
Wave Resistance R_W	Resistance caused by the formation of surface waves
Viscous Resistance R_V	Sum of the Friction Resistance and the viscous pressure Resistance
Residuary Resistance R_R	Is defined as the total resistance minus the skin friction
Pressure Resistance R_P	Sum of the x-component of the pressures on the wetted hull, or the x-components of the resulting normal force on the wetted hull.

As the division above shows, there are three methods to divide the resistance into two major components. These methods of division will be discussed in the following sections.

2.1.1 Residuary Resistance + Skin Friction

When towing tank tests are performed on a single hull, the resistance measured on the towing instruments is the total hull resistance. When we consider towing a bare hull, this total resistance is the total bare hull resistance discussed in this chapter. Because other resistance components are difficult to measure, the definition of the residuary resistance comes into play. The residuary resistance is found by subtracting the skin friction from the bare hull resistance, because the skin friction is an easy calculated value. Therefore the residuary resistance is:

$$R_R = R_{BH} - R_{F0} \quad [2.3]$$

Where the skin friction is determined from the skin friction coefficient and the wetted surface area. This skin friction actually is not the skin friction of the hull tested, but of a flat plate with an equivalent wetted surface area.

$$R_{F0} = \frac{1}{2} \rho V^2 S_c C_{F0} \quad [2.4]$$

The skin friction coefficient of the equivalent flat plate is calculated with the well-known ITTC'57 equation:

$$C_{F0} = \frac{0.0075}{(\log(Re) - 2)^2} \quad [2.5]$$

Once the residuary resistance is known, it can also be made dimensionless in order to scale the total resistance to the full scale vessel. There are two different ways of making this resistance component dimensionless. The most common method used is:

$$C_R = \frac{R_R}{\frac{1}{2} \rho V^2 S} \quad [2.6]$$

There is a second method for making the residuary resistance dimensionless. This method is applied by Gerritsma and Keuning ea. for the DSYHS, where they made use of the displacement of the vessel in stead of the wetted surface area:

$$C_R = \frac{R_R}{\nabla_c \rho g} \quad [2.7]$$

Using this separation of the bare hull resistance components, the form effects and viscous pressure resistance are covered by the residuary resistance. This means that the difference between the skin friction and the friction resistance will be taken into account by the residuary resistance and for this reason, the frictional resistance of the flat plate or skin friction is often referred to as simply the friction resistance as also will be done in the rest of this report. In the equations, the difference can still be seen by the subscript 0 implying the friction resistance of the flat plate or skin friction.

2.1.2 Pressure Resistance + Friction Resistance

In case of using computational fluid dynamics or CFD to calculate the resistance of a vessel, the above method of division is still applicable but a second method looks more appropriate. The results of the numerical calculations performed by the CFD programme allow a division in pressure resistance and friction resistance forces.

Theses pressure and friction forces are the forces working on the hull over the entire dynamic wetted surface. The pressure forces are the forces directed normal to the hull surface while the friction forces are the forces directed parallel to the hull surface. When these forces are integrated over the entire surface and their component in the direction of motion is taken, the results are the pressure resistance and friction resistance. These resistance values are positive when they are directed opposite to the direction of motion of the ship.

$$R_{BH} = R_p + R_f \quad [2.8]$$

In dimensionless form this means:

$$C_{BH} = C_p + C_f \quad [2.9]$$

The coefficients for the bare hull, pressure and friction resistance are all calculated with the following equations:

$$C_{BH} = \frac{R_{BH}}{\frac{1}{2} \rho V^2 S} \quad C_p = \frac{R_p}{\frac{1}{2} \rho V^2 S} \quad C_f = \frac{R_f}{\frac{1}{2} \rho V^2 S} \quad [2.10]$$

2.1.3 Wave Resistance + Transom Resistance + Friction Resistance

There exists a third method of dividing the bare hull resistance. This method uses the wave resistance and the viscous resistance. When wake and wave pattern analysis are performed after towing tank testing or computational fluid dynamics, the wave resistance can be determined. Subtracting the wave resistance from the bare hull resistance delivers then the viscous resistance. However, one should keep in mind that accurate results are more difficult to obtain when using a hull form with a transom stern, as the transom stern

resistance is a separate resistance component from the wave resistance. For transom stern vessel, the bare hull resistance is equal to:

$$R_{BH} = R_W + R_{TR} + R_V \quad [2.11]$$

The coefficients for the wave and viscous resistance are all calculated with the following equations:

$$C_W = \frac{R_W}{\frac{1}{2} \rho V^2 S} \quad C_{TR} = \frac{R_{TR}}{\frac{1}{2} \rho V^2 S} \quad C_V = \frac{R_V}{\frac{1}{2} \rho V^2 S} \quad [2.12]$$

When the viscous pressure resistance is neglected and there is no immersed transom with its complicated flow phenomena, the division of the pressure and friction resistance and the wave and viscous resistance mounts in the same results:

$$C_P = C_W \quad \text{and} \quad C_F = C_V \quad [2.13]$$

2.2 Interference Resistance

The presence of two nearby hulls induces an extra interference resistance on both hulls. It consists of several smaller components as is described in [Müller-Graf, 1997] and later on in this report. For resistance estimation in the conceptual design stage, this interference resistance component is accounted for by the interference factor. This interference factor is multiplied with the wave resistance component or the residuary resistance component in the calculation of the total resistance. In this manner, the increase due to the interference resistance is accounted for in a higher wave resistance term.

$$F_{Icat} = \frac{R_{Rcat}}{2R_{Rmon}} \quad [2.14]$$

$$R_{Icat} = R_{Rcat} - 2 \cdot R_{Rmon} \quad [2.15]$$

Where: R_{Rcat} is the residuary resistance of the catamaran
 R_{Rmon} is the residuary resistance of one demi-hull

Furthermore, the interference resistance can be taken into account by a viscous interference term and a wave interference term, resulting in more accurate results. This method is elaborated in [Schwetz, 2004] and will be the basis of determination of the interference resistance factors in chapter 8.2.

$$R_{Tcat} = \tau \cdot R_{Rmon} + (1 + \beta \cdot k_{mon}) \cdot R_{F_0} \quad [2.16]$$

Where: β is the viscous interference factor

2.3 Windage or Wind Resistance

The windage or wind resistance, or also known as aerodynamic drag, is an important factor in the total resistance of motor catamarans as often, the design requirements state a minimum forward speed in a certain headwind. This resistance contribution is calculated with the following common drag formula:

$$R_{AA} = \frac{1}{2} \rho_A V_R^2 A_V C_{AA} \quad [2.17]$$

Where:

- ρ_A is the air density (1.266 kg/m³)
- A_V is the area exposed to the wind
- C_{AA} is the wind resistance coefficient
- V_R is the sum of the hull speed and the speed component of the wind in the direction of motion:

$$V_R = AWS \cdot \cos(AWA) = TWS \cdot \cos(TWA) + V \quad [2.18]$$

All values in this equation are known except for the drag coefficient or wind resistance coefficient. Again, it is the designer's job to choose or estimate this coefficient to fit his design. The more streamlined the design is, the lower this coefficient will be. In literature, different values for this coefficient can be found. Some examples are given here:

- For passenger catamarans: $C_{AA} = 0.42-0.45$ [Müller-Graf, 1997]
- For freight catamarans: $C_{AA} = 0.45-0.50$ [Müller-Graf, 1997]

From the Aero-Hydro-Sail Force Models lecture notes of the Southampton Institute:

- Hull: $C_{AA} = 0.4$
- Superstructure: $C_{AA} = 0.9$
- Rigging: $C_{AA} = 1.0$
- Mast: $C_{AA} = 0.8$

These values are rough estimates that can be used for the determination of the required engine power in the preliminary design stage. They should not be used for the aerodynamic design of the superstructure. When more accurate estimates are required CFD calculations or wind tunnel tests can be undertaken, depending on the importance and the available budget.

In parallel with this research, VPLP collaborated with a student from the University of Southampton in order to determine drag and lift coefficients for a systematic series of superstructures for catamarans in the Southampton University wind tunnel. In this systematic series, speed, trim angle, hull separation, frontal projected surface and streamlining of the superstructure were varied. The results for the different superstructure lay-outs can be found in Appendix B .

2.4 Appendage Resistance

As for the bare hull resistance, the appendage resistance can be divided into the viscous and residuary component. The appendage resistance can also be taken into account by taking a certain percentage of the bare hull resistance, but this will result in a very rough estimate. More accurate estimates can be found when this resistance component is divided into viscous and residuary resistance. This division introduces the same estimation methods and problems, which will be discussed below.

2.4.1 As function of Hull Skin Friction

With the use of different constants for different types of appendages, the appendage resistance can be defined as a function of the bare hull skin friction. [Holtrop, 1982] defines the appendage resistance with an appendage form factor as seen in equation [2.19]. The appendage form factor constants are based on a large number of experimental tests and can be seen in the table below:

$$R_{AP} = \frac{1}{2} \rho V^2 S_{AP} (1 + k_2)_{eq} C_{F0} \quad [2.19]$$

Appendages	$(1 + k_2)$
rudder behind skeg	1.5 - 2.0
rudder behind stern	1.3 - 1.5
twin-screw balance rudders	2.8
shaft brackets	3.0
skeg	1.5 - 2.0
strut bossings	3.0
hull bossings	2.0
shafts	2.0 - 4.0
stabilizer fins	2.8
dome	2.7
bilge keels	1.4

Table 2.1: Appendage form factors

For motor vessels, the interactions between rudder, strut and propeller play an important role. A lot depends on the speed of the flow through the propeller, as this flow encounters the rudder and the strut of the propeller shaft. This makes the appendage resistance difficult to estimate and is often taken into account as a percentage of the bare hull resistance. Together with the towing tank tests of the bare hull, self propelling towing tank tests can be used in order to determine the appendage resistance but this requires a lot of work and time, and this can only be done in a later design stage when the hull forms and propeller geometry are known.

2.4.2 As function of Appendage Skin Friction

[Keuning, 1997] proposes to decompose the appendage resistance into appendage skin friction and residuary resistance of the keel for sailing yachts. As for the bare hull, the appendage skin friction can be determined by the ITTC 57' method (equation [2.5]).

The term residuary resistance is used here as the subtraction of the skin friction from the total appendage resistance results not only in a small wave resistance component, but also an interference resistance between the appendages and the hull. The magnitude of both components of the residuary appendage resistance is largely dependent on the geometry of the appendage. At the Delft University of Technology, two systematic series were set up to give a parametric quantification of the residuary appendage resistance. [Keuning, 1999]. The Delft Systematic Keel Series or DSKS is a series in which six different keels have been tested underneath two hulls of different beam to draft ratios. The second series is the Delft Various Keel Series or DVKS in which one hull is tested with a series of 13 widely different keels. The residuary appendage resistance of the DSKS is defined as:

$$\frac{R_{Rk}}{\nabla_k \cdot \rho \cdot g} = A_0 + A_1 \cdot \frac{T}{B_{WL}} + A_2 \cdot \frac{T_c + Z_{cbk}}{\nabla_k^{\frac{1}{3}}} + A_4 \cdot \frac{\nabla_c}{\nabla_k} \quad [2.20]$$

Where:

- R_{Rk} is the residuary resistance of the keel
- ∇_k is the displacement volume of the keel
- T is the total draft of hull and keel
- Z_{cbk} is the vertical position of the centre of buoyancy of the keel

The constants of this formula can be found in Appendix C .

From [Hoerner, 1965] and [Abott, 1959], propose a different method to estimate the friction drag as they divide the friction drag into different components that each can be estimated. They assume that the wave resistance component of the appendage resistance can be neglected and the friction drag can be determined with the following formulae:

- Fin Form Drag

$$C_{D_{v,fin}} = C_{F0} \cdot \left(1 + 2 \left(\frac{t}{c} \right)_{mean} + 60 \left(\frac{t}{c} \right)_{mean}^4 \right)_{fin} \quad [2.21]$$

- Wing Tip Losses

$$C_{D_{v,fin tip}} = 0.075 \cdot \left(\frac{t}{c} \right)_{tip}^2 \quad [2.22]$$

- Wing-body junction

$$C_{D_{v,fin root}} = 0.8 \cdot \left(\frac{t}{c} \right)_{root}^3 - 0.0003 \quad [2.23]$$

- Bulb Form Drag

$$C_{D_{v,wei bulb}} = C_{F0} \cdot \left(1 + 1.5 \cdot \left(\frac{d}{l} \right)_{max}^2 + 7 \cdot \left(\frac{d}{l} \right)_{max}^3 \right)_{bulb} \quad [2.24]$$

As explained by Keuning, the Hoerner definition of the form factor for the appendages can be used together with the DSYHS regression of the residuary resistance in order to estimate the entire appendage resistance.

2.1 Resistance due to Lift

The most effective way to reduce the hull resistance can be achieved by lifting up the hull partially or completely out of the water. Displaced volume and wetted area are reduced and by this, the frictional resistance and the wave resistance decrease. [Müller-Graf, 1997]

Lift is mainly created by the hydrodynamic flow, and in a lesser extend by the aerodynamic phenomena. The resistance due to aerodynamic lift will be taken into account in the next section where the wind resistance is discussed.

Hydrodynamic lift originates from the hull and appendages. As a consequence of the lift that is created, a certain amount of induced drag will exist. Foils are a common name for all profiled appendages that deliver lift. This lift is used for different purposes, depending on the foil. The rudder creates lift that is used to manoeuvre the vessel and for sail yachts, it is also used, together with the daggerboard to have an equilibrium in lateral forces and the moment around the vertical axis. Lifting foils are used for lifting the mass of the vessel partly or fully out of the water to decrease resistance or increase stability as is the case for large ocean racing trimarans for example.

2.1.1 Induced drag due to hull lift

At all immersed hull surfaces, mainly at the bottom, hydrodynamic forces are developed which increase with speed. The vertical component of the normal force acts upwards as lift and downwards as suction force. If the vessel is nearly solely supported by the hull lift, the induced drag reaches its maximum with:

$$R_p = \nabla \cdot \rho \cdot g \cdot tg \theta \quad [2.25]$$

Where: θ is the angle between the mean buttock at $\frac{1}{4} B$ of the afterbody and horizontal plane underway: $\theta = \theta_0 + \tau$
 θ_0 is the angle between mean buttock of afterbody and horizontal plane at rest τ is the running trim

This part of resistance is already taken into account in the bare hull resistance, but it is useful to notice that many of the resistance components are linked and cannot be seen separately.

2.1.2 Induced drag due to foil lift

All foils, rudders and daggerboards deliver a certain amount of induced resistance when creating lift. This induced resistance can be calculated using the theory of the Prandtl's Classical Lifting Line Theory. [Anderson, 1991] The induced drag is defines as:

$$D_L = \frac{1}{2} \cdot \rho \cdot V_s^2 \cdot S \cdot C_{D_i} \quad [2.26]$$

Where the induced drag coefficient is depending on the lift coefficient and equal to:

$$C_{D_i} = \frac{C_L^2}{\pi \cdot AR \cdot e} \quad [2.27]$$

Where: AR is the aspect ratio of the foil
 e is the Oswald's efficiency factor by which the induced drag exceeds that of an elliptical lift distribution.

2.2 Resistance due to sea-way

In his paper for the HISWA Symposium 1998, [Keuning, 1998] presented several research results concerning the added resistance due to waves. For sail yachts within the parameter ranges of the Delft Systematic Yacht Hull Series, there are two regression formulae proposed that can be used for the determination of the added wave resistance, where the second formulation is more elaborate, but only increasing accuracy for the shortest average spectral periods.

$$\frac{R_{AW} \cdot 10^2}{\rho \cdot g \cdot L_{WL} \cdot H_{\frac{1}{3}}^2} = a \cdot \left[10^2 \cdot \frac{\nabla_c^{1/3}}{L_{WL}} \cdot \frac{k_{yy}}{L_{WL}} \right]^b \quad [2.28]$$

$$\begin{aligned} \frac{R_{AW} \cdot 10^2}{\rho \cdot g \cdot L_{WL} \cdot H_{\frac{1}{3}}^2} = & \frac{A_1 \cdot k_{yy}}{L_{WL}} \cdot \frac{\nabla_c^{1/3}}{L_{WL}} + A_2 \frac{k_{yy}}{L_{WL}} + A_3 \cdot C_p^2 + A_4 \cdot \frac{L_{WL}}{B_{WL}} + \dots \\ & \dots + A_5 \cdot \left(\frac{L_{WL}}{B_{WL}} \right)^2 + A_6 \cdot \frac{B_{WL}}{T_c} + A_7 \cdot \left(\frac{B_{WL}}{T_c} \right)^2 \end{aligned} \quad [2.29]$$

Both regression formulae can be found in [Keuning, 1998], while the regression constants can be found in the appendix of the same publication.

This method of data gathering can also be applied to hull forms for motor yachts and motor catamarans, but it will take some extensive towing tank testing and calculation work. For the remainder of this report, only the calm water case will be studied and thus, the behaviour of the vessel in waves will not be taken into account.

3 Preliminary Project

In Appendix A , a flow chart is given to explain the lay-out of the entire RCM project, in which the preliminary project of this report is pointed out. In short, the preliminary project consists of three steps. The first step is an extensive literature survey towards the existing and available information concerning catamaran resistance. After that, some of the available information is used to create a regression formula for the estimation of the catamaran resistance and finally, this regression will be validated with the use of resistance values form CFD calculations at full scale. Some conclusions concerning the regression and the used data will be given.

3.1 Available Information

There is not a lot of catamaran resistance information widely available. Three researches on systematic series of catamaran hull forms are worth mentioning: first, the VWS Hard Chine Catamaran Hull Series '89 of Müller-Graf, secondly the Catamaran Series of Molland, which is based on the NPL hull form and finally the research performed by Sahoo with the use of CFD. All researches will be discussed shortly and their most important results and conclusions will be given.

3.1.1 Müller-Graf Data

Somewhere in the mid 80's at the Technical University of Berlin, a research was started on fast and slender hulls both in monohull and catamaran configuration. This research was conducted by Müller-Graf and resulted in the VWS Hard Chine Catamaran Hull Series '89.

Hull Form

The hull form was designed for the German shipbuilding industry for the use as large, high speed catamarans for passenger transportation. The choice of a catamaran configuration was taken as they can fulfil most of the requirements such as low power, large deck area, box shaped superstructures, good transverse stability, good course keeping and manoeuvrability. [Müller-Graph, 2001] The main hull form is shown in Figure 3.1 and can be characterized by its hard chine and its pronounced V-shape of the sections. Also some round bilge versions were tested in this research.

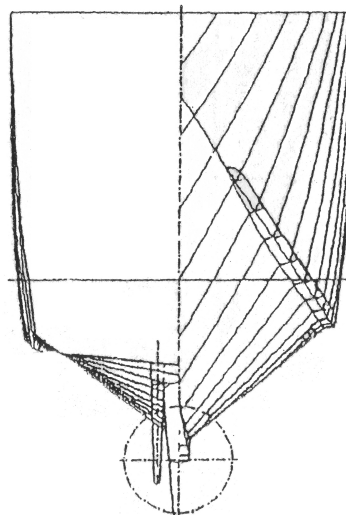


Figure 3.1: VWS series '89 catamaran hull form [Müller-Graf, 1993]

Parameter Range

The series was performed specific for planing catamarans. The hull characteristics that were changed in this systematic series were the deadrise angle, length-to-beam ratio and the cross-sectional shape:

- Deadrise angles of 16°, 27° and 38°
- Length-to-beam ratios of 7.55, 9.55, 11.55 and 13.55
- Round cross-sections and hard chine cross-sections

All important parameter ranges can be found in the table below:

VWS Series '89					
0.2	<	Froude number	<	1	
7.55	<	$\frac{L_{WL}}{B_{WL}}$	<	13.55	
0.38	<	$\frac{LCB}{L_{WL}}$	<	0.43	
6.25	<	$\frac{L_{WL}}{\nabla^{1/3}}$	<	9.67	
		$\frac{s}{L_{WL}}$	=	0.17	
16	<	β_M	<	38	

Table 3.1: Parameter range of the VWS series '89 [Müller-Graf, 1993]

Müller-Graf Results

Müller-Graf did not share the quantitative results from the hydrodynamic research in his paper, however, he discusses the trends in resistance due to the change of the different parameters. Several conclusions were drawn in the publication of this series [Müller-Graf, 1993]:

- Interference resistance:
 - For $\frac{L_{WL}}{B_{WL}} = 7.55$ the interference resistance is 29% of the total resistance.
 - For $\frac{L_{WL}}{B_{WL}} = 13.55$ the interference resistance is 17.5% of the total resistance.
- Influence of length-to-beam ratio:
 - With increasing length-to-beam ratio, the resistance decreases with a minimum for $\frac{L_{WL}}{B_{WL}} = 11.5 - 12.0$
 - At higher length-to-beam ratios, the resistance increases again.
 - Dynamic trim decreases with increasing length-to-beam ratio

- Influence of midship deadrise angle:
 - Below $Fn_{\nabla}=3.0$ the residuary and total resistance increase with decreasing deadrise angle.
 - Above $Fn_{\nabla}=3.0$ the residuary and total resistance increase with increasing deadrise angle.
 - The difference in resistance between deadrise angle 27° and 16° decreases with increasing length to beam ratio.
- Influence of section shape:
 - The round bilge hull form produces up to 10% less resistance below $Fn=1.2$

3.1.1 NPL-Molland Data

The original NPL research focussed on hull shape for fast monohull craft. Both hard shine and round bilge shapes were studied. Molland changed the length-displacement ratio and the length-to-beam ratio to make this hull form applicable for his catamaran research. Only the round bilge shape was studied by Molland.

The NPL and Molland data from the University of Southampton [Molland, 1994] will be used to perform regression analysis using Matlab as a first step in this research. Using the Molland data, the importance of the different parameters could be examined and the applicability of the Matlab programme could be tested. In this paragraph, the results for this regression analysis are given en shortly discussed.

Hull Form

The NPL hull form is characterized by its round bilge, the large V sections at the bow. It is a high speed planing hull form designed to be used for high speed catamarans. The sections of this hull form can be seen in Figure 3.2 below.

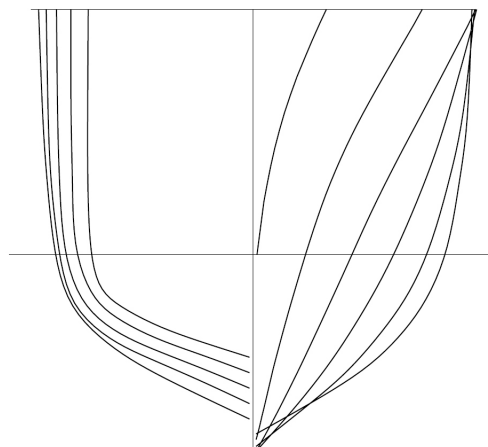


Figure 3.2: The NPL parent hull form

Parameter Range

The initial monohull systematic series of the NPL research was focussed on hull shape for fast monohull craft. Therefore the Froude numbers that are applied range from 0.3 to 1.5. Furthermore, 4 different length-displacement ratios were used:

- $L/Disp = 4.76$ $L/B = 3.42$
- $L/Disp = 5.83$ $L/B = 4.00$
- $L/Disp = 5.93$ $L/B = 4.39$
- $L/Disp = 6.10$ $L/B = 4.97$

The high speed resistance data of Molland [1994] was generated for higher length-displacement ratios and speeds only up to a Froude number of 1.00.

NPL-Molland Series				
0.2	<	Froude number	<	1.00
7.00	<	$\frac{L_{WL}}{B_{WL}}$	<	15.10
0.436	<	$\frac{LCB}{L_{WL}}$	<	0.455
1.5	<	$\frac{B_{WL}}{T_c}$	<	2.5
6.3	<	$\frac{L_{WL}}{\nabla^{1/3}}$	<	9.5
0.653	<	C_P	<	0.733
0.2	<	$\frac{s}{L_{WL}}$	<	0.5

Table 3.2: Parameter range of the Molland catamaran series [1994]

NPL-Molland Results

In the figure below, a sample of the Molland results is given. It can be seen that there are some obvious trends: at the speed where the hump in wave resistance takes place, it is shown that the resistance increases with decreasing separation between the hulls. However, at higher speeds, the catamaran with the smallest separation ratio has the lowest resistance.

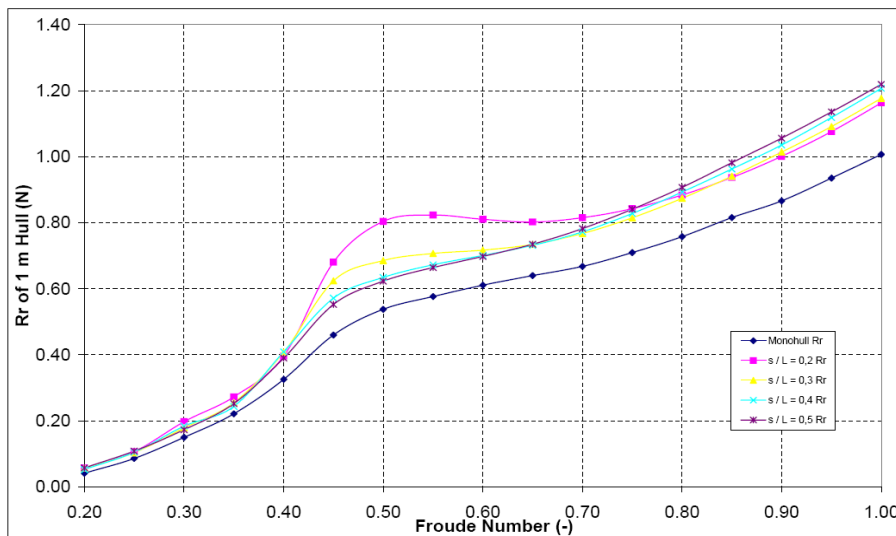


Figure 3.3: Residuary resistance of model 5a at scale of 1 metre

From the above trends, it should be expected that the monohull, considered as a catamaran with infinite separation between the hulls, should have a higher resistance at high speeds than the catamarans. This is clearly not the case, implying some bad correlation between the monohull and catamaran test results from this research. This will be discussed further on in the report when the towing tank tests and the CFD results for this research will be presented.

3.1.2 Schwetz-Sahoo Data [2002]

A big difference with the two researches indicated above is the research performed at the Australian Maritime College. Schwetz [2002] prepared a generic series of hull forms for high speed catamarans. Using these hull forms, CFD calculations were performed using SHIPFLOW.

Hull Form

The generic series of hull forms ranges from wide hard chine planing hull forms to narrow round bilge hull forms with and without bulbous bows as can be seen in the illustration below:

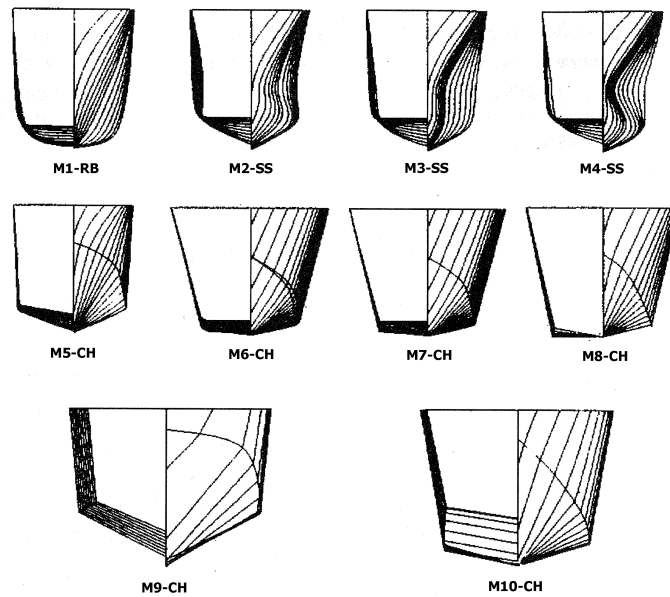


Figure 3.4: Schwetz systematic series of hull forms

Parameter Range

Schwetz Systematic Series				
0.5	<	Froude number	<	1.5
8.8	<	$\frac{L_{WL}}{B_{WL}}$	<	15.3
0.4	<	$\frac{LCB}{L_{WL}}$	<	0.49
6.3	<	$\frac{L_{WL}}{\nabla^{1/3}}$	<	9.56
0.46	<	C_B	<	0.68
0.2	<	$\frac{s}{L_{WL}}$	<	0.4

Table 3.3: Parameter range of the Schwetz and Sahoo research [2002]

As can be seen from the table above, the data is based on high speed calculations which can't be used for cruising catamarans that operate between Froude number 0.2 and 0.9

Schwetz-Sahoo Results

The results from the CFD calculations were used to create regression formulae to determine the wave resistance of catamaran and monohull hull forms falling in the parameter range shown before.

$$C_{W_{mon}} = C_1 \cdot \left(\frac{L_{WL}}{\nabla^{1/3}} \right)^{C_2} \cdot \left(\frac{LCB}{LCF} \right)^{C_3} \cdot \left(\frac{B}{T} \right)^{C_4} \cdot C_B^{C_5} \quad [3.1]$$

$$C_{W_{cat}} = C_1 \cdot \left(\frac{L_{WL}}{\nabla^{1/3}} \right)^{C_2} \cdot \left(\frac{s}{L_{WL}} \right)^{C_3} \cdot \left(\frac{LCB}{LCF} \right)^{C_4} \cdot i_E^{C_5} \cdot C_B^{C_6} \cdot \left(\frac{B}{T} \right)^{C_7} \quad [3.2]$$

Where: i_E is the half waterline entry angle

The constants of this regression can be found in Appendix C.3 .

3.1.3 Sahoo Data [2004]

The previous research of Schwetz and Sahoo used a very extend range of different hull shapes for the systematic series. In [Sahoo, 2004], Sahoo presents a new systematic series, directed more towards the high-speed ferry industry in Australia. For this research, the hull forms were also analysed with the use of CFD calculations using SHIPFLOW.

Hull Form

The hull forms for the new systematic series are based on typical hull forms used by the high-speed ferry industry in Australia. These hull forms have round bilge sections and are very slender as can be seen in Figure 3.5:

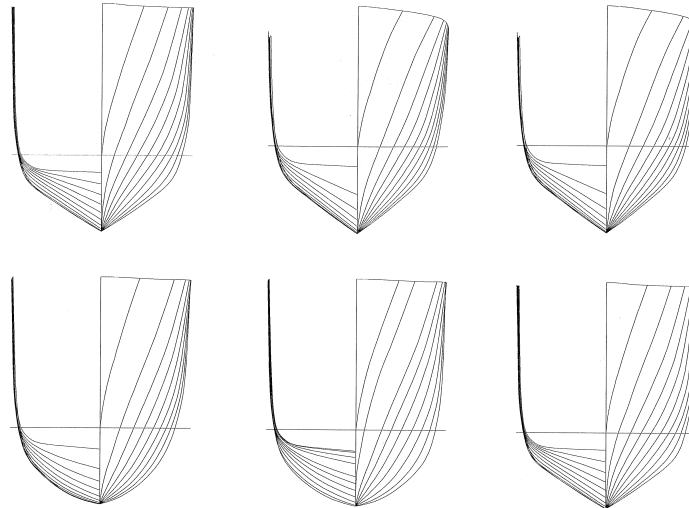


Figure 3.5: Sahoo systematic series of hull forms

Parameter Range

Sahoo Systematic Series					
0.2	<	Froude number	<	1	
10.0	<	$\frac{L_{WL}}{B_{WL}}$	<	15.0	
0.45	<	$\frac{LCB}{L_{WL}}$	<	0.47	
8.04	<	$\frac{L_{WL}}{\nabla^{1/3}}$	<	11.20	
0.40	<	C_B	<	0.50	
0.2	<	$\frac{s}{L_{WL}}$	<	0.4	

Table 3.4: Parameter range of the Sahoo research [2004]

The parameter range for this research was directed towards very slender hulls with high length-displacement ratios. These ratios are too high for cruising catamarans, and thus not applicable for determining the resistance of luxurious cruising catamarans.

Sahoo Results

Again, two regression formulae were formulated to determine the wave resistance for both the catamaran as well as the monohull configuration.

$$C_{W_{mon}} = e^{C_1} \cdot \left(\frac{L_{WL}}{B}\right)^{C_2} \cdot C_B^{C_3} \cdot \left(\frac{L_{WL}}{\nabla^{1/3}}\right)^{C_4} \cdot (i_E)^{C_5} \cdot (\beta)^{C_6} \quad [3.3]$$

Where: β is the half waterline entry angle

$$C_{W_{cat}} = e^{C_1} \cdot \left(\frac{L_{WL}}{B}\right)^{C_2} \cdot \left(\frac{B}{T}\right)^{C_3} \cdot C_B^{C_4} \cdot \left(\frac{L_{WL}}{\nabla^{1/3}}\right)^{C_5} \cdot (i_E)^{C_6} \cdot (\beta)^{C_7} \cdot \left(\frac{s}{L_{WL}}\right)^{C_8} \quad [3.4]$$

Where: i_E is the half waterline entry angle

The constants of this regression can be found in Appendix C.4 .

3.2 Regression Analysis

In order to build an accurate and reliable regression, a thorough study has to be performed. First off all, the different regression methods have to be studied, together with the software that needs to be used. Finally, before creating the regression formula, the different parameters that are varied need to be discussed. All these subjects are elaborated in this chapter, which is closed off with the final lay-out of the regression and its regression constants.

3.2.1 Regression Method

There are different regression analysis methods and some of the most common methods were tested in the scope of this research, however, the method used for building the regression, which is discussed here is

the linear regression analysis. The linear regression describes the data points as a linear combination of one or more model parameters. Using linear regression analysis for each specific speed value in the entire speed range is known to give a good simulation for the resistance of a vessel. This method is extensively used for the Delft Systematic Yacht Hull Series.

The linear regression method makes use of the Least Squares Method. This method creates a *regression line* or *least squares line*. This line is determined such that the sum of the *squared* distances of all the data points from the line is the lowest possible. This method gives a lot of freedom to choose build-up depending on the variables. However, more freedom also means more possibilities and more work to find the correct regression variables to best describe the data available.

3.2.2 Matlab

Matlab is a high-level language and interactive environment to perform intensive computations. Matlab can be used to calculate regressions, statistics and artificial neural networks. This programme requires some programming knowledge to get started, but once the required m-files are programmed, the regression analysis and plotting of the results is automated. The possibilities for regression analysis in Matlab will be elaborated in the following section. The following information concerning two Matlab functions can be found in Chapter 6 of the Matlab Manual [2007].

Multiple Linear Regression

The multiple linear regression is a linear regression as explained in the previous section. The multiple system makes use of more than two independent variables to describe the dependant variable. In Matlab this regression can be calculated using the \ (back-slash) operator or the Matlab function REGRESS. The REGRESS function not only gives the solution to the system, but also delivers the statistical values of the system.

Stepwise Regression

There are two common stepwise regression methods: the forward and the backward stepwise regression. The forward stepwise regression starts with no terms in the regression model and at each step, the statistically most significant term (the one with the highest F statistic and lowest p-value) is added to the regression model, until there are none left. The backward regression starts with all the terms in the model and removes the least significant terms, until all the remaining terms are statistically significant. The function name in Matlab is STEPWISE. Using this function, an interactive graphical interface is started that can be used to compare competing models. This graphical interface makes it possible to research the influence of the different variables in the regression.

3.2.3 Regression Parameters

Study Different Parameters and the Regression Stability

The most important parameters are discussed here on their relevance with respect to the regression analysis:

- Length-displacement ratio $\frac{L_{WL}}{\nabla^{1/3}}$:

This parameters is the most important one with respect to the resistance of slender hulls, as it gives a better representation of the slenderness than $\frac{L_{WL}}{B_{WL}}$ because the displacement term includes all geometrical parameters like L, B, T and C_b .

- Separation ratio $\frac{s}{L_{WL}}$:

For catamarans this parameter is of major importance as changing it will result in different interference effects and different speeds at which these interference effects take place.

- Beam-to-draft ratio $\frac{B_{WL}}{T_c}$:

When changing the $\frac{L_{WL}}{\nabla^{1/3}}$ ratio, also $\frac{L_{WL}}{B_{WL}}$ and/or $\frac{B_{WL}}{T_c}$ will change, making them important parameters. When building the regression, the beam-to-draft ratio could be replaced by displacement-WSA ratio $\frac{\nabla^{2/3}}{S_c}$ as this ratio represents about the same, but is said to result in a more robust regression.

- Slenderness ratio $\frac{L_{WL}}{B_{WL}}$:

The same applies as for the beam-to-draft ratio.

- LCB position $\frac{LCB}{L_{WL}}$:

The position has a large influence on the fullness of the hull form towards the bow or the stern, thus influencing the wave resistance.

- Prismatic coefficient C_p :

This parameter is also important, describing the fullness of the hull with respect to the maximum section area.

Some important notes to take into account:

- Concerning the use of the parameters in the mathematical regression, it can be said that, the more parameters used, the more accurate the regression will be. But at the same time, the more parameters used, the more tests are needed to make a robust regression.
- From practice it was found that the LCB position was required for an accurate regression, but due to the very small range of in LCB values of the Molland series, the regression is very sensitive to LCB changes as will be shown during the validation process of the regression in the next section.

3.2.4 Final Regression

With the use of the parameters studied above, an extensive Matlab file was written in such a way that these different parameters could easily be excluded or included in order to study directly their importance. The final regression is a linear regression with the form given in equation [3.5]. All the parameters from this regression formula are dimensionless and dependant on the length-displacement ratio.

$$C_R = \left(a_1 + a_2 \cdot \frac{LCB}{L_{WL}} + a_3 \cdot \frac{B}{L_{WL}} + a_4 \cdot \frac{B}{T} + a_5 \cdot \frac{s}{L_{WL}} \right) \cdot \frac{\nabla^{1/3}}{L_{WL}} \quad [3.5]$$

Where:

$$C_R = \frac{R_R}{\frac{1}{2} \rho V^2 S_c} \quad [3.6]$$

The above definition for the residuary resistance coefficient is used because this was the method applied by Molland [1994] and introduces the lowest number of sources for inaccuracies in the further calculations.

The constants a_1 to a_5 for this regression can be found in Appendix C . The constants are presented separately for the monohull and catamaran configuration. The division between the monohull data and the catamaran data was required, as the Molland data did not show a consistence trend in the resistance with respect to the separation ratio. First tests with the combined data showed that the resulting regression gave non accurate estimates for the monohull configuration due to the different shape of the resistance curve. For the monohull configuration one can see that:

$$a_5=0$$

[3.7]

3.3 Validation and Accuracy

In the course of this research, as will be shown later on in this report, CFD calculations were performed on a VPLP hull form. The results from the regression above will be compared to these CFD results. Two different CFD software packages are used, which are called ISIS and ICARE. Both are based on the RANS theory and will be discussed more thoroughly, together with the results in chapter 5.

3.3.1 Monohull Resistance

As two regressions are built, one for the monohull and one for the catamaran configuration, these regressions will be validated separately.

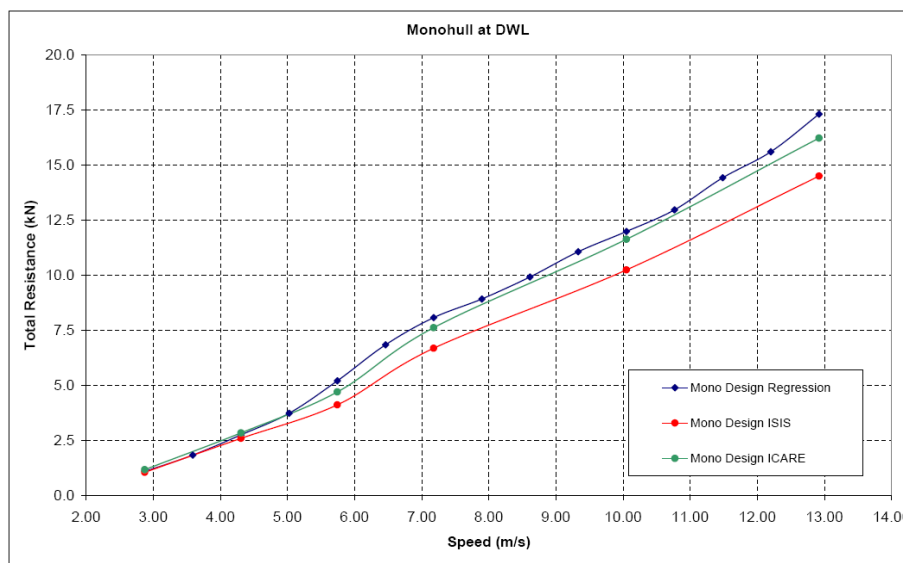


Figure 3.6: Regression results in comparison with CFD for the design displacement case

The parameters of the heavy displacement configuration are similar to those of model 4b of the Molland data and therefore, it could be assumed that the resistance of this configuration is estimated more accurately as can be seen on the following page, implying that the ISIS results could be more accurate than the ICARE results.

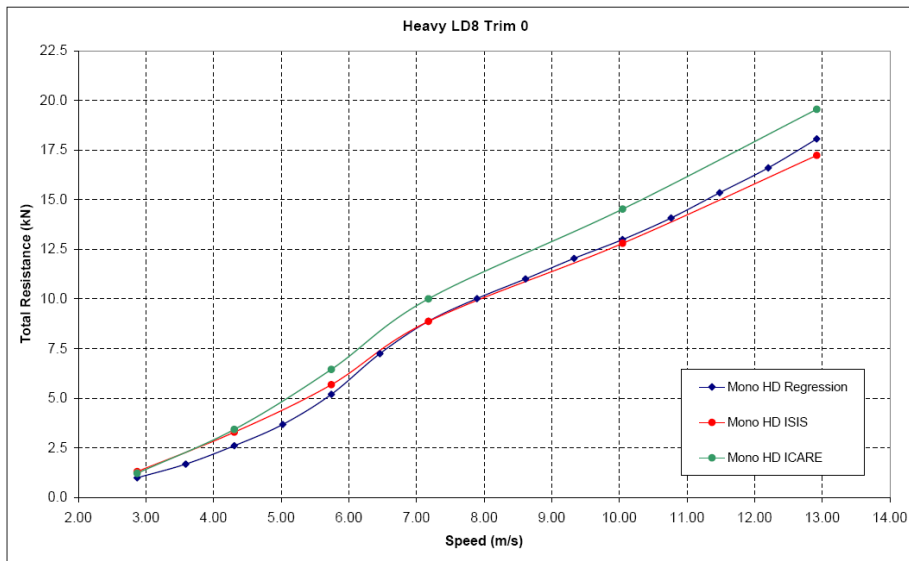


Figure 3.7: Regression results in comparison with CFD for the heavy displacement case

In Figure 3.8, the effect of an out-of-range LCB position on the results of the regression can be seen. Due to the small range of LCB position available from the Molland test data, the regression is very sensitive to changes in LCB. It is therefore important to incorporate more LCB variations in the VPLP test data in order to create the final VPLP catamaran regression.

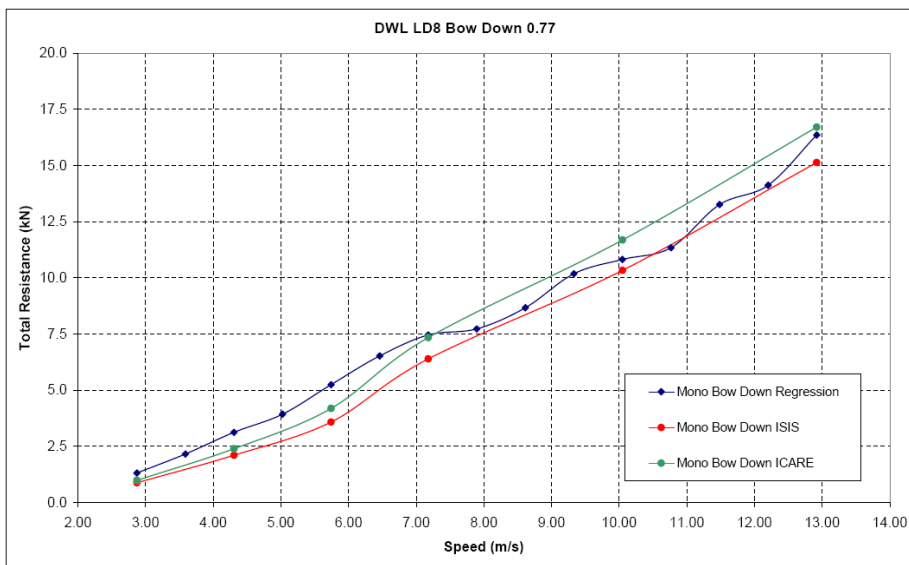


Figure 3.8: Influence of out-of-range LCB position on the regression results

3.3.2 Catamaran Resistance

With respect to the catamaran configuration, it should be noted that the interaction factor from the CFD shows no interaction or even negative interaction for speeds higher than $F_n = 0.7$. In the Molland research, catamaran resistance is larger than the monohull resistance for all speeds, which is reflected in the regression. This is one of the reasons to perform a new VPLP systematic series on full scale CFD and large model scale towing tank tests in order to clarify the differences in the total interference factor.

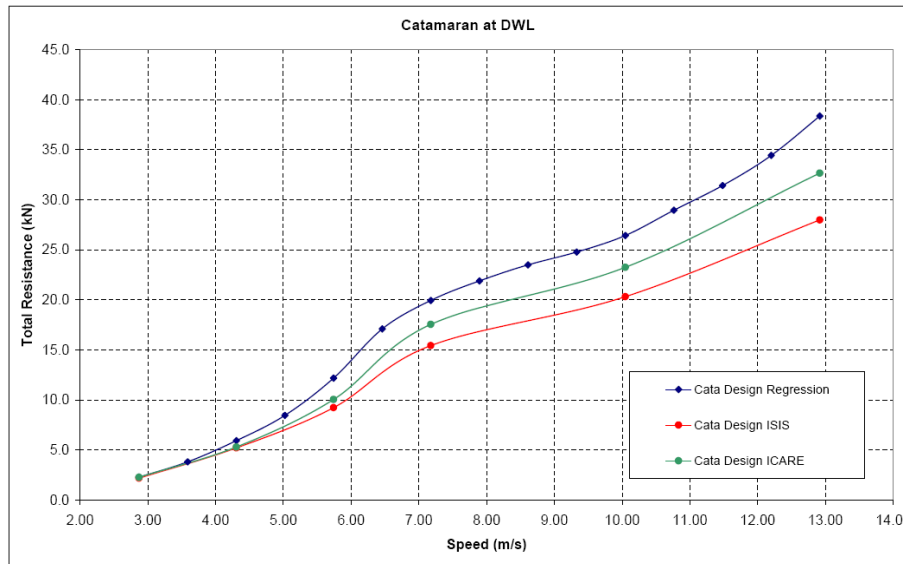


Figure 3.9: Catamaran regression results in comparison to CFD results

The differences observed in the Molland data between the monohull resistance and the catamaran resistance is clearly reflected in the regressions. If compared to the CFD results, it looks as the catamaran regression overestimates the catamaran resistance, while the monohull resistance seems to be estimated more accurately. This would imply that the Molland data for the monohull configurations is accurate while the catamaran results are too high. The inconsistencies in the available data and thus the regressions based on this data point out the need for extra investigation and new towing tank tests on a bigger matrix to build a more precise data set and corresponding regressions.

3.4 Conclusion

The first and far most important conclusion from this chapter is the lack of applicable data for the estimation of the resistance of cruising catamarans. At this stage, only the parameter range of the Molland data is usable, but some of his results should be handled with care. Furthermore, the hull shape of hull used by Molland is not suited for luxurious cruising catamarans, but can give a first indication of the bare hull resistance. The most important point to take into account is the inconsistency in the Molland data between monohull and catamaran results.

The above conclusions prove the need to produce VPLP Systematic Catamaran Series. This series is required for extra investigation and towing tank tests to build a more precise data set and corresponding regressions.

4 Final Project

The final project consists of a personalized series of hull forms specifically designed for VPLP. In this chapter, the final project will be elaborated thoroughly and the importance of the different research topics will be explained here. Furthermore, the VPLP hull form will be presented together with the useful information concerning the CFD calculations and the towing tank tests. Finally, the applied test matrices of the final project will be discussed.

4.1 Project Lay-out

In this paragraph, the final project and its lay-out will be discussed. This can be seen as an extensive introduction for the rest of this chapter and the coming chapters, describing the goals, the method and the boundary conditions of the project.

4.1.1 Project Goals

The main goal of the final project is to find an accurate resistance prediction for cruising motor catamarans in the range of 15-30 meters. This goal can be achieved by gathering as much information as possible in order to perform different analysis on different fields. Once this goal is reached, the resistance estimation method can be included into the existing VPP for cruising motor catamarans of VPLP. The entire project flow chart can be found in Appendix A .

4.1.2 Working Method

The flow chart of the project, not only gives the project goal as mentioned above, but also gives an overview how to get to this goal. It can be seen, moving upwards from the final goal, how the work is divided into smaller portions which are explained in this report. The idea to achieve the above goal is to perform CFD calculations or towing tank test on a systematic series of motor catamaran hull forms. With the use of the preliminary CFD calculations, performed with two different software packages, and towing tank tests, a trade-off can be made between these three different methods. Once this has happened, the data can also be used to study other research fields that are required for the accurate resistance prediction of the VPP. These research fields include:

- Estimation of the Bare Hull Resistance
- Determination of the Form Factor
- Estimation of the Interference Resistance
- Estimation of the Transom Resistance
- Validation of the Scaling Methods

These research topics will be explained briefly in the next paragraph and discussed elaborately in their proper chapters afterwards.

4.1.3 Boundary Conditions

The research project is bounded by some boundary conditions resulting in the final project lay-out. With respect to the CFD calculations, the matrix of tested configurations is kept limited in size in order to comply with the research budget and the goal to perform those calculations with two different software packages for a better comparison. The cost for such CFD calculations is quite extensive compared to towing tank testing due to the high required calculation power and time. Towing tank tests aren't cheap either, but once the model is built, increasing the size of the test matrix doesn't increase the cost dramatically.

Another boundary condition for the CFD calculations is the size of the grid applied. The size of the grid has to be an optimum with respect to the precision of the calculations and the calculation time. As for the towing tank tests, the boundaries are more drawn up by the available equipment and set-up. However intended at the start of the project, no values are available for the dynamic wetted surface area of the hull and transom due to the large size of the model. At the same time, towing time was limited to 4 weeks, limiting the size of the test matrix of speeds and configurations.

4.2 Research Topics

The purpose of this section is to explain the followed research path, resulting in the final goal of accurately estimating the bare hull resistance for full scale motor catamarans. The use of CFD calculations and towing tank tests stands central in this discussion and it will be seen that, however both are entirely different, they can be used together to solve the research questions.

First of all, the bare hull resistance will be discussed, introducing the need for further investigation into the use of the form factor and different scaling laws. Thus, as a results, the form factor will be elaborated, introducing new investigation fields in the form of the interference resistance and the transom stern resistance.

4.2.1 Bare Hull Resistance

The base of the entire research is an accurate estimation of the bare hull resistance, and thus a precise determination of the bare hull resistance from the CFD calculations and the towing tank tests. Therefore the division of the bare hull resistance for both the CFD calculations and the towing tank tests will be given here.

Computational Fluid Dynamics

Using CFD for the determination of the bare hull resistance, results in the pressure resistance and the friction resistance of the full scale vessel. Using these results, two regression formulae could be made as an estimation method which could be incorporated in the motor catamaran VPP.

However, the full scale vessel in this research is 21 meters, and of course, not all the motor yachts designed at VPLP will be of this length. Therefore, attention should be taken in how to scale these results to the according waterline length. In order to scale these CFD determined bare hull resistance values, they need to be divided into the pressure resistance and the friction resistance. This can be done in two ways, depending on the pressure resistance of the monohull or the catamaran as can be seen below:

$$R_{BHcat} = R_{Pcat} + (1 + \beta \cdot k) \cdot R_{F0} \quad [4.1]$$

$$R_{BHcat} = \tau \cdot R_{Pmon} + (1 + \beta \cdot k) \cdot R_{F0} \quad [4.2]$$

These equations will not be elaborated at this point, as they only are used here to show the importance of studying the interference resistance and the different interference factors. More information can be found in chapter 8.2.

Towing Tank Tests

When performing towing tank tests, the total bare hull resistance of the model is found. In order to use it to determine the resistance of a vessel at full scale, it has to be divided into the residuary resistance component and the skin friction component as is explained in section 2.1.1. As for the CFD calculations, there are two ways to divide the bare hull resistance. One is to use the residuary resistance of the catamaran, while the second one uses the residuary resistance of the monohull and the total interference factor:

$$R_{BHcat} = R_{Rcat} + R_{F0} \quad [4.3]$$

$$R_{BHcat} = R_{Rmon} \cdot F_{Icat} + R_{F0} \quad [4.4]$$

This again shows the importance of a third interference factor that will be elaborated in chapter 8.1.

4.2.2 Form Factor

As shown in the previous section, the form factor comes into play when scaling the CFD results to the required waterline length of the designed vessel. However, it is also used when trying to scale the towing tank results more accurately than only using the residuary resistance and skin friction. This division of the bare hull resistance is already shown in equations [4.1] and [4.2], making these equations also valid for the towing tank test results.

When the form factor is determined from slow speed towing tank test, as will be explained more elaborate in chapter 6 , some precautions should be taken. First of all, a constant form factor for the entire speed range will be found and secondly, when performing slow speed towing tank tests with a hull form with an immersed transom, the transom introduces a resistance component that makes this kind of form factor determination invalid. Thus meaning that the form factor needs to be determined without immersed transom and introducing an estimation method for the transom resistance. The influence of the immersed transom on the form factor will be studied in chapter 6.3, while the estimation method for the transom resistance will be discussed in chapter 9 .

When CFD calculations are used to determine the form factor, a form factor, depending on the speed is found. This variable form factor will be compared to the form factor determined from the towing tank tests later on in this report with a more in-depth discussion of the form factor.

4.2.3 Scaling Methods

There are two scaling methods to be used and analysed in this case. The first method, uses the division of residuary resistance and skin friction. This leaves out the use of the form factor, which can be assumed to be accurate as the form factor for this type of hull forms are expected to be very small.

However, using the form factor could increase the precision. If the form factor is to be used, the bare hull resistance is divided into pressure resistance and friction resistance.

As seen from the previous paragraph, the form factor can be determined with or without the transom resistance incorporated. This results in three scaling methods that will be elaborated and compared in chapter 7 .

4.2.4 Interference Resistance

In the previous sections, it is already shown how important the interference resistance and interference factors are in the determination of a catamarans resistance. The three different interference factors mentioned before will be elaborated in chapter 8 . The two equations, showing the three interference factors, are repeated here in order to give reminder of the three different interference factors:

$$R_{Tcat} = R_{Rmon} \cdot F_{Icat} + R_{F_0} \quad [4.5]$$

$$R_{Tcat} = \tau R_{Pmon} + (1 + \beta \cdot k) \cdot R_{F_0} \quad [4.6]$$

Where: F_{Icat} is the total interference factor
 β is the viscous interference factor
 τ is the wave interference factor

4.2.5 Transom Stern Resistance

As was mentioned before, the immersed transom has a big influence on the form factor determined from slow speed towing tank tests for hull forms with immersed transoms. It is therefore recommended to determine the form factor without immersed transom, and to estimate the transom resistance as a separate resistance component. Two methods of transom resistance estimation will be proposed in chapter 9 , after which their results will be briefly compared.

4.3 VPLP Catamaran

Due to the lack of relevant research information on cruising catamarans, VPLP started its own research. For this purpose, different hull shapes were studied and a parent hull form was designed specifically for this research. This hull form will be elaborated in the first section, while the parameter range of the test cases will be explained in section 4.3.2.

4.3.1 Hull Form

The purpose of this hull form is to resemble the hull forms used by VPLP in their design of cruising motor catamarans. This hull form needs to be "simple" in order to easily comprehend all the flow phenomena and determine the resistance components. For this reason, several elements are not taken into account, which may be used in the actual designs of VPLP. For example, the hull is designed without spray-rails, without trim flap and without a bulbous bow. However, it was decided to introduce a tunnel at the stern to place the propeller as this would always be required for the cruising motor catamarans designed at VPLP. More information can be found in Appendix D, where the entire design process of the parent hull is documented. The sections of the VPLP hull form can be seen in Figure 4.1.

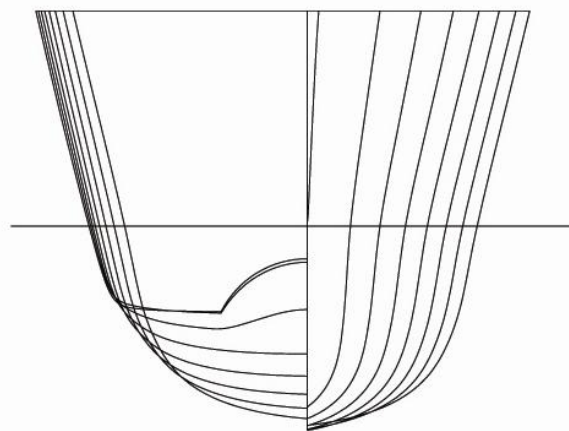


Figure 4.1: VPLP V-shape parent hull form

4.3.2 Parameter Range

As mentioned before a preliminary matrix of hull configurations are tested, which will be extended in the near future with CFD calculations or towing tank tests. The preliminary parameter range displayed here comes from one parent hull form testes with different trim angles and displacements. The purpose of the entire RCM project is to extend this parameter range with scaled versions of the parent hull form to build precise and robust regressions for different resistance components.

VPLP research				
0.2	<	Froude number	<	0.9
0.419	<	$\frac{LCB}{L_{WL}}$	<	0.479
7.50	<	$\frac{L_{WL}}{\nabla^{1/3}}$	<	8.50
1.9	<	$\frac{B_{WL}}{T_{WL}}$	<	2.4

Table 4.1: Parameter range of the VPLP research

4.4 Facilities / Programme

Testing a catamaran in the towing tank only requires building one of the two catamaran hulls. Towing this hull near the side of the towing tank will simulate the catamaran, as the waves will be reflected by the towing tank wall. This makes it possible to use large models, giving more accurate resistance measurements. The same can be done for the CFD calculations. The plane of symmetry with the appropriate boundary conditions will make one half of the catamaran redundant. In this paragraph, the used CFD software and models will be discussed and the facilities of the towing tank will be elaborated.

4.4.1 Computational Fluid Dynamics

The CFD calculations are performed by two independent subcontractors with the use of two different calculation codes, both based on RANS. The calculations are performed on the hull at full scale of 21 metres. A major disadvantage of CFD calculations, even with the powerful computers nowadays is the required computational time and required computing power. The main advantages of performing CFD calculations are listed below:

- Easy division of resistance into pressure resistance and friction resistance.
- Easy deduction of form factor
- Easy determination pressure distribution on the transom
- Easy deduction viscous and wave interference resistance

These CFD calculations will be used to make a trade off between the two CFD packages used and are used as a comparison for the towing tank test results. Both CFD packages will be explained briefly.

ISIS

ISIS is a CFD calculation code that is incorporated in the commercial package FINE™/Marine from NUMECA Flow Integrated Environments (FINE™). FINE™/Marine is dedicated to marine applications and is the latest CFD product from NUMECA International. It offers high accuracy flow simulation results on arbitrary and complex geometries, leading to shorter design cycles. FINE™/Marine is developed in collaboration with Ecole Centrale de Nantes, Centre National de la Recherche Scientifique (CNRS), and NUMECA International. The synergy results in a product consisting of:

- Full-hexahedral automated unstructured mesh generator HEXPRESS™;
- Incompressible RANS solver ISIS;
- Flow visualization and analysis tool CFView.

The code uses the RANS theory to solve the Navier-Stokes equations. Furthermore, it is a Volume Of Fluid method, which uses an interface capturing method for the free-surface. The calculations are performed by Yann Roux from the company k-Epsilon. There are two kinds of grids used for the calculations, which are a structured mesh and an automated unstructured mesh. The turbulence model applied to solve the equations is the k-omega (SST Menter) model.

ICARE

As for ISIS, ICARE is also developed at the Ecole Centrale de Nantes. The CFD calculations were performed by Erwan Jacquin of the company HydroOcean. In contradiction to ISIS, ICARE is not available as a commercial CFD packages, and only few spin-off companies of the Ecole Centrale de Nantes own licences to use this package.

ICARE makes use of an interface tracing mesh, where the grid cells deform after each time step in order for the mesh to follow the free surface. The advantage of this method is that it requires less grid cells as there is no grid for the air, however, this introduces also some disadvantages. First of all, the calculation time with less grid cells does not decrease due to the grid deformation iteration which is required. Secondly, a number of cells perpendicular to the hull surface are required. This gives a limit in the minimum thickness of the bow

wave against the hull, which could give some inaccuracies. Further disadvantages include the impossibility to model spray and a difficult convergence of the solution the unwetting of the transom stern.

4.4.1 Towing Tank Tests

The towing tank tests for this research are performed at the Delft University of Technology. A brief summary with the characteristics of the towing tank will be given below, together with some information concerning the used model, also built in-house at the University.

Delft Towing Tank

The Delft University of Technology own two towing tanks that can be found in the building of the Maritime Engineering Department. The largest one of the two is used during this research in order to use the biggest model possible for accurate results. The characteristics of the large towing tank can be found in Table 4.2. The model is suspended underneath a chariot that rides on rails and is powered by four electrical engines. The model is connected to the chariot with the use of in-house manufactured sensors for resistance and side force. Only the two degrees of freedom sinkage and trim are kept free and their values are read out by a high precision optical sensor.

Length	142.00	m
Width	4.22	m
Maximum Water Depth	2.50	m
Maximum Towing Speed	8.00	m/s

Table 4.2: Delft towing tank characteristics

Towing Tank Model

The models for the Delft Towing Tank are manufactured in the in-house workshop of the Maritime Engineering Department. The model is built from high density foam, which is milled numerically. The model has a water line length of 4.2 meters at its design displacement, which gives a scaling factor of 1:5. The main hydrostatic values of the model at its design displacement can be found in the table below:

DISPL kg	LCB m	VCB mm	LWL m	draft mm	BWL m	WSA m ²	Star m ²	SWL m ²	Cp -	Cb -
144.7	2.11	76.2	4.205	225.2	0.390	2.17	0.00942	1.21	0.660	0.386

Table 4.3: Main hydrostatic values of the model

The turbulence simulation is performed with the use of four turbulence strips with carborundum or silicium carbide grains of 40mm width placed at 0.5 metre intervals.

4.4.2 Test Results

The different CFD calculation methods and the towing tank tests, all have their specific output values. For the CFD calculations, these output values not only depend on the calculation tool, but also the communication with the subcontractors. For the towing tank tests, the output depends largely on the possible set-up and the model size. The output values which were recuperated from the different tests are given in Table 4.4.

	ICARE	ISIS	Towing Tank
Total Resistance			X
Pressure Resistance	X	X	
Friction Resistance	X	X	
Transom Stern Resistance		X	
Side Force		X	X
Yaw Moment		X	X
Sinkage	X	X	X
Trim	X	X	X
Dynamic WSA		X	
Transom Dynamic WSA		X	
Wave Height (betw Hulls)	X	X	

Table 4.4: Output from CFD and towing tank tests

4.5 Test Data

For the three different test methods, different test configurations and different test speeds are applied, depending on the foreseen use of the results. These test data will be briefly explained in this paragraph.

4.5.1 Test Configurations

The two main fields of research are the form factor determination and the resistance determination of cruising motor catamarans, while the two major testing methods are the towing tank tests and the CFD calculations. Therefore, three tables of test configurations will be discussed: firstly the towing tank test configurations for the slow speed form factor tests, secondly the full speed range CFD calculations and finally the full speed range towing tank tests.

For the research towards the form factor using the slow speed towing tank tests, the influence of the transom stern is studied by the use of configurations at different trim angles. A second research field with these tests was studying the effect of the tunnel for the propeller on the form factor. All configurations were tested in the middle of the towing tank as the monohull configuration as well as in the close proximity of the tank wall in order to simulate the catamaran configuration with separation ratios 0.30 and 0.50.

		Trim	Tunnel Cases	
			With Tunnel	Without Tunnel
Trim Cases	WL at Bottom Transom	2.59°	Mono Cata	Mono Cata
	WL at Half of Tunnel	1.34°	Mono Cata	---
	WL at Top of Tunnel	0.00°	Mono Cata	Mono Cata

Table 4.5: Form factor test matrix

The full speed range tests are performed with both CFD calculations and towing tank tests. The CFD calculations are performed on a less extensive list of configurations as these calculations demand a lot of computing power and time. 5 configurations were tested with the two RNAS CFD packages ICARE and ISIS. Table 4.6 shows the configurations, where the catamaran configuration has a separation ratio of 0.30.

		Trim Cases		
		Bow Up (0.77 degrees)	Normal (0 degrees)	Dow Down (-0.77 degrees)
Displacement Cases	Light $\left(\frac{L}{\nabla^{1/3}}=8.5\right)$	---	Mono	---
	Design $\left(\frac{L}{\nabla^{1/3}}=8.0\right)$	Mono	Mono Cata	Mono
	Heavy $\left(\frac{L}{\nabla^{1/3}}=7.5\right)$	---	Mono	---

Table 4.6: Resistance test matrix (CFD)

The test matrix for the towing tank tests is much more extensive and gathers 18 different configurations. The catamaran configurations noted here in Table 4.7, are for three different separation ratios, namely 0.25, 0.30 and 0.40.

		Trim Cases		
		Bow Up (0.77 degrees)	Normal (0 degrees)	Dow Down (-0.77 degrees)
Displacement Cases	Light $\left(\frac{L}{\nabla^{1/3}}=8.5\right)$	Mono	Mono Cata	Mono
	Design $\left(\frac{L}{\nabla^{1/3}}=8.0\right)$	Mono	Mono Cata	Mono
	Heavy $\left(\frac{L}{\nabla^{1/3}}=7.5\right)$	Mono	Mono Cata	Mono

Table 4.7: Resistance test matrix (towing tank)

4.5.2 Test Speeds

Two types of tests were performed in the scope of this research. For the determination of the form factor by the use of towing tank tests, slow speed tests are used to generate the Prohaska and Hughes plots. The towing speeds used for the model of 4.2 meters are listed in Table 4.8. In order to be able to determine the different resistance components for the entire speed range applicable to the cruising motor catamarans designed at VPLP, both CFD calculations and towing tank tests were performed at Froude numbers of 0.2 to 0.9, which results in the test speeds summarized in Table 4.9.

Froude Number	Model Speed (m/s)
-	$L_{WL} = 4.2$ meter
0.000	0.000
0.100	0.642
0.125	0.802
0.150	0.963
0.175	1.123
0.200	1.284
0.225	1.444
0.250	1.605
0.275	1.765
0.300	1.926

Table 4.8: Model Test speeds for form factor determination

Froude Number	Model Speed (m/s)	Full Scale Speed (m/s)
-	$L_{WL} = 4.2$ meter	$L_{WL} = 21$ meter
0.20	1.284	2.871
0.30	1.926	4.306
0.40	2.568	5.741
0.50	3.209	7.177
0.70	4.493	10.047
0.90	5.777	12.918

Table 4.9: Model and full scale resistance test speeds

4.5.3 Nomenclature

To organize all test results, both CFD and towing tank tests, the results are clearly indicated by a name, summarizing all required info. The lay-out of the names will be explained by the use of two examples:

- Cat0.3_Disp-D_Tr0_ISIS
- Mon0_Disp-L_Tr0.77_TTT

The information intervals in the name are separated by underscore sign (_) and explain the configuration of the tested case, together with the calculation or test method used.

- The first entry clarifies if the hull is tested in monohull or catamaran configuration, and gives the applicable separation ratio. The possible entries in this research are: Mon0 , Cat0.25, Cat0.3, Cat0.4, Cat0.5
- Secondly, the displacement case is given, with the following possible entries: Disp-L for light displacement, Disp-D for design displacement and Disp-H for heavy displacement.
- The third entry states the trim angle at which the hull is tested. The angle is directed positive to port (a positive angle equals a nose down trim). As a result, here are the possible entries for the trim angles applied in this research: Tr0, Tr-0.77, Tr0.77, Tr1.34 or Tr2.59
- The last entry specifies the determination method of the test results, which can be towing tank tests (TTT), CFD calculations with ISIS (ISIS) or CFD calculations with ICARE (ICARE)

5 Bare Hull Resistance

The bare hull resistance is the main resistance component on which this research is based. Its value is determined here with the use of computational fluid dynamics and towing tank tests. The results of both determination methods will be given in this chapter, while also the trim and sinkage values will be compared without the need of complicated scaling methods. Comparison of other resistance components will follow in the subsequent chapters.

5.1 Bare Hull Resistance Determination

For this research, the bare hull resistance was determined with the use of two CFD packages and a large series of towing tank tests. In this paragraph, the bare hull resistance results, determined with these three methods will be shown and discussed.

5.1.1 Towing Tank Tests

In the determination of the bare hull resistance with the use of towing tank tests, the turbulence simulation for the model is important. The friction resistance of the turbulence strips applied will be discussed here, together with the bare hull resistance results.

Turbulent Strips

In order to simulate the correct turbulent flow around the towed model with respect to the full scale vessel, turbulence strips are applied to the model to trip the boundary layer and induce an artificial transition from the laminar boundary layer towards the turbulent boundary layer. Based on experience, all tests were performed with 4 double turbulence strips of 40 mm width attached to the model at about half a meter intervals. The latest configuration was tested with these double strips, as well as with 4 single strips of 20 mm in order to determine the added frictional resistance of the strips. The strip friction coefficient based on the strip surface is plotted below.

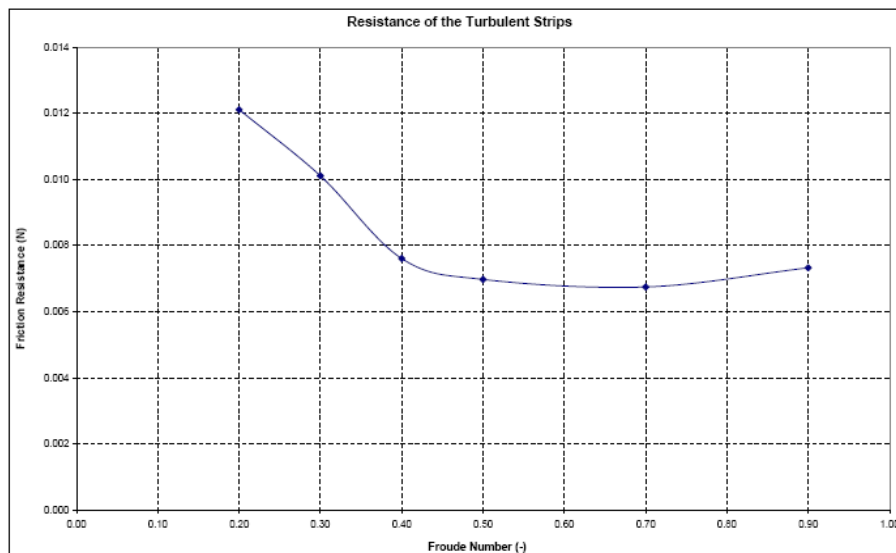


Figure 5.1: Friction resistance of the turbulence strips

The mean strip friction coefficient resulted to 0.007167 and is used to subtract the strip resistance of all the towing tank test data that was gathered.

Froude Number	ΔR_F	$C_{F_{Strips}}$
0.400	0.933	0.007611
0.500	1.337	0.006977
0.700	2.534	0.006749
0.900	4.551	0.007332
Mean Value		0.007167

Table 5.1: Friction resistance of the turbulence strips

Measurements

The first results proposed here, are the full speed range results for the bare hull resistance of the monohull and the catamaran configuration at different separation ratios. The trend for decreasing separation ratio, which increases the hump drag is clearly visible.

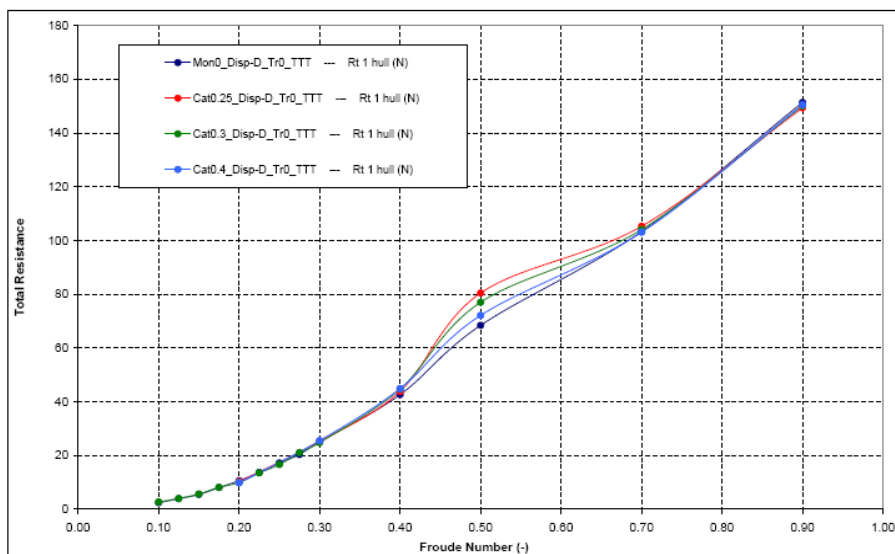


Figure 5.2: Example of the gathered towing tank test resistance data

Remembering the results from Molland's research (Figure 3.3), where the monohull resistance at high speeds is clearly lower than the catamaran resistance, it can be seen here that at high speeds, the monohull resistance and the catamaran resistance in fact result in about the same values.

Furthermore, it can be seen that for these slender hull forms, the hump in the resistance curve is very limited in size and is located at higher Froude numbers than for hull forms with lower length-displacement ratios. The hull form testes here has its hump at a Froude number of 0.5 and the hump is directly a function of the separation ratio.

On the next page, the same hull configurations are used to plot the trim angle and the sinkage. From both plots it can be seen that at the position of the hump, both the trim angle trend and the sinkage trend depends nicely on the separation ratio. However, at higher speeds, the configuration with a separation ratio of 0.3 seems to behave different than the trend followed by the other catamaran and monohull configurations. It can be seen that this configuration trims down the bow faster after the hump and raises faster out of the squat of the hump into the semi-planing mode, where a large part of the vessels displacement is carried by the upwards pressure forces. This change in attitude however isn't reflected in the resistance of the vessel.

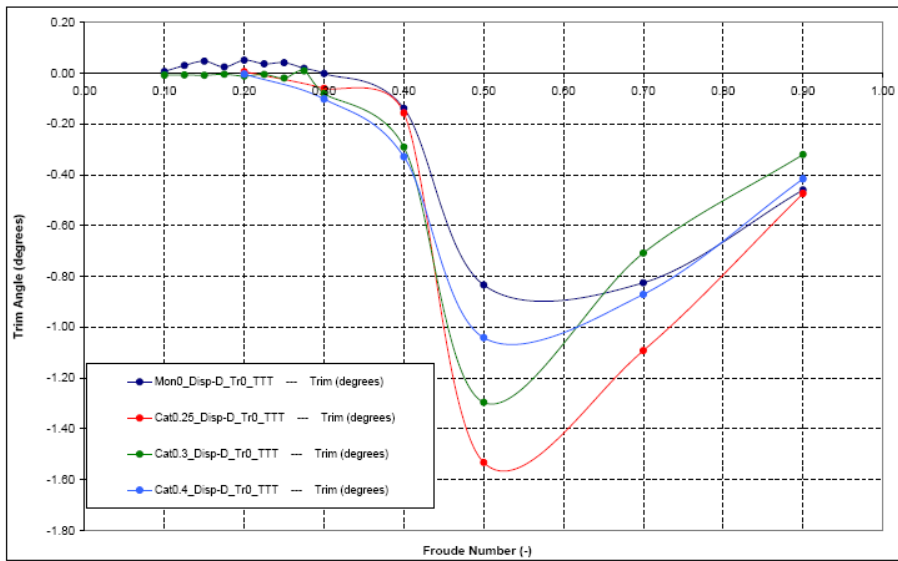


Figure 5.3: Example of the gathered towing tank test trim data

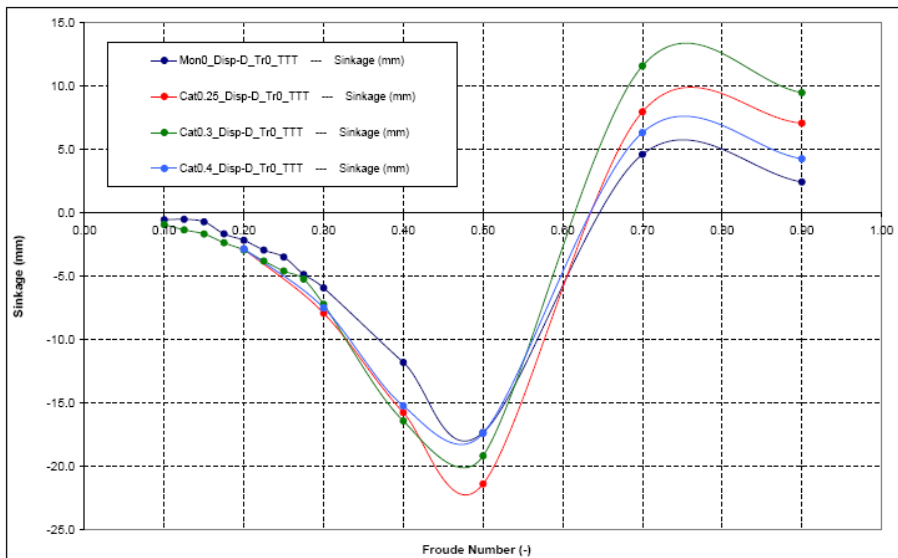


Figure 5.4: Example of the gathered towing tank test sinkage data

5.1.2 CFD Calculations

Computational fluid dynamics calculations are known to output the forces action tangential and perpendicular to the hull surface, which are the pressure and friction forces respectively. The total bare hull resistance is the sum of the components of these pressure and friction forces in the direction opposite to the velocity direction of the vessel.

$$R_{BH} = R_P + R_F \tag{5.1}$$

The subdivision of the pressure and friction resistance can be seen below, where the friction resistance and the total bare hull resistance is plotted. The difference between the total bare hull resistance and the friction resistance corresponds to the pressure resistance.

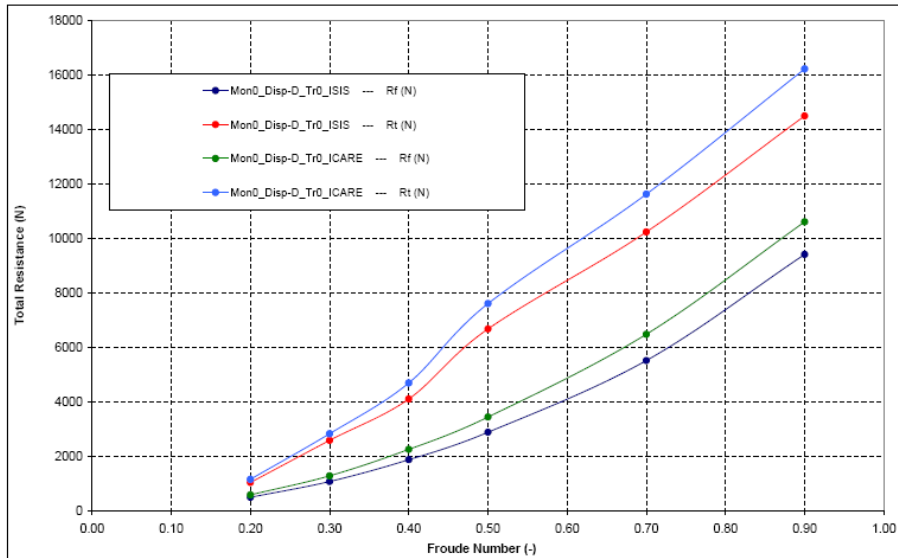


Figure 5.5: ISIS and ICARE results for friction and total resistance

Another comparison between the CFD packages can be seen in Figure 5.6, where the trim angle for the monohull and catamaran are plotted against the Froude number. They clearly show the same trends, but as for the resistance, there is a quantitative offset between the results of the two CFD packages.

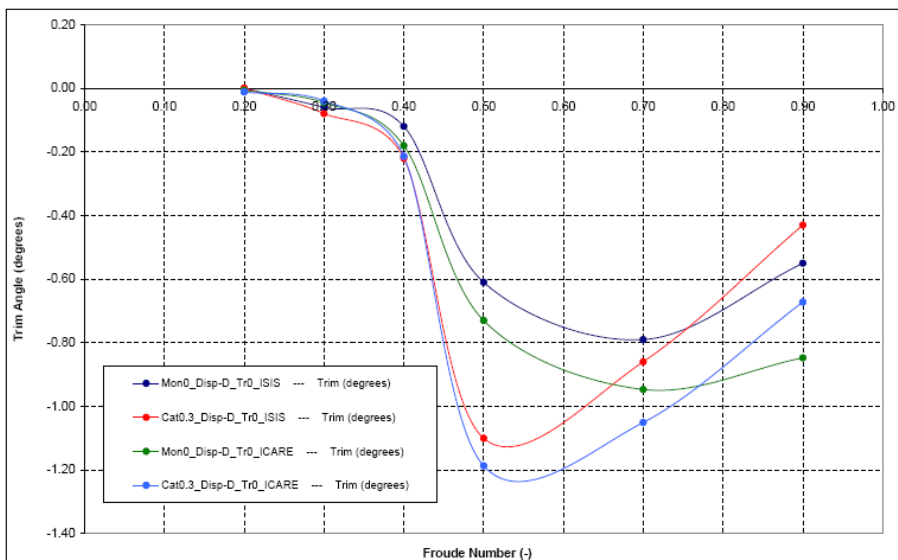


Figure 5.6: ISIS and ICARE trim angle for monohull and catamaran

5.2 Comparison

The trim angle and the sinkage values of the CFD and towing tank tests can be directly compared, without complex scaling. As said before, the CFD results show to same trend for the trim angle, while the towing tank results show a fastest re-trimming after the hump. At the hump it looks as the CFD is underestimating the trim angle, while overestimating it at a Froude number of 0.9.

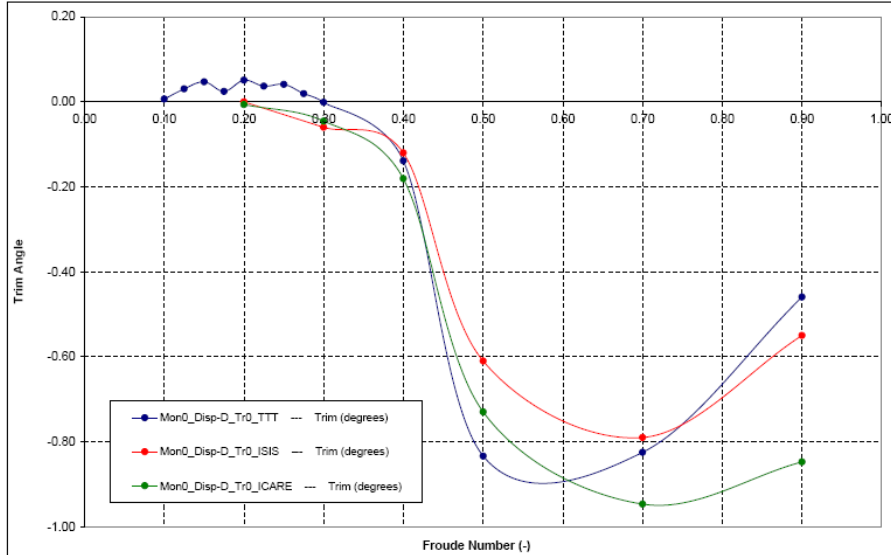


Figure 5.7: Comparison of trim angle between CFD and towing tank tests

The same trend in difference between the CFD results and the towing tank test results for the trim angle can be seen for the sinkage in even more exaggerated quantities. The CFD is underestimating the sinkage by 40 to 50% in displacement mode, while in the semi-displacement mode, wrongly describing the hydrodynamic lift at high speeds. This comes to no surprise as it is known that current CFD codes are able to give good predictions on resistance, but are less accurate on the determination of trim and sinkage.

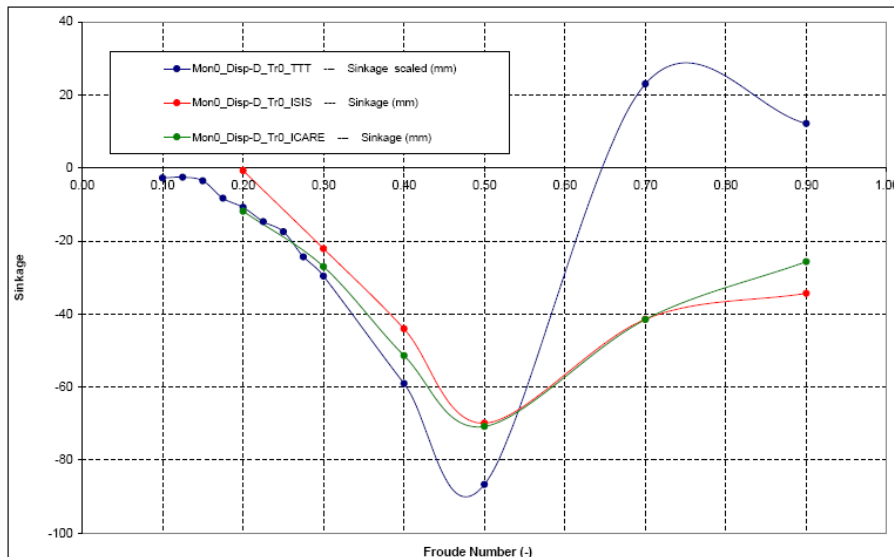


Figure 5.8: Comparison of sinkage between CFD and towing tank tests

5.3 Conclusion

An important fact to review is the constant value found for the friction coefficient of the turbulence strips. Finding a constant value for this coefficient is an important implication that the test method results in coherent results. This constant coefficient is taken into account in all the towing tank results, showing the importance of its coherent value.

Concerning the towing tank results, the most important thing to remember at this point is the clear trend of the hump drag with respect to the separation ratio. Such a consistent trend will ease the creation of an accurate regression formula for the estimation of the bare hull resistance. Furthermore, it was seen from the towing tank test results that the previous results of Molland showed inconsistencies between the monohull resistance and the catamaran resistance. At high speeds, the monohull and catamaran resistance converge to about the same value.

Further conclusions can be drawn for the CFD results when they are compared to the towing tank results. The trim angle and the sinkage of the CFD results do not seem to be very accurate. Especially at higher speeds, the differences are significant. How these differences reflect themselves in the resistance estimations has to be examined in the subsequent chapters concerning the form factor and the scaling between towing tank tests and full scale results.

6 Form Factor

For the scaling of resistance from model scale towards full scale, the form factor is a very important concept. Using the Froude analogy to scale the wave resistance, the form factor is required to accurately determine the wave resistance from the total bare hull resistance and the ITTC'57 determination of the skin friction. The concept of the form factor and its use will be elaborated in this chapter. Furthermore, the existing methods to determine the form factor will be explained, after which some existing estimation methods are proposed. The chapter will be finished by discussing the findings from the CFD data and the towing tank tests and the final conclusions concerning the form factor.

6.1 Definition

As seen in Figure 2.1, the friction resistance can be divided into the ITTC skin friction and form effects. Physically, this division can be explained by saying that the skin friction is the friction resistance of a flat plate of the same wetted surface area, while the form effect count for the friction resistance of the 3 dimensional shape of the body. These form effects are calculated by the use of the coefficient, i.e. the form factor.

$$R_{BH} = R_p + R_f = R_p + (1 + k) \cdot R_{F0} \quad [6.1]$$

Where: R_{F0} is the skin friction as defined in equation [2.4]
 $1 + k$ is the form factor

6.2 Form Factor Determination

The concept of the form factor was already set up in the previous section. The use of the form factor is a simplified way of implementing the magnitude of the resistance due to form effects as a percentage of the friction resistance. There exist different methods to determine the form factor. Each of these methods has their advantages and limitations as will be elaborated in the section.

6.2.1 Slow Speed Tests

The most used method to determine is the use of slow speed towing tank tests. With the results of these tests, two methods can be used to determine the form factor. Both methods, Prohaska's method and Hughes' method, will be elaborated in this section.

Prohaska's Method

The most common method applied is Prohaska's method, using slow speed towing tank tests to determine the form factor. The total resistance at low speeds can be described as given in the formula below from the ITTC (ITTC 7.5-02-02-01):

$$C_T(Re, Fn) = C_w(Fn) + (1 + k) \cdot C_{F0}(Re) \quad [6.2]$$

It is assumed that for low speeds (below $Fn = 0.2$) C_w is a function of Fn^4

The straight line plot of $\frac{C_T}{C_{F0}}$ versus $\frac{Fn^4}{C_{F0}}$ will intersect the ordinate ($Fn = 0$) at $(1 + k)$. This is a visual way to derive the form factor from the slow speed towing tank tests. This method is widely applied for slow speed vessels without immersed transoms. Its application to transom sterns is questionable because of the different flow regime in the transom area. Furthermore, with slender hulls, the drag at slow speed is so small as to be difficult to measure accurately. [Couser, 1997] For these slender hulls at these slow speeds, the flow can remain laminar, resulting in different resistance measurements.

Hughes' Method

Hughes' method uses the total resistance coefficient, plotted against the Reynolds number. For decreasing speed, this total resistance coefficient converges towards the friction resistance coefficient. From this friction resistance coefficient, the form factor can be deduced as shown in the figure below:

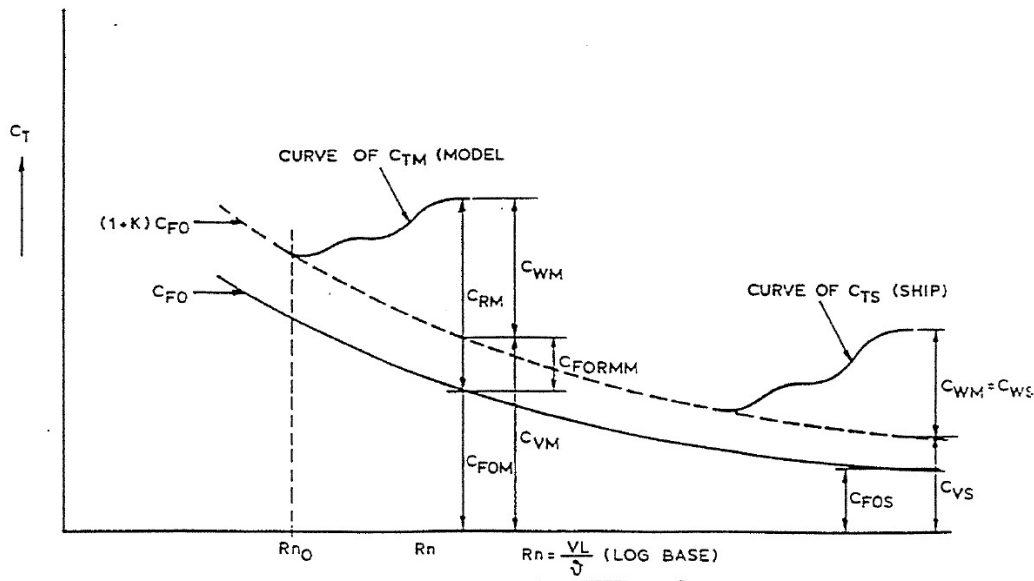


Figure 6.1: Hughes method of determining the form factor

With precise measuring results, these two methods should result in the same form factors. As the determination of the form factor with both methods is subjected to a large subjectivity, using both methods parallel help finding more objective results.

6.2.2 Computational Fluid Dynamics

Potential codes may be used to derive the pressure resistance due to inviscid flow characteristics. The boundary layer integral method can be used to estimate the boundary layer growth in areas separations does not occur. Full Reynolds averaged Navier Stokes (RANS) codes may be used to predict the flow where separation occurs. However, these methods are extremely computationally intensive. The form factor can then be determined by dividing the friction resistance results from the calculations by the ITTC skin friction.

$$R_{Fmon} = (1 + k_{mon}) \cdot R_{F0} \quad [6.3]$$

$$R_{Fcat} = (1 + k_{cat}) \cdot R_{F0} \quad [6.4]$$

6.2.3 Wind tunnel measurements

Wind tunnel experiments enable direct measurement of the viscous resistance since no free surface waves are generated. When using wind tunnel tests, Reynolds' analogy is used to scale the friction resistance from the wind tunnel model to the full scale vessel, resulting in very accurate friction resistance values. However, very careful consideration of the flow around the transom is required.

6.2.4 No free surface

By mirroring the vessel at the water line and calculating with CFD or testing in the towing tank, the influence of the free surface is eliminated and the total calculated or measured resistance is the viscous resistance. The form factor can then be calculated from following equation. Again the effects of separation at an immersed transom should be taken into account.

$$(1+k) = \frac{R_T}{R_{F0}} \quad [6.5]$$

Determination wave pattern resistance: By measuring the wave pattern resistance, it can be subtracted from the total resistance, leaving only the viscous resistance. Comparing the ITTC friction resistance and this viscous resistance, the form factor can be determined.

$$(1+k) = \frac{R_T - R_{WP}}{R_{F0}} \quad [6.6]$$

6.2.5 Full scale tests

By using both full scale tests and model tests (or more general tests at different scale) the form factor can be deduced from the equation [6.8]. This equation is simply found when eliminating the wave resistance from ITTC equations for ship and model found below:

$$R_{T_{ship}} = R_W + R_{F0_{ship}} \cdot (1+k) \quad \text{and} \quad R_{T_{model}} = R_W + R_{F0_{model}} \cdot (1+k) \quad [6.7]$$

$$\rightarrow \frac{R_{T_{model}} - R_{T_{ship}}}{R_{F0_{model}} - R_{F0_{ship}}} = (1+k) \quad [6.8]$$

6.3 Form Factor Estimation

There may exist different determination methods for the form factor, a single estimation method however doesn't exist. The magnitude of the form factor is difficult to estimate since there is no well based or generally accepted formulation known to describe it. From different researches, some values for monohulls and catamarans and will be discussed here.

6.3.1 Monohull

Different estimation methods for the form factor of monohulls are proposed in literature. They are summarized in this section, to show the extend of existing attempts to find that one accurate formulation.

Eight-oared rowing shells

When talking about rowing shells, two important things should be noted: it concerns very slender hulls without an immersed transom. For rowing shells, the length-displacement ratio is positioned somewhere

between 15 and 20: $15 < \frac{L}{\nabla^{1/3}} < 20$ [Scragg and Nelson, 1993]

$$k = 0.0097 (\theta_{entry} + \theta_{exit}) \quad [6.9]$$

Where: θ_{entry} is the half angle (in degrees) of the bow at the waterplane

θ_{exit} is the half angle (in degrees) of the stern at the waterplane

Delft Systematic Yacht Hull Series:

For the DSYHS, a large number of yacht hull forms were tested. Prohaska's method was used to determine the form factor as these yacht hulls didn't have immersed transoms. This resulted in very small

form factors in the range of 0.03 to 0.07. For the DSYHS it was therefore decided to leave this small resistance component into the residuary resistance.

Container Ships

This regression comes from [Holtrop, 1982] and can be used for container ships.

$$(1+k) = C_{13} \left(0.93 + C_{12} \left(\frac{B}{L_R} \right)^{0.92497} (0.95 - C_P)^{-0.521448} \left(1 - C_P + 0.0225 \frac{LCB_{mid}}{L_{WL}} \right)^{0.6906} \right) \quad [6.10]$$

Where: LCB_{mid} is the longitudinal position of the centre of buoyancy, forward of 0.5 L
 L_R is a parameter reflecting the length of the run according to:

$$\frac{L_R}{L_{WL}} = 1 - C_P + \frac{0.06 C_P \frac{LCB_{mid}}{L_{WL}}}{4 C_P - 1} \quad [6.11]$$

In the equation for the form factor, the constants are:

$$C_{12} = \left(\frac{T}{L_{WL}} \right)^{0.2228446} \quad \text{when } \frac{T}{L_{WL}} > 0.05$$

$$C_{12} = 48.20 \left(\frac{T}{L_{WL}} - 0.02 \right)^{2.078} + 0.479948 \quad \text{when } 0.02 < \frac{T}{L_{WL}} < 0.05 \quad [6.12]$$

$$C_{12} = 0.479948 \quad \text{when } \frac{T}{L_{WL}} < 0.02$$

$$C_{13} = 1 + 0.003 C_{stern} \quad [6.13]$$

Afterbody form	C_{stern}
V-shaped sections	-10
Normal section shape	0
U-shaped sections with Hogner stern	10

Table 6.1: Constants for Holtrop form factor determination

Holtrop Parameter Range				
0.55	<	C_P	<	0.85
3.90	<	L/B	<	14.9
2.10	<	B/T	<	4.00
0.05	<	Froude Number	<	1.00

Table 6.2: Parameter range for Holtrop form factor determination

6.3.2 Catamaran

Molland [Molland, 1994] started the research on a systematic catamaran series based on the existing parent hull form of the NPL series. As part of this research, Molland determined the form factor by subtracting the wave pattern resistance from the measured total resistance as seen in equation. The wave pattern resistance was determined by the use of a wave pattern analysis based on multiple longitudinal cuts.

$$R_{FO} \cdot (1+k) = R_{BH} - R_{WP} \quad [6.14]$$

The results differ for monohulls and catamarans. For the monohulls the form factor (1 + k) was in the range of 1.22 to 1.45 while for the catamarans it was higher in the range of 1.38-1.65 But this research was reviewed by Armstrong [Armstrong, 2000] where he claimed that these form factors contradict the expectation that long slender hull forms would have low form factor values. Armstrong [2000] remarks that the calculation of the form factor didn't took the transom resistance into account. Furthermore it should be noted that the models used by Molland were small (Lwl = 1.6m). At very low Froude numbers, the viscous effects are dominant, particularly for the small model hulls used in the experiments. These effects will be far less for full-scale vessels, meaning that the form factors for the full scale vessel could be a lot smaller than the ones stated by Molland.

In his publication, Schwertz [Schwetz, 2002] sites Armstrong [Armstrong, 2000], giving a regression formula in order to determine the form factor for model en full scale ships:

$$(1+k)_{model} = 1.45 - 0.139 \cdot \left(\frac{L}{\nabla^{1/3}} \right)^{0.6} \cdot \left(\frac{B}{T} \right)^{-0.1} \quad [6.15]$$

$$(1+k)_{ship} = 1.72 - f \cdot \left(\frac{L}{\nabla^{1/3}} \right)^g \cdot \left(\frac{B}{T} \right)^{-0.1} \quad [6.16]$$

Where:

$$1 \cdot 10^9 < Re < 2 \cdot 10^9$$

$$f = 2.25 \cdot Fn^2 - 4.47 \cdot Fn + 1.61 \quad \text{valid for } 0.6 < Fn < 1.0$$

$$f = 0.61 \quad \text{valid for } Fn > 1.0$$

$$g = 0.76 - 1.09 \cdot f$$

High speed catamarans: Couser [1997] compared form factor data from calculations of different researches and compared them with full scale tests. The data from the researches were corrected for transom stern effects. Assuming that the form factor remains constant with Froude number and demi-hull separation, he found that the primary geometric parameter for the form factor was the length-displacement ratio. This resulted in suggested form factors for high-speed, round bilge hull forms.

Couser, together with Molland and Armstrong, [Couser, 1997] reviewed the previous results obtained by Molland in order to correct the data for the influence of the transom resistance on the form factor. Their results are summarized in the Table 6.3:

$\frac{L_{wl}}{\nabla^{1/3}}$	Monohull Form factor	Catamaran Form Factor
6.3	1.35	1.48
7.4	1.21	1.33
8.5	1.17	1.29
9.5	1.13	1.24

Table 6.3: Suggested form factors according to Couser [1997]

6.4 Data Analysis

In this paragraph, the results from the CFD calculations and the towing tank tests will be presented and discussed.

6.4.1 Computational Fluid Dynamics

The method to determine the form factor from the CFD results was briefly mentioned before and is very straight forward. The form factor is found by dividing the friction resistance components, which is an exact value coming from the CFD, by the skin friction determined with the use of the ITTC correlation line.

$$R_{F_{mon}} = (1 + k_{mon}) \cdot R_{F0} \quad [6.17]$$

$$\rightarrow (1 + k_{mon}) = \frac{R_{F_{mon}}}{R_{F0}} \quad [6.18]$$

The found values of the form factor for the different configurations are very consistent and therefore, the mean values are presented here in Table 6.4. The different configurations include the three displacement configurations (light, design and heavy) and the trimmed configurations (bow down and bow up). This shows that for the tested hull form, it can be concluded that the form factor is not depending on the sinkage or trim angle. This fact will be used later on when discussing the form factor determination with the use of the towing tank tests.

Froude Number	ICARE $(1 + k_{mon})$	ISIS $(1 + k_{mon})$	Difference $1 - \frac{ISIS}{ICARE}$
0.20	1.167	0.988	0.154
0.30	1.202	1.007	0.162
0.40	1.235	1.030	0.166
0.50	1.247	1.046	0.161
0.70	1.255	1.068	0.149
0.90	1.287	1.136	0.117

Table 6.4: CFD form factor for monohull

From the above table, it can be seen that the ISIS results give form factors that are between 12 and 17 % smaller than those of ICARE. Some doubt could exist on the small form factors found with the use of ISIS. This fact will be discussed when these results are compared to the towing tank test results.

Froude Number	ICARE	ISIS	Difference
	$(1+k_{cat})$	$(1+k_{cat})$	$1 - \frac{ISIS}{ICARE}$
0.20	1.135	0.988	0.129
0.30	1.166	1.009	0.134
0.40	1.197	1.037	0.133
0.50	1.206	1.029	0.147
0.70	1.218	1.041	0.145
0.90	1.272	1.130	0.111

Table 6.5: CFD form factor for catamaran

In Table 6.5, the catamaran form factor is presented. These results differ from the monohull configurations, implying some kind of interference effect that will be discussed in chapter 8.4. The results of ISIS and ICARE seem to be closer in the case of the catamaran, resulting in differences between 11 and 15 %. Both the results for the monohull and catamaran configuration of ISIS and ICARE are shown in the plot below. Here it is clearly visualized that both methods tend to the same trend in form factor depending on the speed, but again, as was seen for the resistance values, an offset is present, resulting in higher values from ICARE.

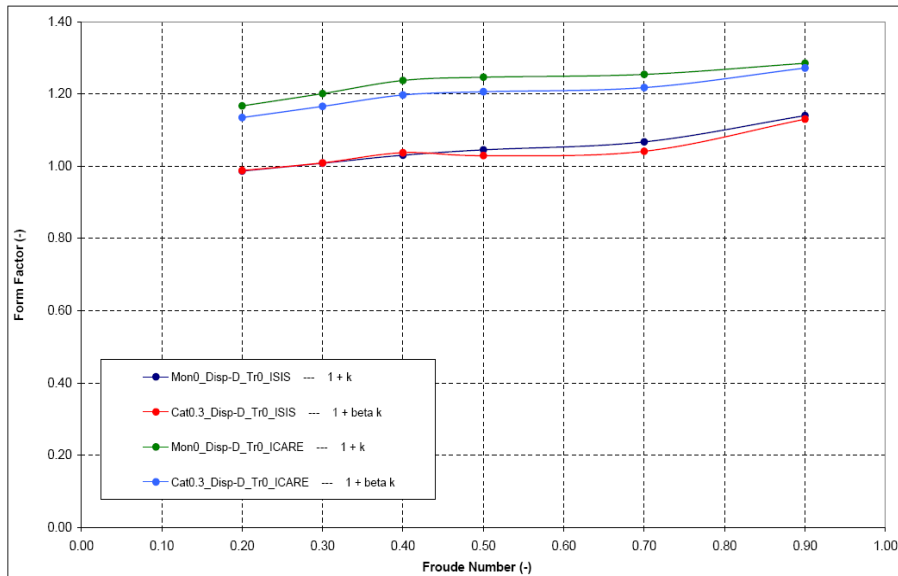


Figure 6.2: Form factor results from CFD

If the form factor is plotted for the different configurations, it can be seen that the form factor is quasi independent of the configuration except for the higher speeds. The fact that the form factor is independent of the trim angle or the displacement will be useful when determining the form factor from slow speed towing tank tests as will be elaborated in the following section.

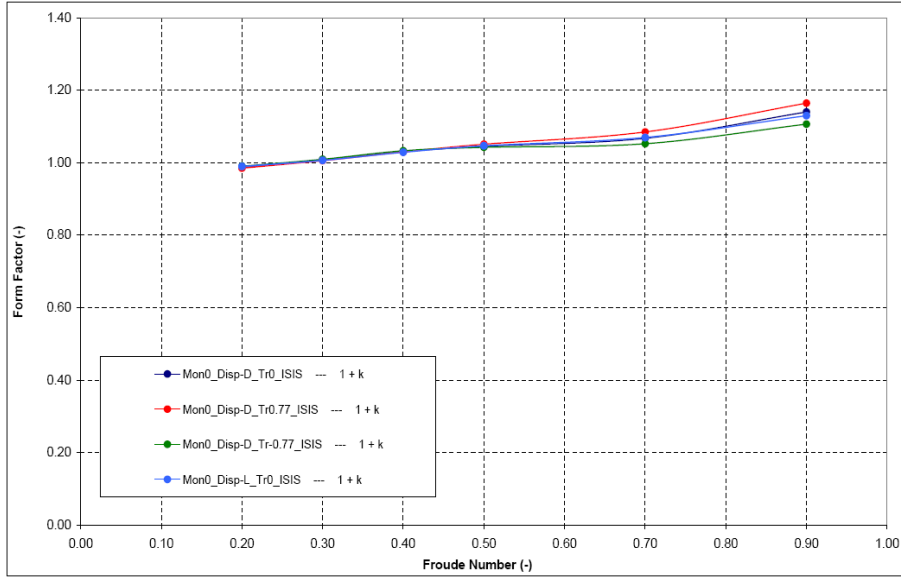


Figure 6.3: Form factor results from ISIS for different configurations

6.4.2 Towing Tank Tests

The Prohaska method presented before and equation [6.2] will be used to determine the form factor. However, caution should be taken as the value of total resistance coefficient C_T , as defined in the equation of the ITTC, is actually calculated from the bare hull resistance, therefore, the form factor will be determined with the following formula for the total resistance coefficient:

$$C_T = \frac{R_{BH}}{\frac{1}{2} \rho V^2 S_c} \quad [6.19]$$

The configurations tested for the form factor determination are found in Table 4.5. The build-up of this matrix is mainly used to study the influence of the immersed transom on the form factor for both the monohull and catamaran configurations. Secondly the hull form with and without tunnel for the propeller is tested to examine its influence on the form factor.

Slow Speed Test Results

In order to analyse the slow speed test results,

$$R_{BH} = R_w + R_{TR} + R_F \quad [6.20]$$

For both the catamaran and monohull configurations, the following formula is valid, including the interference effects as shown in chapter 2.2 and explained fully in chapter 8. In this equation, an extra value is added in order to take into account the resistance of the immersed transom in the slow speed tests.

$$R_{BH} = \tau \cdot R_w + (1 + \beta \cdot k_{mon} \cdot X) \cdot R_{F0} \quad [6.21]$$

Where: X takes into account the resistance component of the immersed transom in the form factor towing tank tests
 $X = 1$ without immersed transom
 $\beta = 1$ and $\tau = 1$ for the monohull

Results from Prohaska plot and the Hughes plot give similar results as is expected. The Prohaska results for $(1 + \beta \cdot k_{mon} \cdot X)$ are found in the tables below:

	Trim (degrees)	0.000	1.337	2.591
	s / Lwl (-)			
Mono	1.0	1.410	1.120	1.045
Cata	0.5	1.565	1.105	1.060
Cata	0.3	1.510	1.138	1.080

Table 6.6: Measured values for the hull with tunnel: $(1 + \beta \cdot k_{mon} \cdot X)$

	Trim (degrees)	0.000	1.337	2.591
	s / Lwl (-)			
Mono	1.0	1.493	-	1.038
Cata	0.5	1.489	-	1.087
Cata	0.3	1.501	-	1.101

Table 6.7: Measured values for the hull without tunnel: $(1 + \beta \cdot k_{mon} \cdot X)$

Form Factor Results

Because of the hull shape with an immersed transom, the form factor is determined from the bow down trimmed configuration where the transom runs clear at all low speeds. One may imply that this method is not valid, as the trimmed configuration shows different characteristics than the configuration at zero trim. However, the characteristics of the flow around the vessel not changed severely due to the use of the U-sections. These sections near the bow are characterized with their parallel side walls, which means that the entrance angle at the bow isn't changed with changing trim. The fact that the form factor is not changed by the changing trim angle is shown by the form factor results of the CFD calculations (Figure 6.3). The configuration with the bow trimmed down 2.591 degrees makes the transom run clear and can be assumed to be the form factor without transom resistance component ($X = 1$):

		With tunnel	Without tunnel
	s / Lwl (-)		
Mono	1.0	1.045	1.038
Cata	0.5	1.060	1.087
Cata	0.3	1.080	1.101

Table 6.8: Form factor without transom resistance component: $(1 + \beta \cdot k_{mon})$

Table 6.8 shows, as was seen from the CFD results, a form factor that consists of very small values. They even seem too small to be valid. However, when looking to the history of the correlation lines, it can be seen that Hughes proposes the following friction line for the determination of the skin friction:

$$C_{F0_{HUGHES}} = \frac{0.067}{(\log_{10} Re - 2)^2} \quad [6.22]$$

When comparing this to the correlation line proposed by the ITTC (equation [2.5]), it can be seen that the ITTC already incorporates a form factor of 12 % on top of the Hughes friction line, explaining the possibility of finding very low form factors when using the skin friction coefficient of the ITTC.

6.4.3 Comparison

In the following figure, the comparison between the CFD results and the towing tank tests can be found.

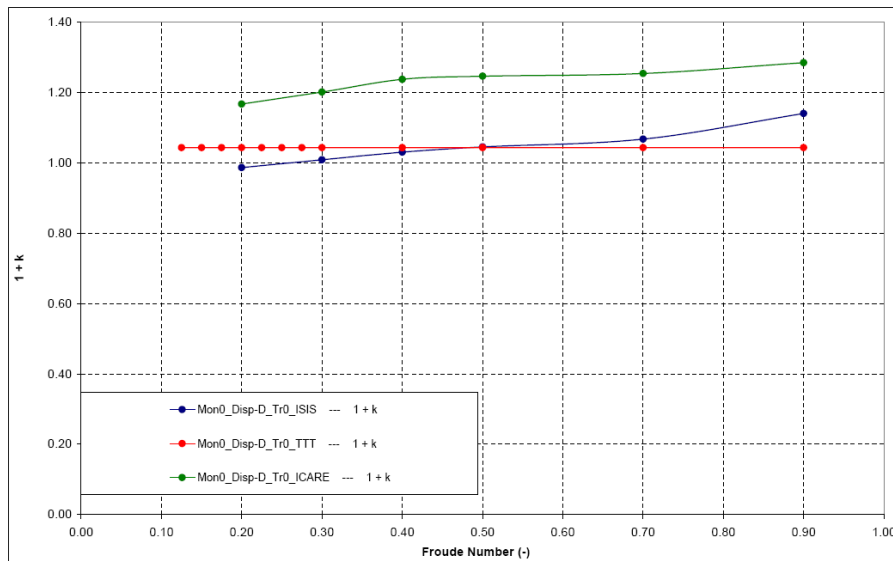


Figure 6.4: Form factor comparison

It can be observed that the form factor determined with the ISIS results come in close comparison with the result from the towing tank test, with the single difference that the towing tank test form factor is independent on the speed, while the CFD form factors increase in value for increasing speeds.

For a hull form with a length-displacement ratio of 8, Couser [1997] finds a form factor of 1.19 from the Molland data after correction for the immersed transom stern. When comparing this to 1.04 found in this research for the hull shape without tunnel, questions should be posed concerning the determination of the wave pattern resistance and the size of the towing tank models.

6.5 Conclusion

There are two important and interesting conclusions to be found from this chapter. Two similarities are found between towing tank tests and the CFD data for a hull form with a length-displacement ratio of 8. First of all, the towing tank tests performed during this project and the ISIS calculation results deliver small form factor in the range of roughly 1.00 – 1.14. The second similarity is the resemblance between the ICARE form factor results and the form factors found by Couser and Molland, which lay roughly in the range of 1.15 – 1.30. It has to be concluded that the towing tank tests in this research are more accurate than the data from Couser and Molland, as in this research, the immersed transom is eliminated. This results in the fact that the ISIS result are more accurate than the ICARE results for the determination of the form factor. This seems logical, as ICARE has difficulties of simulating the flow at the transom. The differences between the form factor for the monohull configuration and the catamaran configuration need to be studied to determine the interference effects that are part of the friction resistance. Furthermore, more research towards the effects of the immersed transom on the form factor is required. Both topics will be discussed in the following chapters.

7 Scaling Results

Scaling methods are a very important part of this research, as the towing tank results need to be scaled to full scale and even the CFD results require scaling if vessels of different length are studied. Three methods will be used and compared here. First, scaling will be done without the use of the form factor and afterwards, two different form factors will be used, respectively the form factor determined with immersed transom and the form factor determined from the trimmed model. All three methods will be compared to draw some conclusions at the end of this chapter.

7.1 Scaling Methods

In this section, the two applied scaling methods will be elaborated, showing the difference in theory between the method using the form factor and the method without using the form factor.

7.1.1 Without Form Factor

When towing tank tests are performed on a hull, the resistance measured on the towing instruments is the total hull resistance. When we consider towing a bare hull, this total resistance is the total bare hull resistance discussed in this chapter. Because other resistance components are difficult to measure, the definition of the residuary resistance comes into play. The residuary resistance is found by subtracting the skin friction from the bare hull resistance, because the skin friction is an easy calculated value. Therefore the residuary resistance is:

$$R_R = R_{BH} - R_{F0} \quad [7.1]$$

The skin friction is determined from the skin friction coefficient and the wetted surface area. This skin friction actually is not the skin friction of the hull tested, but of a flat plate with an equivalent wetted surface area.

$$R_{F0} = \frac{1}{2} \rho V^2 S_c C_{F0} \quad [7.2]$$

The skin friction coefficient of the equivalent flat plate is calculated with the well-known ITTC'57 equation [ITTC, 2002]:

$$C_{F0} = \frac{0.0075}{(\log(Re) - 2)^2} \quad [7.3]$$

Once the residuary resistance is known, it can also be made dimensionless in order to scale the total resistance to the full scale vessel. There are two different ways of making this resistance component dimensionless. The most common method used is:

$$C_R = \frac{R_R}{\frac{1}{2} \rho V^2 S} \quad [7.4]$$

There is a second method for making the residuary resistance dimensionless. This method is applied by Gerritsma and Keuning ea. for the DSYHS, where they made use of the displacement of the vessel in stead of the wetted surface area:

$$C_R = \frac{R_R}{\nabla_c \rho g} \quad [7.5]$$

Using this separation of the bare hull resistance components, the form effects and viscous pressure resistance are covered by the residuary resistance. This means that the difference between the skin friction and the friction resistance will be taken into account by the residuary resistance and for this reason, the frictional resistance of the flat plate or skin friction is often referred to as simply the friction resistance as also will be done in the rest of this report. In the equations, the difference can still be seen by the subscript 0 implying the friction resistance of the flat plate or skin friction.

7.1.2 With Form Factor

When the form factor is determined as described in the previous chapter, it can be used for scaling the towing tank test results to the full scale resistance.

$$R_W = R_{BH} - (1 + k) \cdot R_{F0} \quad [7.6]$$

When using a smooth hull, where no separation occurs and no immersed transom, the pressure resistance approaches the wave resistance. This results in the above equation, which is the equation most often found in the literature. As this research is based on a hull form with an immersed transom and two kinds of form factors were found, both form factors will be used for the scaling. Equation [7.6] gives the determination of the pressure resistance which includes the transom resistance as the form factor is found from the trimmed configuration eliminating the immersed transom, while equation [7.7] is used to determine the wave resistance from the form factor determined with an immersed transom.

$$R_P = R_{BH} - R_F = R_{BH} - (1 + k) \cdot R_{F0} \quad [7.7]$$

$$R_W = R_{BH} - R_F = R_{BH} - (1 + k \cdot X) \cdot R_{F0} \quad [7.8]$$

These formulae are applicable for the monohull configuration, as the viscous interference factor needs to be added in the case of the catamaran resistance. The applied form factor for both of the above equations, then become:

$$(1 + k \cdot \beta) \quad \text{and} \quad (1 + k \cdot \beta \cdot X) \quad [7.9]$$

7.2 Skin Friction

In order to study the scaling methods, the results of each method will be plotted against the full scale resistance determined with both CFD packages, ICARE and ISIS. When the skin friction is determined with the use of the ITTC'57 correlation line, and no form factor is used as explained above, only the skin friction coefficient is scaled, while the residuary resistance coefficient remains constant for both scales. The results of this scaling method can be seen in Figure 7.1.

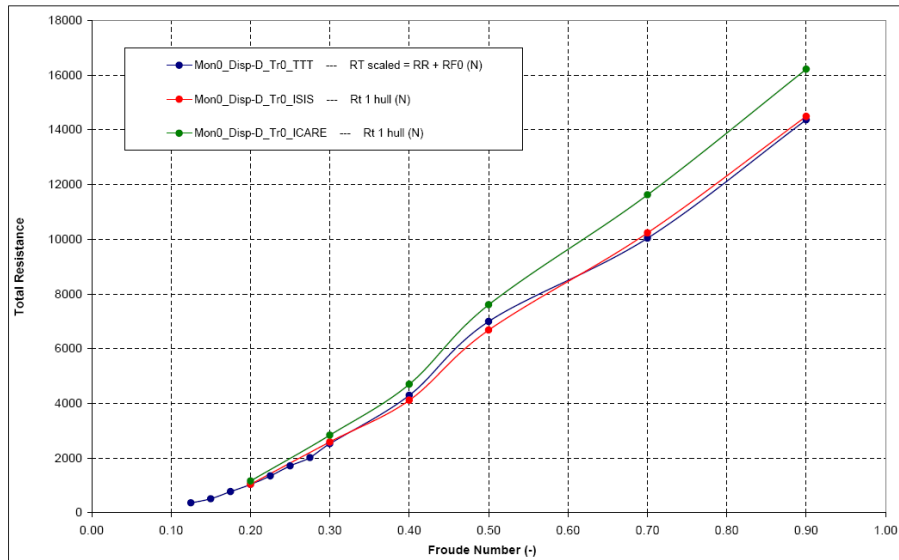


Figure 7.1: Scaling of towing tank results without the form factor

From these results, different issues can be discussed. First of all, it can be stated that both ISIS calculation results and the scaled towing tank test results are very similar. Knowing that the towing tank results precisely simulate the wave system and thus the progression of the resistance curve, it can be concluded that ISIS underestimates the wave system at the hump and overestimate its effect at higher speeds. ICARE gives the same trend, but with a consistent 12 - 14% of overestimation of the total bare hull resistance. Both CFD methods have the same dynamic wetted surface areas, and as a result this means that ICARE uses a different and probably less accurate method of calculating friction forces and the turbulence.

7.3 Friction Resistance with Transom Resistance

Form factors that were determined from slow speed towing tank tests with an immersed transom were found to be up to 48 % larger. For the hull with tunnel for example, the form factors with immersed transom was found to be 35 % larger than the trimmed hull without immersed transom:

$$\frac{(1+k \cdot X)}{(1+k)} = \frac{1.410}{1.045} = 1.35 \quad [7.10]$$

The resulting form factor is too large, meaning that a too large part of the total resistance is subject to the scaling as function of the Reynolds Number. This results in a scaled resistance, which severely underestimates the full scale resistance as can be seen in Figure 7.2.

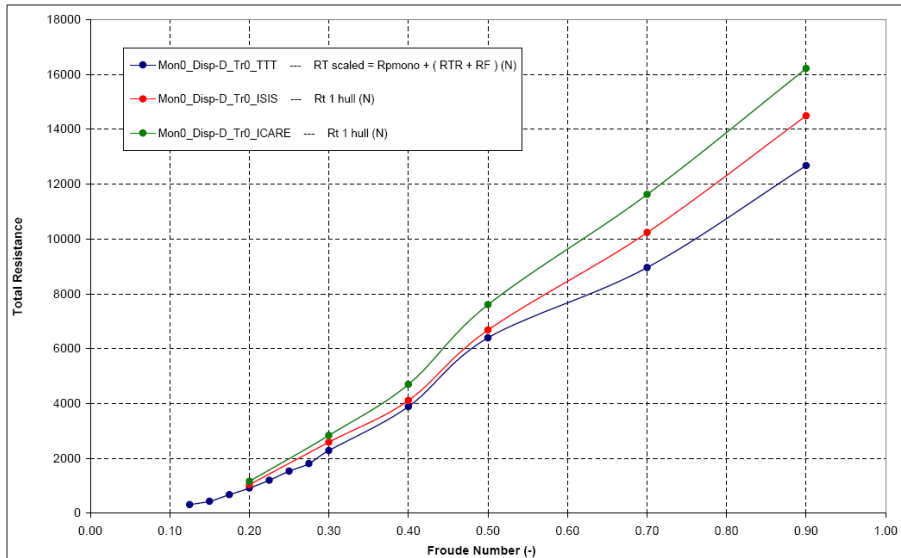


Figure 7.2: Scaling of towing tank results with the form factor determined with immersed transom

7.4 Friction Resistance

When the form factor is deducted from the hull trimmed to eliminate the immersed transom, a more clear view of the actual friction resistance presents itself. Due to the small value of the form factor, this results in approximately the same conclusions as for the case where no form factor was used (paragraph 7.2).

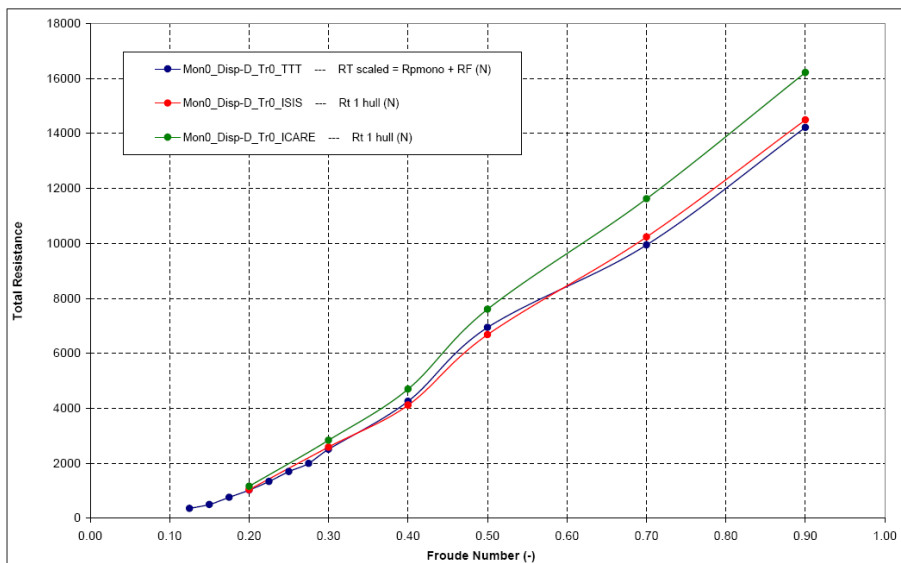


Figure 7.3: Scaling of towing tank results with the form factor

To give a better view on the differences between these results, the separate results for the pressure resistance and the friction resistance are given in the following plots.

The first thing that can be noticed from the friction resistance figure is the close similarity of the scaled towing tank friction resistance and the results from ISIS, except for the highest speed. This trend is also visual in the plot of the pressure resistance, but the inverse happens at the highest speed, resulting in a very close resemblance for the total resistance as seen above. The pressure resistance however is slightly underestimated at Froude 0.4 and 0.5, explaining the higher hump drag of the towing tank results for the total bare hull resistance.

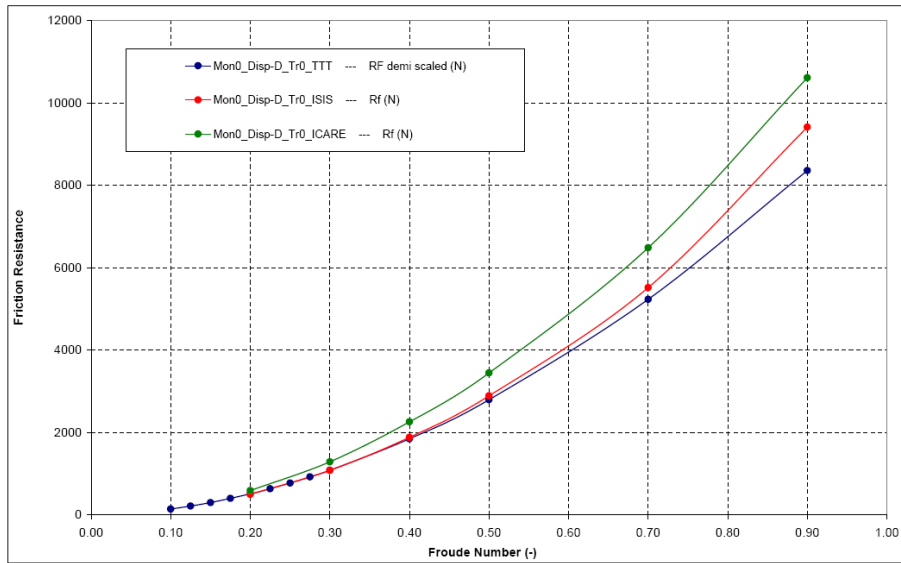


Figure 7.4: Friction resistance scaling

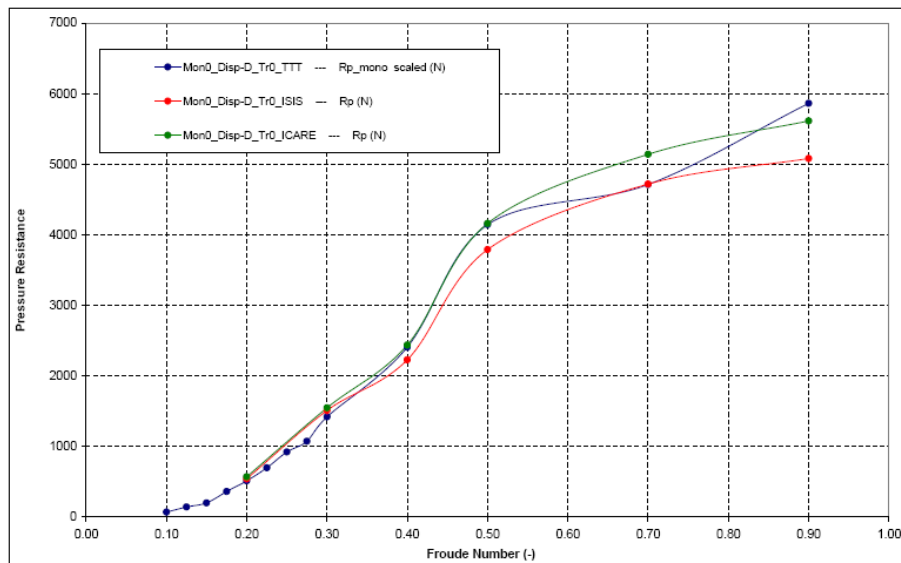


Figure 7.5: Pressure resistance scaling

7.5 Comparison

The three scaling methods are compared here to the ISIS CFD results to get a better understanding of the differences between the three methods. In this comparison, it is not to goal to discuss good or bad estimation methods for the bare hull resistance, as there is not quantitative correct value available. This comparison is used to elaborate on which method could be the most applicable method for the estimation of the bare hull resistance of slender hulls in monohull and catamaran configuration.

As can be seen from the graphs below, both the monohull configuration and the catamaran configuration result in the same trends between the different estimation methods, with a slightly larger pronounced difference between the different methods.

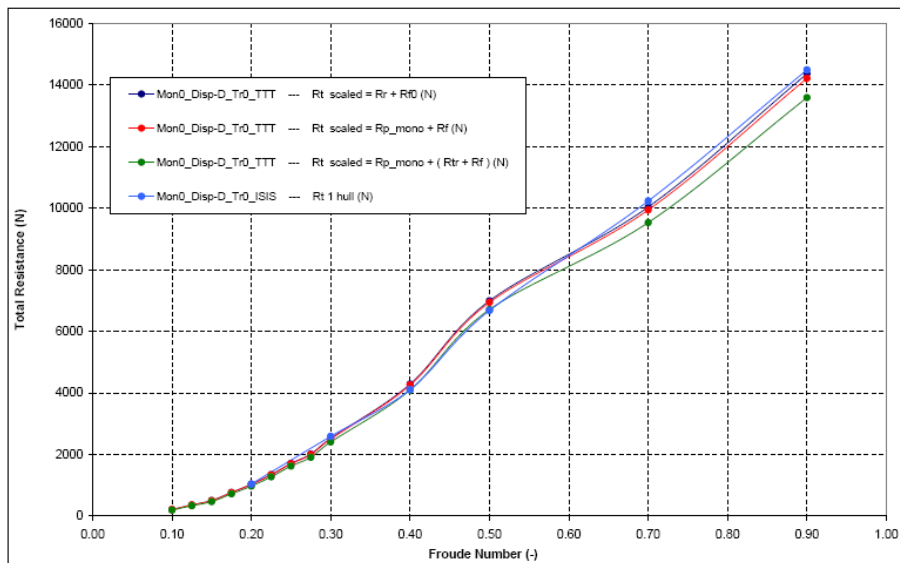


Figure 7.6: Scaled bare hull resistance of the monohull configuration

Using the residuary resistance, without the use of the form factor, the full scale result gives a small overestimation with respect to the resistance based upon the friction resistance, where the form factor is used. When using the form factor that includes the transom effects, the results are clearly underestimated.

As known, results are more accurate when using the form factor, however, with these small values for the form factor, also scaling without the form factor results in an acceptable precision. It could even be said to be beneficial not to use the form factor in order to keep the scaling as simple as possible and use the overestimation as a small factor of safety.

This method can prove to be useful for hull forms of which the form factor isn't known. At the same time, this method can be used for hull forms without U-shaped sections at the bow and a transom stern. The form factor of these hull forms can't be determined with the bow down towing tank tests, as the flow phenomena will change when changing the trim angle. Therefore, a method without form factor is easy to apply.

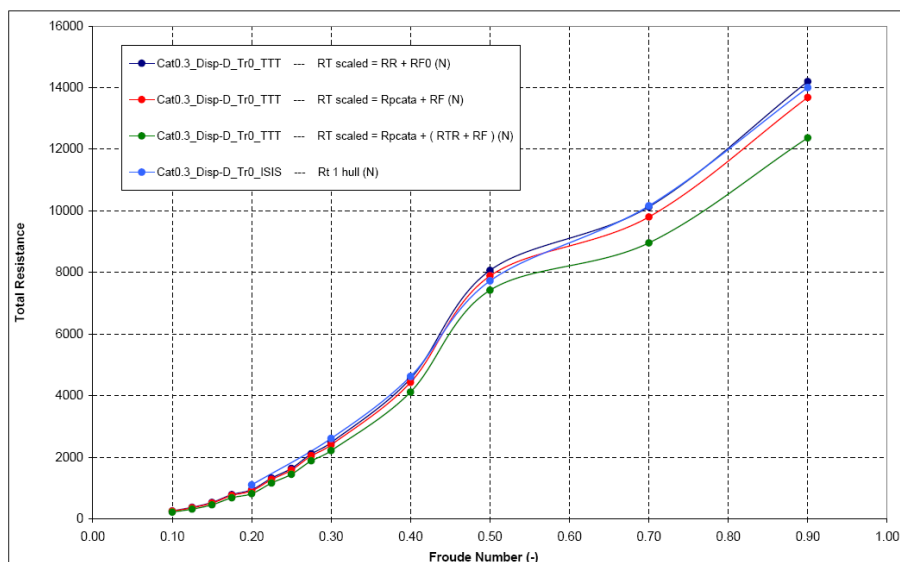


Figure 7.7: Scaled bare hull resistance of the catamaran configuration

7.6 Conclusions

Looking at the results of the different estimation methods, including scaling towing tank tests and full scale CFD calculations, several conclusions can be made.

First of all, it is shown that both the ICARE results and the scaled results based on the form factor with transom stern effects, are distant from the rest of the results, implying that they are less accurate.

Next to the fact that the ISIS results show a slight different trend in hump resistance and high speed resistance, the two scaling methods, one without the use of the form factor, the other with its use, and the ISIS calculations are within 2 - 3 % of each other, which can be defined as very accurate. From this it can be said that ISIS delivers very satisfactory results and that due to the small value of the form factors, its use could be neglected for these slender hull forms.

8 Interference Resistance

As this entire research turns around the resistance of catamarans, it is logical that the interference resistance between the two hulls will be discussed elaborately. In the first section, the total interference resistance and total interference factor will be defined and explained. In the following section 8.2, the total interference resistance will be divided into components, which will be elaborated. Results from previous researches will be discussed, and finally, the different interference resistance components will be estimated from CFD calculations and towing tank tests.

8.1 Definition

The interference resistance can be defined as the increase in resistance due to the hull of the catamaran being in close proximity to each other. This resistance can be quantified as the total interference resistance, or as a factor, describing the ratio between the resistance of the catamaran hull with respect to that of equivalent monohull. Both terms will be explained briefly in this section.

8.1.1 Total Interference Resistance

The total interference resistance can be determined by the use of CFD calculations or towing tank tests and is then defined as the difference in resistance of the catamaran, and twice the resistance of one of the hulls tested as monohull.

$$R_{Icat} = R_{Tcat} - 2 \cdot R_{Tmon} \quad [8.1]$$

When using the ITTC '57 formula for the skin friction, this equation can also be written as:

$$R_{Icat} = R_{Rcat} - 2 \cdot R_{Rmon} \quad [8.2]$$

Where: R_{Rcat} is the residuary resistance of the catamaran
 R_{Rmon} is the residuary resistance of one demi-hull

8.1.2 Total Interference Factor

In order to study the total interference resistance of a number of different catamarans, the total interference factor is used. It is a dimensionless parameter, giving the relation between the residuary resistance of the catamaran and twice the residuary resistance of one of the demi-hulls:

$$F_{Icat} = \frac{R_{Rcat}}{2R_{Rmon}} \quad [8.3]$$

8.2 Components

For catamarans, the presence of two hulls nearby causes additional resistance components due to interference effects. When the overall resistance increase is defined as the total interference resistance as mentioned above. Furthermore, this total interference resistance can be divided into two important interference resistance components as listed below [Müller-Graf, 1997]:

- The wave pattern resistance increment due to the superposition of the inner bow and stern waves.
- The frictional resistance increment due to the increased velocity at the inner underwater sides of the hulls.

[Pham, 2001] sites Insel and Molland [Insel, 1992] in order to determine these interference resistance components. The monohull total resistance coefficient is defined as:

$$C_{T_{mon}} = C_{W_{mon}} + (1 + k_{mon}) C_{F_0} \quad [8.4]$$

When this equation is applied for the catamaran, it results in:

$$C_{T_{cat}} = C_{W_{cat}} + (1 + k_{cat}) C_{F_0} \quad [8.5]$$

Combining both equations and adding the different interference component factors, the total catamaran coefficient can be written as:

$$C_{T_{cat}} = \tau C_{R_{mon}} + (1 + \phi k) \sigma C_{F_0} \quad [8.6]$$

Where: τ is the hull interference factor
 ϕ takes into account the change in the pressure field around the demi-hull
 σ takes account for the velocity augmentation between the hulls

For practical purposes, ϕ and σ can be combined into a viscous resistance interference factor β :

$$C_{T_{cat}} = \tau C_{R_{mon}} + (1 + \beta k_{mon}) C_{F_0} \quad [8.7]$$

Where: β is the viscous interference factor

8.3 Existing Research

Not a lot of information on the interference factors is available in literature. Two researches discussing the same results will be very briefly mentioned her.

Molland

In his research, explained before in this report, Molland used the monohull and catamaran form factor data to calculate the viscous interference factor is explained above. Molland presents all his results, but does not give conclusion on the results of the viscous interference factor.

Couser

After Couser and Molland, [Couser, 1997] reviewed the results for the form factor, they also published the results they found for the viscous interference factor. These results are summarized in the table below:

$\frac{L_{wl}}{\nabla^{1/3}}$	Monohull Form factor	Catamaran Form Factor	Viscous Interference Factor	Form Factor Increase
	(1 + k)	(1 + β k)	β	%
6.3	1.35	1.48	1.371	9.63
7.4	1.21	1.33	1.571	9.92
8.5	1.17	1.29	1.706	10.26
9.5	1.13	1.24	1.846	9.73

Table 8.1: Suggested form factors and corresponding viscous interference factor from Couser [1997]

These viscous interference factors result in an increase of the form factor of about 10 %.

8.4 Data Analysis

In this section the different interference factors will be discussed and the differences between the towing tank results and the CFD results will be compared.

8.4.1 Total Interference Factor

The definition of the total interference resistance was given in equation [8.3]. This method is valid for application on both the CFD results as on the towing tank test results.

In Figure 8.1, the towing tank test results for the total interference factor are presented to study their trend as function of the separation ratio.

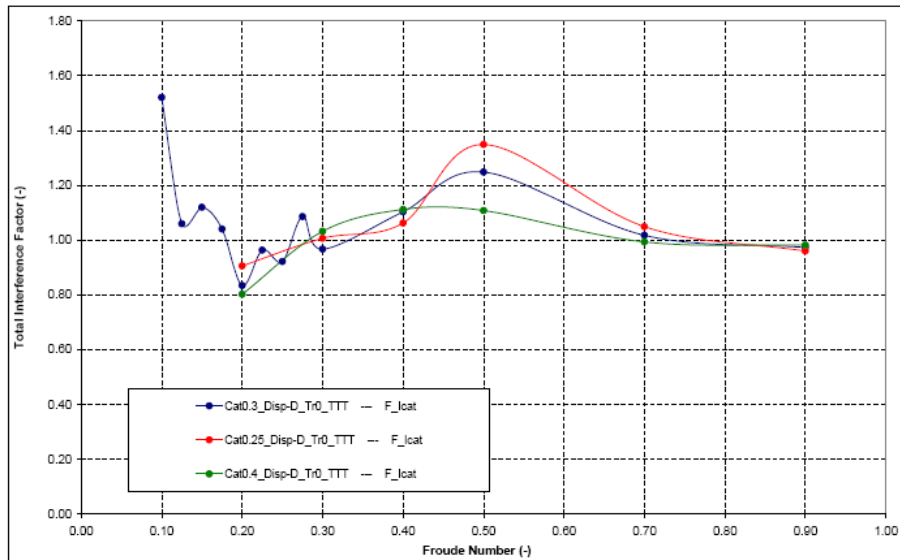


Figure 8.1: The total interference resistance factor as a function of the separation ratio

From Froude number 0.5 and upwards, the trend with respect to the separation ratio is clearly visible, with the highest interference for the smallest separation, as can be expected. However, at lower speeds, the trends become less clear due to the oscillating nature of the interference. This probably depend on the wave length of the wave system at low speeds and the separation ratio.

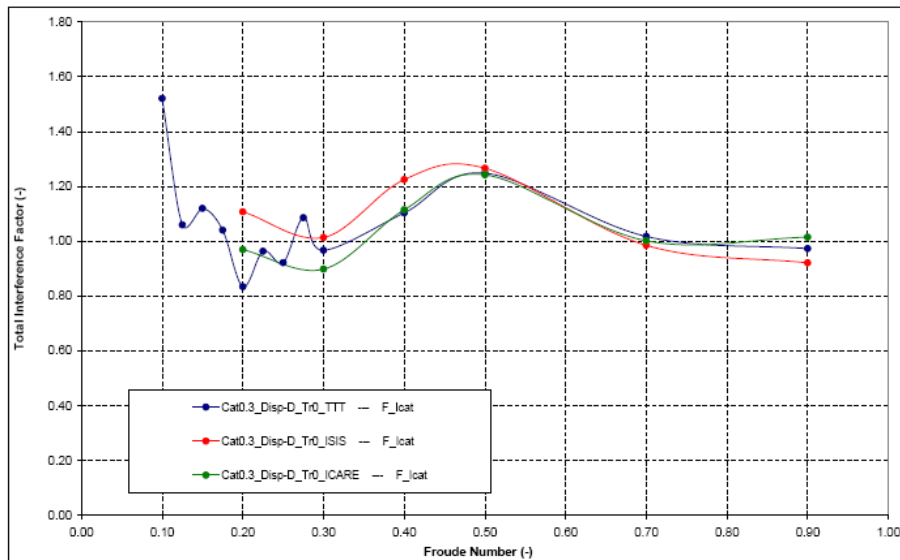


Figure 8.2: Total interference factor

8.4.2 Viscous Interference Factor

The viscous interference factor is a measure for the increase of friction resistance due to the higher speed of the flow between the two hulls. It is expressed as a part of the form factor. In this section, an explanation will be given on how to define this factor from the towing tank tests results and the CFD calculations, after which a comparison will be given.

Computational Fluid Dynamics

With the use of CFD calculations, the monohull and catamaran form factor and as a result, the viscous interference factor can be calculated from for each speed. How the form factor is calculated is already explained in chapter 6.2. Equation [6.3] can be rewritten as:

$$(1+k_{mon})=\frac{C_{Fmon}}{C_{F0}} \quad [8.8]$$

$$\rightarrow k_{mon}=\frac{C_{Fmon}-C_{F0}}{C_{F0}} \quad [8.9]$$

The same thing can be done for the catamaran test results::

$$(1+k_{cat})=\frac{C_{Fcat}}{C_{F0}} \quad [8.10]$$

Where: $k_{cat}=\beta k_{mon}$

$$k_{cat}=\frac{C_{Fcat}-C_{F0}}{C_{F0}} \quad [8.11]$$

$$\rightarrow \beta=\frac{k_{cat}}{k_{mon}}=\frac{C_{Fcat}-C_{F0}}{C_{Fmon}-C_{F0}} \quad [8.12]$$

The results found from the ISIS and ICARE CFD calculations are summarized below:

Froude Number	Monohull Form factor	Catamaran Form Factor	Viscous Interference Factor
	$(1+k_{mon})$	$(1+k_{cat})=(1+\beta k_{mon})$	β
0.20	1.167	1.135	0.807
0.30	1.201	1.166	0.824
0.40	1.237	1.197	0.831
0.50	1.246	1.206	0.837
0.70	1.254	1.218	0.856
0.90	1.285	1.272	0.954

Table 8.2: Form factors and corresponding viscous interference factor from ICARE

Froude Number	Monohull Form factor	Catamaran Form Factor	Viscous Interference Factor
	$(1 + k_{mon})$	$(1 + k_{cat}) = (1 + \beta k_{mon})$	β
0.20	0.987	0.988	0.882
0.30	1.008	1.009	1.111
0.40	1.030	1.037	1.235
0.50	1.045	1.029	0.646
0.70	1.067	1.041	0.612
0.90	1.140	1.130	0.929

Table 8.3: Form factors and corresponding viscous interference factor from ISIS

From the results from ISIS, it can be seen that, due to the small form factors, the even small changes in catamaran form factor result in large variations in viscous interference factors.

Towing Tank Tests

because the slow speed towing tank tests result in one form factor for each configuration which is independent of the speed, also one viscous interference factor is to be found.

		Tunnel	No tunnel	Tunnel	No tunnel
	$s / Lwl (-)$	$(1 + \beta \cdot k_{mono})$		β	
Mono	1.0	1.045	1.038	1.000	1.000
Cata	0.5	1.060	1.087	1.333	2.302
Cata	0.3	1.080	1.101	1.778	2.672

Table 8.4: Viscous interference factor

Due to small form factor values, small errors in form factor determination might be reflected in large deviations in viscous interference factor and thus result in an uncertainty of the exact value of the viscous interference factor.

Comparison

First of all, it is useful to compare the form factor of the catamaran configuration, including the viscous interference factor, as this is the basis for the determination of the viscous interference factor. The towing tank form factor for the catamaran configuration is found to be within the range of the speed dependant form factor found from ISIS, while the ICARE catamaran form factor is found to be higher.

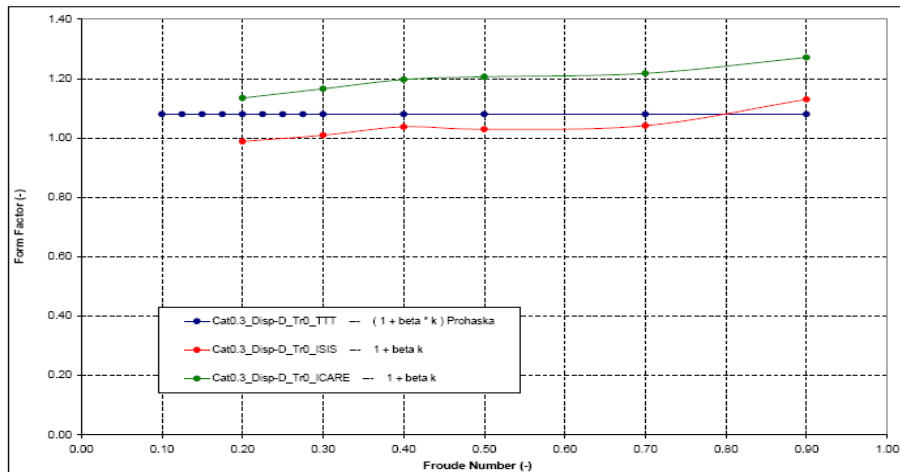


Figure 8.3: Form factor with viscous interference factor $(1 + \beta \cdot k)$

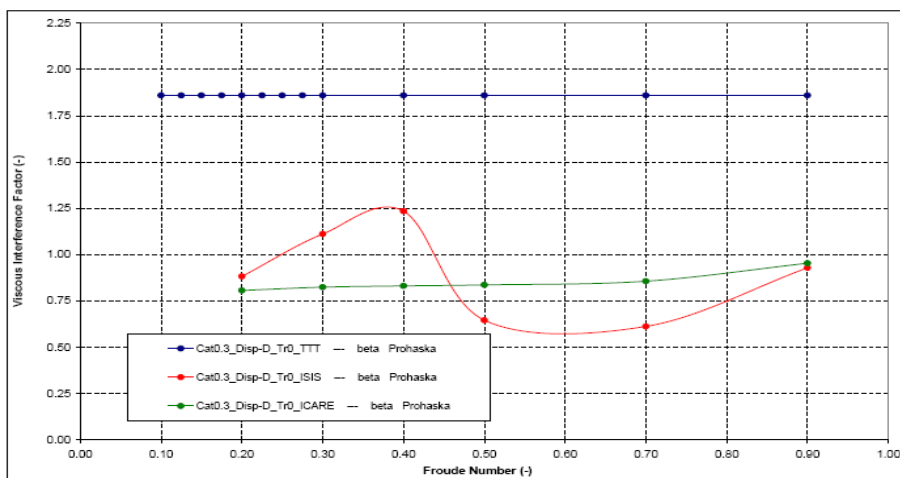


Figure 8.4: Viscous interference factor β

The two most important conclusions that can be taken is that fact that the CFD results show a slightly negative viscous interference factor, while the towing tank tests result in a very high positive viscous interference factor.

The presence of the two neighbouring hulls, introduced an increased velocity between the two hulls, thus increasing the friction resistance. The towing tank tests validate this idea, however, the CFD results find a decreased friction resistance. The most logical explanation could be the difference in simulation of turbulence between the CFD and the towing tank tests.

8.4.3 Wave Interference Factor

As for the viscous interference factor, the wave interference factor is determined differently from the CFD results than from the towing tank tests. Both methods will be discussed briefly, after which both results will be compared.

Computational Fluid Dynamics

The exact formulation of the wave interference resistance is given in equation [8.13].

$$\tau = \frac{C_{Wcat}}{C_{Wmon}} \quad [8.13]$$

However, the data from the CFD calculations consist of the pressure resistance and the friction resistance. Thus, in order to define the wave interference factor, it is assumed that the ratio of wave resistances doesn't

differ a lot from the ratio of pressure resistances. This is valid as it is assumed that the transom stern resistance can be formulated as a constant percentage of the pressure resistance, without being dependant on the fact that the tested configuration is that of a catamaran or a monohull. As the transom resistance is relatively small with respect to the wave resistance, it is assumed here that this method is valid, resulting in:

$$\tau = \frac{C_{Wcat}}{C_{Wmon}} \approx \frac{C_{Pcat}}{C_{Pmon}} \quad [8.14]$$

Towing Tank Tests

Using equation [8.13] as the definition of the wave resistance interference factor, this factor can be determined from the towing tank test result using the following equation:

$$\tau = \frac{C_{Wcat}}{C_{Wmon}} = \frac{[C_T - (1 + \beta k_{mon}) C_{F_0}]_{cat}}{[C_T - (1 + k_{mon}) C_{F_0}]_{mon}} \quad [8.15]$$

Comparison

When looking at the different results from the towing tank tests and the CFD calculations, the most obvious conclusion is that all three methods result in similar trends, showing a low or even negative wave interference factor at a Froude number of 0.3, a maximum interference at Froude 0.5 and decreasing from there on.

The wide spread of the test results at low speed for the towing tank tests can be explained by the oscillating nature of the interference between wave systems. Therefore it is difficult to compare the interference at Froude 0.2 as was also the case for the total interference factor.

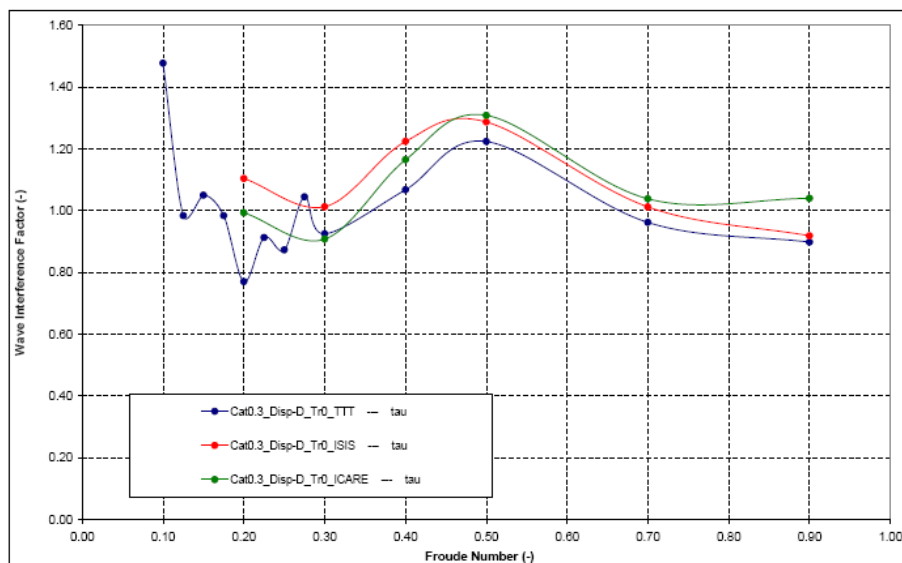


Figure 8.5: Total interference factor τ

From Froude 0.3 onwards, the deviation between the towing tank tests and ISIS are very limited, ranging from about 10% to 2.5% at the highest speed. The differences between ISIS and ICARE range from a positive 11% at low speed and a negative 9 % at the highest speed.

8.5 Conclusion

Total interference factor is difficult to predict at low speeds due to the oscillating nature of the wave interference between the hulls. However, at higher speeds clear trends are shown. The same counts for the wave interference factor which shows largely the same overall behaviour.

No conclusion can be drawn on the quantity of the viscous interference resistance factor. The CFD calculations give negative values, while existing results and the towing tank tests give positive values that change with the length-displacement ratio, the separation ratio and hull shape. It can be concluded that this viscous interference factor is specific to each case. With respect to the form factor, the existing results of Couser show an increase of 10% due to the viscous effects while in this research an increase of 3 – 6 % is found.

9 Hydrostatic Transom Resistance

As can be seen from the form factor results in chapter 6 , the immersed transom has a large influence on the form factor determination. This is caused by the transom stern resistance component. In this chapter, the theory of the hydrostatic transom resistance will be explained and compared to the results from CFD calculations. One way to try to estimate the hydrodynamic transom resistance is to approach it from a static point of view. The definition of the static transom resistance will be explained in this section. Furthermore, an existing regression to determine the transom dynamic wetted surface will be given, and a second regression will be built in the scope of this project. Both regressions will be compared to reach some conclusions.

9.1 Definition

The hydrostatic transom resistance is defined as the resistance of the missing hydrostatic pressure on the transom when the transom starts to unwet with increasing speed. The geometry of the problem is given in the figure below from [Doctors, 2007]:

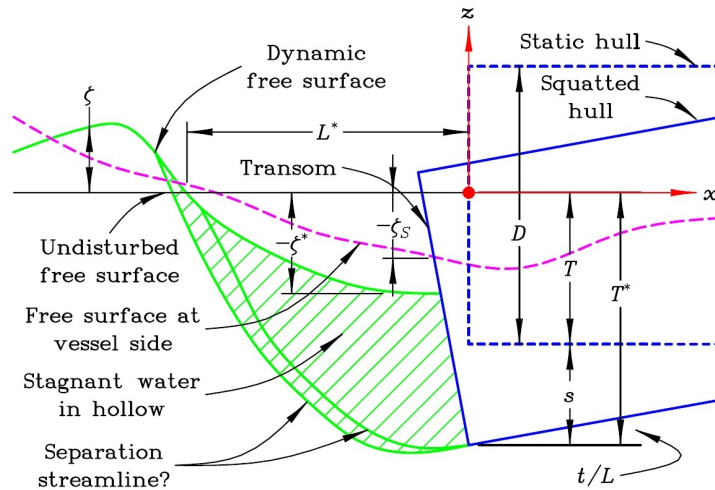


Figure 9.1: Definition of the geometry of transom unwetting [Doctors, 2007]

The pressure force on the immersed transom of a hull can be written as:

$$R_{TR} = \rho \cdot g \int_{T_{TR,dyn}}^{\zeta} (z - \zeta) \cdot b_{TR}(x, z) dz \quad [9.1]$$

Where:

- $T_{TR,dyn}$ is the dynamic transom draft
- ζ is the elevation of the stagnant water in the hollow immediately behind the transom
- $b_{TR}(x, z)$ is the local transom width dependant of the height and the local x-position

In order to be able to solve this integral, several parameters of the immersed transom should be known. First of all, the geometry of the entire stern is required as the integral depends on the local beam of the transom at every height. Secondly, the elevation of the stagnant water on the transom is needed. The geometry is known from the design, while the the elevation of the stagnant water can be calculated from the percentage of the dynamic wetted surface of the immersed transom with respect to the static value of this wetted surface. This percentage can be estimated with the use of regression formula. In the following sections, an existing regression formula from Doctors [2007] will be proposed, after which a new regression is built from the CFD data of this research.

9.2 Regression Doctors

In a collaboration between the University of Tasmania and the University of New South Wales, towing tank test are used to analyse the flow behaviour at transom sterns and how this can be used to estimate the transom resistance. Doctors presents a regression formula for the determination of the unwetted surface area of the transom [Doctors, 2006] and its regression constants [Doctors, 2007]. The regression formula has the following form:

$$\eta_{dry} = C_1 \cdot Fn_{TR}^{C_2} \cdot \frac{B}{T}^{C_3} \cdot Re_{TR}^{C_4} \quad [9.2]$$

Where:

$$\eta_{dry} = 1 - \frac{S_{TR \text{ dynamic}}}{S_{TR \text{ static}}} \quad [9.3]$$

$$Fn_{TR} = \frac{V}{\sqrt{g \cdot T_{TR}}} \quad [9.4]$$

$$Re_{TR} = \frac{\sqrt{g \cdot T_{TR}^3}}{\nu} \quad [9.5]$$

Where: T_{TR} is the draft of the transom

The constants for this regression formula can be found in Doctors' publication [Doctors, 2007] and are summarized in Appendix C .

9.3 Regression VPLP

With the data available form the ISIS calculations, a regression formula of a different form is proposed. The VPLP regression is based on a summation of different components in stead of a multiplication as presented in the previous section. For the determination of the regression formula, η_{dry} is discretized from 0.0 to 1.0 to give a good representation of the unwetting curves presented in Figure 9.2. With these values for η_{dry} the following regression can be found using Matlab:

$$Fn_{TR} = a_1 \cdot \eta_{dry} + a_2 \cdot \frac{B_{WL}}{T_c} + a_3 \cdot \frac{LCB}{L_{WL}} + a_4 \frac{S_{TR}}{A_X} \quad [9.6]$$

Where: S_{TR} is the (static) wetted surface area of the transom (m²)
 A_X is the maximum section area (m²)
 Fn_{TR} is the Transom Froude Number (-) and is defined as:

$$Fn_{TR} = \frac{V}{\sqrt{g \cdot T_{TR}}} \quad [9.7]$$

Where: T_{TR} is the draft of the transom

When $\eta_{dry} = 1.0$ the transom emerged entirely from the water, the corresponding Fn_{TR} value is the speed at which the flow separates at the transom and the entire transom is dry.

When $0 < \eta_{dry} < 1.0$ the transom is still immersed, and η_{dry} can be used to determine the transom resistance by integrating the hydrostatic transom pressure (equation [9.1]) over the dynamic wetted surface of the immersed transom.

The constants for the regression are given in Appendix C.6 . The data used to determine this regression is coming from the CFD calculations with ISIS on the VPLP parent hull form and the hull form of Noah '76 and is visualized in Figure 9.2.

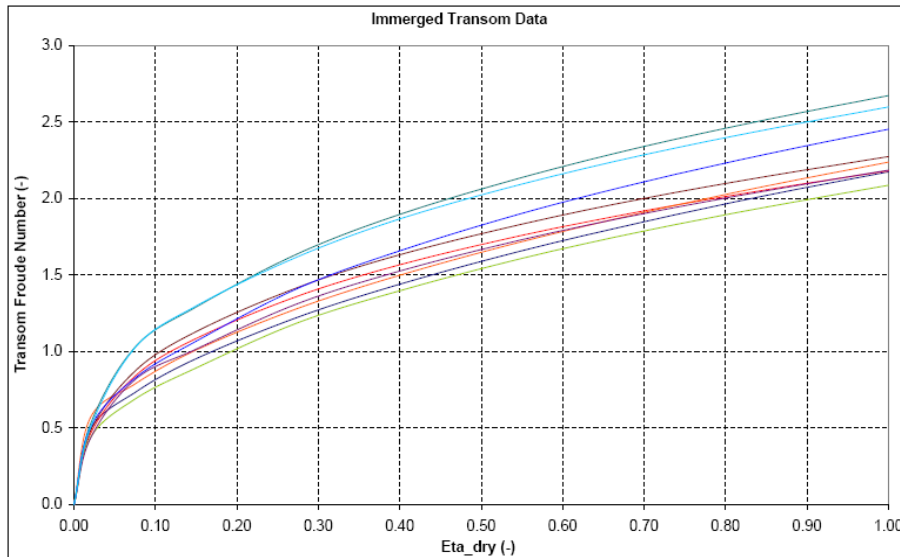


Figure 9.2: Ratio of dynamic WSA of the transom and the static WSA of the transom

At the moment, the regression constants are based on 2 different hull forms and a total of 9 different configurations. More resistance data should be incorporated in this regression to make it more precise and more robust, but in this report, it acts as a first indication in the search for the useful parameters to simulate the immersion of the transom stern of cruising motor catamarans.

An important note concerning this regression is the fact that the gathered data comes from ISIS CFD calculations of the bare hull, without appendices or propeller. Adding a working propeller to the hull increases the velocity of the flow at the transom, accelerating the separation of the flow at the transom. Additional CFD calculations were performed with the presence of the propeller, which did concur these phenomena. However, not enough calculations were performed to quantify this phenomenon for inclusion in the regression formula.

9.4 Comparison VPLP - Doctors

First of all, it should be noted that both regression formulae are based on different test data, while Doctors regression is based on a large number of low speed towing tank tests, the VPLP regression is based on unwetting curves from only 3 to 4 CFD calculation points each. It is expected that for the moment the Doctors regression is more accurate, but as the number of CFD calculations for the VPLP Catamaran Series will increase, the updated regression constants will also result in more precise estimations. The VPLP regression could already be more accurate if transom area results would have been available from the towing tank tests performed at the Delft University of Technology, however, due to the large scale of the model and difficulties with the equipment set-up, these results are not available.

In Figure 9.3, the unwetting of the parent hull at design displacement and trim zero is shown. It can be clearly seen that both regression formulae result in the same trend of the transom unwetting, with a slight offset with respect to the speed. This means that the VPLP regression underestimates the unwetted surface with respect to the Doctors regression. This results in a small overestimation of the transom resistance.

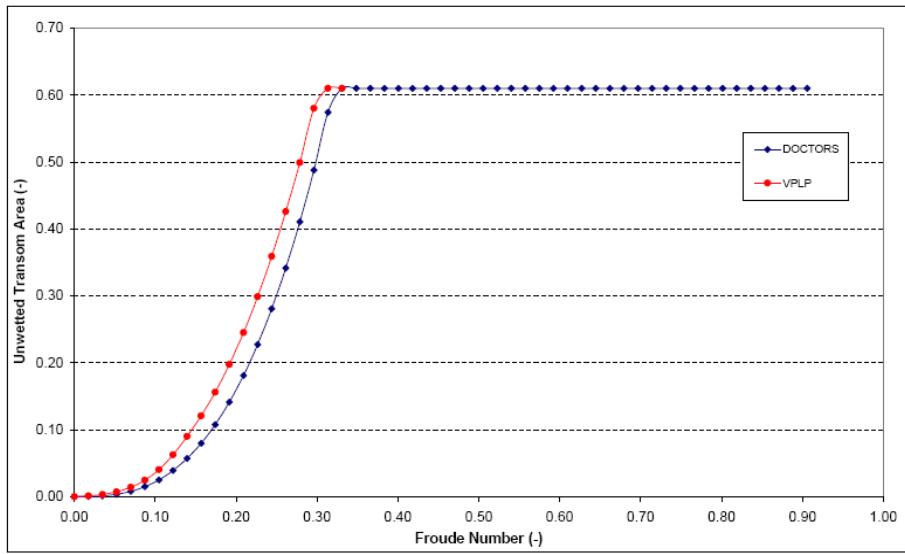


Figure 9.3: VPLP regression and Doctors regression for transom unwetting

Conclusions

The purpose of this research was to study the prediction of the resistance of cruising motor catamarans. From the available data, the performed CFD calculations and towing tank tests, several conclusions can be drawn.

From the available data from previous researches, a regression formula was built in order to give a first estimation of the resistance of catamarans. Regression analysis of the Molland results gives a good representation of the towing tank tests performed by Molland, but is very sensitive to changes in position of the longitudinal centre of buoyancy. This can be credited to the small range of LCB values in the available research data.

In the next step of the project, CFD calculations and towing tank tests are performed on a hull form designed especially for this project. From the comparison between the two CFD tools, ISIS and ICARE, and the towing tank tests, it was shown that:

- There are large differences between the results of the two CFD codes. The results from ICARE are about 15% higher than those of ISIS.
- When comparing the CFD results to the towing tank test results, it can be seen that the ISIS results are the closest to the towing tank test data. From this, it can be assumed that ISIS is more accurate than ICARE for this type of calculations.
- Comparison between this test data and the Molland test data shows a significant difference in the behaviour of the monohull and catamaran resistance. From this research, it can be concluded that the monohull and catamaran resistance results at high speeds converge to same value. Molland showed an offset between the converging resistance of catamarans of different separation ratio and the resistance of monohulls. This difference indicates some incorrectness of the resistance tests of the monohull and catamaran configurations performed by Molland.

From the available data, it was shown that more test data was required for analysis in order to have a more precise resistance prediction method. It was concluded that the following fields of research required more attention:

- The determination of the form factor, required for accurate scaling of test results
- Different methods of scaling of test and calculation results
- The interference resistance components for catamarans with different separation ratios
- The transom resistance of the immersed transom

All these topics are studied, and several more important conclusions can be drawn.

It was shown from the CFD calculations that the form factor can be determined from towing tank tests with the hull trimmed bow down so that the transom runs clear. However, it was assumed here that this is only valid for slender hull forms with U-sections at the bow, so that the changes of the waterlines of the trimmed hull form stay acceptable.

The form factors obtained from the towing tank tests and the CFD calculations were compared and as for the resistance determination, the ISIS results gave a good approximation with respect to the towing tank results. As for the total resistance, ICARE overestimates the form factor.

The form factors from Molland and corrected for transom resistance by Couser remain too high with respect to the form factors found in this report. This can indicate that the hydrostatic transom resistance used by Couser, to correct the Molland data, still underestimates the total transom resistance and therefore overestimates the form factor.

Three scaling methods were introduced and from the comparison of their results with the full scale CFD results, the following conclusions can be summarized:

- The ICARE results and the scaled results based on the form factor with transom stern effects, are distant from the rest of the results, implying that they are less accurate.
- The ISIS results show a slight different trend in hump resistance and high speed resistance with respect to the scaled towing tank test results. The two scaling methods, one without the use of the form factor, the other with its use, and the ISIS calculations are within 2 - 3 % of each other, which can be defined as very accurate, implying that both scaling methods can be used for slender hull forms.

Concerning the different interference resistance components, the conclusions drawn in the corresponding chapter can be repeated:

- The total interference factor is difficult to predict at low speeds due to the oscillating nature of the wave interference between the hulls. However, at higher speeds clear trends are shown
- The CFD calculations give negative values for the viscous interference factor, while existing results and the towing tank tests give positive values that change with the length-displacement ratio, the separation ratio and hull shape. It can be concluded that this viscous interference factor is specific to each case. With respect to the form factors, the existing results of Couser show an increase of 10% due to the viscous effects while in this research an increase of 3 – 6 % is found.
- The wave interference factor shows the same overall behaviour as the total interference factor.

For the determination of the transom resistance, two determination methods for the dynamic wetted surface area of the transom are presented. From the comparison between both, it can be said that:

- The VPLP regression underestimates the unwetted surface with respect to the Doctors regression. This results in a small overestimation of the transom resistance.
- More towing tank test data for the dynamic wetted surface area of the transom is required to build a more accurate regression.
- The question remains if the method of the missing hydrostatic transom pressure is a good simulation of the transom resistance.

Recommendations

For the succession of the RCM project at VPLP Yacht Design, it can be concluded from this research, as both the results of the towing tank tests and the ISIS computations are proven to be accurate, that it is beneficial to use one of these methods to perform extra tests with different configurations in order to build a large database. This database then can be used for building regressions to estimate the catamaran resistance at high precision. From the point of view of the costs involved, the towing tank test will be more cost effective than the CFD when testing a large number of configurations per hull form. When using towing tank tests for increasing the database of results, it will be important to have the wetted surface area of the transom stern at low speed in order to better compare it to the hydrostatic transom resistance.

For slender hull forms, the ITTC scaling method using the residuary resistance and no form factor can be used for accurate scaling of towing tank tests. However, as the scaling factor becomes larger, it is advised to take into account the form factor, as the overestimation of the resistance increases with increasing scaling factor.

Furthermore, more research towards the transom resistance is required, as the difference between the form factors found by Couser from the Molland data and the form factors from this research suggest that the transom resistance is higher than the hydrostatic transom resistance.

References

- [1] Abott, I.H., A.E. Von Doenhoff
Theory of wing sections
Dover Publications, Inc. New York, 1959
- [2] *Aero-Hydro-Sail Force Models: 3rd year lecture notes*
Southampton Institute
- [3] Anderson, J.D.
Fundamentals of Aerodynamics
McGraw-Hill International Editions, 1991
- [4] Armstrong, N.A.
On the Viscous Resistance and Form Factor of High-Speed Catamaran-Ferry Hull Forms
Sydney: University of New South Wales, 2000
- [5] Bailey, D
The NPL High Speed round bilge Displacement Hull Series
The Royal Institute of Naval Architects, 1976
- [6] Barkley, G.S.
Resistance and Propulsion
Southampton Institute, 2001
- [7] Beaulac, M.
Investigate into windage effects on the superstructures of catamaran motor yachts
University of Southampton, 2007
- [8] Couser, P.R., A.F. Molland, N.A. Armstrong, I.K.A.P. Utama
Calm Water Powering Predictions For High Speed Catamarans
International Conference on Fast Sea Transportation, 1997
- [9] Couser, P.R., A. Mason, e.a.
Artificial Neural Networks for Hull Resistance Prediction
Formation Design Systems, 2004
- [10] Doctors, L.J.
Influence of the Transom-Hollow Length on Wave Resistance
Proceedings of the Twenty-First International Workshop on Water Waves and Floating Bodies, 2006
- [11] Doctors, L.J., G.J. Macfarlane, R. Young
A Study of Transom-Stern Ventilation
International Shipbuilding Progress, 2007
- [12] Faltinsen, O.M.
Hydrodynamics of High-Speed Marine Vehicles
Cambridge: Cambridge University Press, 2005
- [13] Hoerner, S.F.
Fluid Dynamic Drag
Published by the author, 1965

- [14] Holtrop, J., G.G.J. Mennen
An Approximate Power Prediction Method
International Shipbuilding Progress, Vol.29, No. 335, 1982
- [15] Insel, M, A.F. Molland,
An investigation into Resistance Components of High-Speed Displacement Catamarans
Transactions of RINA, 1992
- [16] ITTC 7.5-0.2-0.2-0.1
ITTC Recommended Procedures
23rd ITTC 2002
- [17] Keuning, J.A., Binkhorst, B-J.
Appendage Resistance of a Sailing Yacht Hull
Chesapeake Sailing Yacht Symposium, 1997
- [18] Keuning, J.A., J. Gerritsma, P.F. van Terwisga
Resistance tests of a series planing hull forms with 30 degrees deadrise angle, and a calculation model base don this and similar systematic series
Delft: Delft University of Technology, 1992
- [19] Keuning, J.A., R. Onnink, A. Versluis and A.A.M. van Gulik
The Bare Hull Resistance of the Delft Systematic Yacht Hull Series
International HISWA Symposium on Yacht Design and Yacht Construction, 1998
- [20] Keuning, J.A., Sonnenberg, U.B.
Approximation of the Hydrodynamic Forces on a Sailing Yacht based on the 'Delft Systematic Yacht Hull Series'
International HISWA Symposium on Yacht Design and Yacht Construction, 1998
- [21] Keuning, J.A., Sonnenberg, U.B.
Approximation of the Calm Water Resistance on a Sailing Yacht based on the 'Delft Systematic Yacht Hull Series'
Chesapeake Sailing Yacht Symposium, 1999
- [22] Keuning, J.A., Katgert, M.
A Bare Hull Resistance Prediction Method Derived From the Results of the Delft Systematic Yacht Hull Series Extended to Higher Speeds'
International Conference on Innovation in High Performance Sailing Yachts, 2008
- [23] Matlab Manual
Chapter 6: Linear Models
MathWorks, 2007
- [24] Molland, A.F., Wellicome, J.F., Couser, P.R.
Resistance experiments on a systematic series of high speed displacement catamaran forms:variation of length- displacement ratio and breadth-draft ratio forms
Ship Science Report, University of Southampton, 1994
- [25] Molland, A.F., Lee, A.R.
Resistance Experiments on a Series of High Speed Displacement Catamaran Forms : Variation of Prismatic Coefficient
Ship Science Report, University of Southampton, 1995
- [26] Müller-Graf, B.
Widerstand und Propulsion: Erste Ergebnisse der VWS-Gleitkatamaran-Serie '89

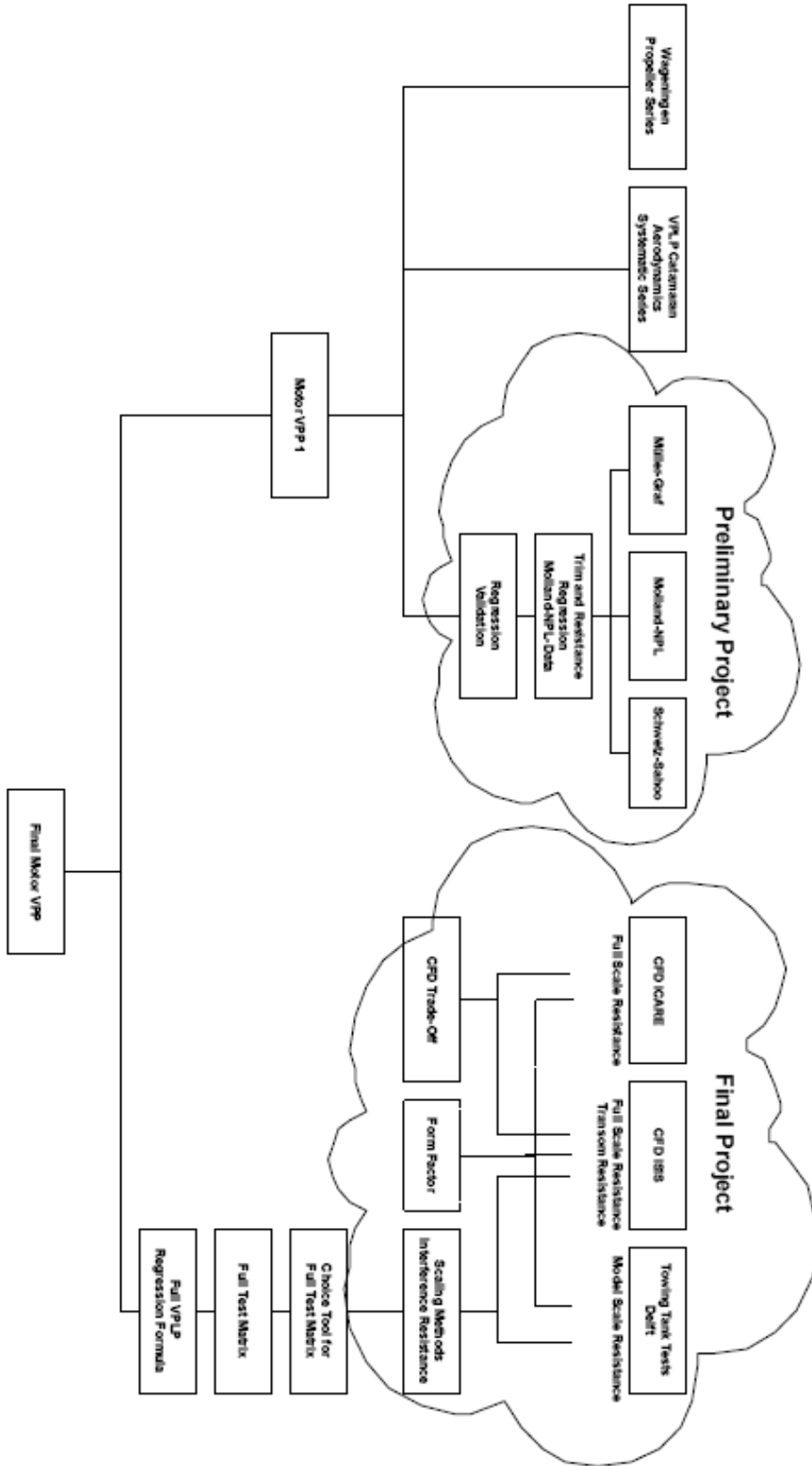
University of Berlin, 1993

- [27] Müller-Graf, B.
Resistance Components of High Speed Small Craft
Athens: Small Craft Technology, 1997
- [28] Müller-Graph, B., D. Radojicic, A. Simic
Resistance and Propulsion Characteristics of the VWS Hard Chine Catamaran Hull Series '89
University of Berlin, 2001
- [29] Pham, X.P., K. Kantimahanthi, P.K. Sahoo
Wave Resistance Prediction of Hard-Chine Catamarans through Regression Analysis
Proceedings of 2nd International EuroConference on High-Performance Marine Vehicles, 2001
- [30] Sahoo, P.K., N.A. Browne, M. Salas
Experimental and CFD Study of Wave Resistance of High-Speed Round Bilge Catamaran Hull Forms
Australian Maritime College, 2004
- [31] Schlichting, H.
Boundary-Layer Theory
New York: McGraw-Hill Book Company, 1979
- [32] Schwetz, A., P.K. Sahoo
Wave Resistance of Semi-Displacement High-Speed Catamarans through CFD and Regression Analysis
Australian Maritime College, 2002
- [33] Scragg, C.A., B.D. Nelson
The Design of an Eight-Oared Rowing Shell
Marine Tech., Vol. 30, No. 2, Apr. 1993, pp. 84-99.
- [34] Zouridakis, F.
A Preliminary Design Tool for Resistance and Powering Prediction of Catamaran Vessels
Massachusetts Institute of Technology, 2005

Appendices

Appendix A Project Flow Chart.....	I
Appendix B Aerodynamic drag and lift of catamarans.....	III
B.1 Model.....	III
B.2 Narrow: $B/L = 0.4$ $s/L = 0.28$	IV
B.3 Large: $B/L = 0.5$ $s/L = 0.38$	V
Appendix C Summary of Regression Formulae.....	VII
C.1 DSYHS.....	VII
C.2 NPL-Molland Regression.....	IX
C.3 Schwetz-Sahoo Resistance Regression.....	XII
C.4 Sahoo Resistance Regression.....	XIII
C.5 Doctors Transom Wetted Surface Area.....	XV
C.6 VPLP Transom Wetted Surface Area.....	XV
Appendix D Design of the VPLP Hull Form.....	XVII
D.1 Hull Form Concepts.....	XVII
D.2 Choice of VPLP Hull Form.....	XVIII
D.3 Final Design VPLP Hull Form.....	XVIII
Appendix E Test Matrices.....	XXI
E.1 Form Factor Test Matrix.....	XXI
E.2 Validation Resistance Matrix.....	XXI
E.3 Proposed Total Resistance Matrix.....	XXII
Appendix F Van Peteghem Lauriot Prévost Yacht Design.....	XXIII

Appendix A Project Flow Chart



Appendix B Aerodynamic drag and lift of catamarans

In collaboration with the University of Southampton, VPLP had performed a systematic series of wind tunnel tests to determine laws concerning the lift and drag of catamarans with head wind. In this appendix, the results of these wind tunnel tests are given.

B.1 Model

The model was built in a modular way, such that the trim angle, the superstructure lay-out and the separation ratio could be changed. A picture of an example configuration is shown in Fig.App 1.

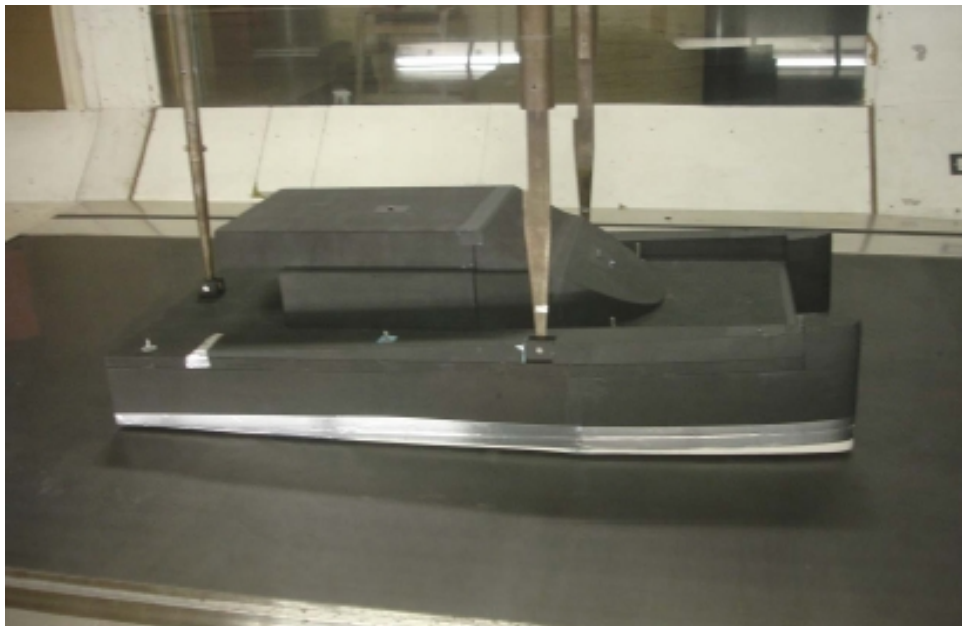


Fig.App 1: Model set-up in the Southampton windtunnel

B.2 Narrow: $B/L = 0.4$ $s/L = 0.28$

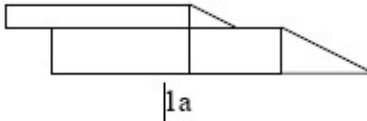
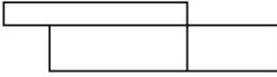

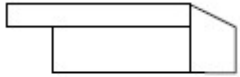
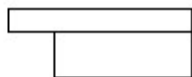
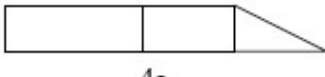
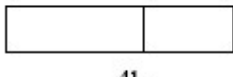
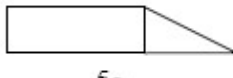
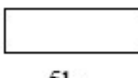
NARROW SPACING		Trim angle 0°		Trim angle 2°		Trim angle 4°	
Superstructure arrangements	Speed (m/s)	Cd	Cl	Cd	Cl	Cd	Cl
 1a	10 m/s	0.431	0.097	0.474	0.462	0.503	0.741
	20 m/s	0.436	0.093	0.474	0.440	0.525	0.700
 1b	10 m/s	0.554	0.128	X	X	0.646	0.712
	20 m/s	0.542	0.117	X	X	0.632	0.681
 2a	10 m/s	0.472	0.096	0.557	0.452	0.542	0.691
	20 m/s	0.471	0.089	0.526	0.420	0.569	0.658
 2b	10 m/s	0.512	0.102	X	X	X	X
	20 m/s	0.511	0.094	X	X	X	X
 3	10 m/s	X	X	0.611	0.471	0.612	0.709
	20 m/s	X	X	0.597	0.447	0.648	0.676
 4a	10 m/s	0.451	0.183	0.494	0.532	0.532	0.761
	20 m/s	0.455	0.172	0.487	0.503	0.572	0.729
 4b	10 m/s	0.504	0.168	X	X	X	X
	20 m/s	0.504	0.158	X	X	X	X
 5a	10 m/s	0.496	0.156	0.577	0.507	0.687	0.976
	20 m/s	0.498	0.147	0.558	0.483	0.675	0.717
 5b	10 m/s	0.548	0.147	X	X	X	X
	20 m/s	0.557	0.137	X	X	X	X

Fig.App 2: Drag and lift coefficients of catamaran superstructures with narrow hull spacing

B.3 Large: $B/L = 0.5$ $s/L = 0.38$

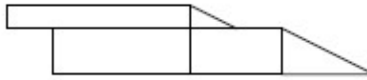
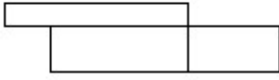

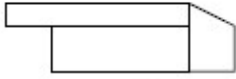
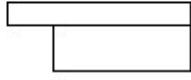
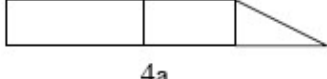
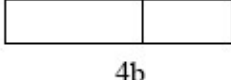
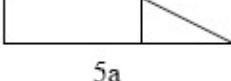
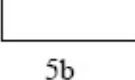
LARGE SPACING		Trim angle 0°		Trim angle 2°		Trim angle 4°	
Superstructure arrangements	Speed (m/s)	Cd	Cl	Cd	Cl	Cd	Cl
 1a	10 m/s	0.476	0.242	0.540	0.448	0.531	0.742
	20 m/s	0.469	0.137	0.520	0.428	0.609	0.759
 1b	10 m/s	0.549	0.172	X	X	X	X
	20 m/s	0.578	0.155	X	X	X	X
 2a	10 m/s	0.484	0.151	0.561	0.460	0.584	0.755
	20 m/s	0.500	0.139	0.522	0.427	0.594	0.732
 2b	10 m/s	0.525	0.160	X	X	X	X
	20 m/s	0.559	0.143	X	X	X	X
 3	10 m/s	X	X	0.675	0.455	X	X
	20 m/s	X	X	0.699	0.431	X	X
 4a	10 m/s	0.503	0.213	0.557	0.511	0.593	0.812
	20 m/s	0.509	0.197	0.555	0.488	0.619	0.792
 4b	10 m/s	0.555	0.205	X	X	X	X
	20 m/s	0.577	0.189	X	X	X	X
 5a	10 m/s	0.518	0.206	0.603	0.499	0.695	0.805
	20 m/s	0.517	0.190	0.605	0.476	0.699	0.702
 5b	10 m/s	0.569	0.194	X	X	X	X
	20 m/s	0.574	0.179	X	X	X	X

Fig.App 3: Drag and lift coefficients of catamaran superstructures with large hull spacing

Appendix C Summary of Regression Formulae

In this appendix, all regression formulae discussed in the report will be summarised while their regression constants will be given in the following appendix. When using these formulae, think about the importance of the parameter ranges where they are applicable. Also be careful using these formulae for any arbitrary hull, as most of them are only accurate for certain types of hull form. These points of attention will be stated at the beginning of each subsection below.

C.1 DSYHS

The Delft Systematic Yacht Hull Series or DSYHS is based on different families of sailing yacht hull forms. This systematic series is very extensive, resulting in a wide field of applicability. Even hull forms with parameters out of the parameter ranges can be accurately estimated, but when doing this extra caution should be considered.

Keuning All Series [Keuning, 1998]

Regression formula

$$\frac{R_r}{\nabla_c \rho g} = a_0 + \left(a_1 \frac{LCB_{fpp}}{L_{wl}} + a_2 C_p + a_3 \frac{\nabla_c^{2/3}}{A_w} + a_4 \frac{B_{wl}}{L_{wl}} \right) \frac{\nabla_c^{1/3}}{L_{wl}} + \left(a_5 \frac{\nabla_c^{2/3}}{S_c} + a_6 \frac{LCB_{fpp}}{LCF_{fpp}} + a_7 \left(\frac{LCB_{fpp}}{L_{wl}} \right)^2 + a_8 C_p^2 \right) \frac{\nabla_c^{1/3}}{L_{wl}} \quad [\text{APP 1}]$$

Parameter range

DSYHS 1998				
0.10	<	Froude number	<	0.6
2.73	<	$\frac{L_{WL}}{B_{WL}}$	<	5.00
2.46	<	$\frac{B_{WL}}{T_c}$	<	19.38
4.34	<	$\frac{L_{WL}}{\nabla_c^{1/3}}$	<	8.50
0.52	<	C_p	<	0.60

Table.App 1: Parameter range of the DSYHS [Keuning, 1998]

Regression Constants

Froude No.	a_0	a_1	a_2	a_3	a_4	a_5	a_6	a_7	a_8
0.10	-0.00086	-0.08614	0.14825	-0.03150	-0.01166	0.04291	-0.01342	0.09426	-0.14215
0.15	0.00078	-0.47227	0.43474	-0.01571	0.00798	0.05920	-0.00851	0.45002	-0.39661
0.20	0.00184	-0.47484	0.39465	-0.02258	0.01015	0.08595	-0.00521	0.45274	-0.35731
0.25	0.00353	-0.35483	0.23978	-0.03606	0.01942	0.10624	-0.00179	0.31667	-0.19911
0.30	0.00511	-1.07091	0.79081	-0.04614	0.02809	0.10339	0.02247	0.97514	-0.63631
0.35	0.00228	0.46080	-0.53238	-0.11255	0.01128	-0.02888	0.07961	-0.53566	0.54354
0.40	-0.00391	3.33577	-2.71081	0.03992	-0.06918	-0.39580	0.24539	-3.52217	2.20652
0.45	-0.01024	2.16435	-1.18336	0.21775	-0.13107	-0.34443	0.32340	-2.42987	0.63926
0.50	-0.02094	7.77489	-7.06690	0.43727	0.11872	-0.14469	0.62896	-7.90514	5.81590
0.55	0.04623	2.38461	-6.67163	0.63617	1.06325	2.09008	0.96843	-3.08749	5.94214
0.60	0.07319	-2.86817	-3.16633	0.70241	1.49509	3.00561	0.88750	2.25063	2.88970

Table.App 2: DSYHS regression constants 1998

Keuning All Series at Higher Speeds [Keuning, 2008]

Regression formula

$$\frac{R_r}{\nabla_c \rho g} = a_0 + \left(a_1 \frac{LCB_{fpp}}{L_{wl}} + a_2 C_p + a_3 \frac{\nabla_c^{2/3}}{A_w} + a_4 \frac{B_{wl}}{L_{wl}} \right) \frac{\nabla_c^{1/3}}{L_{wl}} + \left(a_5 \frac{LCB_{fpp}}{LCF_{fpp}} + a_6 \frac{B_{wl}}{T_c} + a_7 C_m \right) \frac{\nabla_c^{1/3}}{L_{wl}} \quad [\text{APP 2}]$$

Parameter range

Caution should be taken as the parameter ranges changes for the different speed regimes. At lower speeds, the entire DSYHS data is incorporated, however, at higher speeds, only part of the DSYHS hulls are used for the regression formula, making the formulae less precise at higher speeds for some hull forms.

DSYHS 2008					
0.15	<	Froude number	<	0.75	
2.73	<	$\frac{L_{WL}}{B_{WL}}$	<	5.88	
2.46	<	$\frac{B_{WL}}{T_c}$	<	19.38	
4.34	<	$\frac{L_{WL}}{\nabla_c^{1/3}}$	<	8.50	
0.52	<	C_p	<	0.60	

Table.App 3: Parameter range of the DSYHS [Keuning, 2008]

Regression Constants

Froude No.	a_0	a_1	a_2	a_3	a_4	a_5	a_6	a_7
0.15	-0.0005	0.0023	-0.0086	-0.0015	0.0061	0.0010	0.0001	0.0052
0.20	-0.0003	0.0059	-0.0064	0.0070	0.0140	0.0013	0.0005	-0.0020
0.25	-0.0002	-0.0156	0.0031	-0.0021	-0.0070	0.0148	0.0010	-0.0043
0.30	-0.0009	0.0016	0.0337	-0.0285	-0.0367	0.0218	0.0015	-0.0172
0.35	-0.0026	-0.0567	0.0446	-0.1091	-0.0707	0.0914	0.0021	-0.0078
0.40	-0.0064	-0.4034	-0.1250	0.0273	-0.1341	0.3578	0.0045	0.1150
0.45	-0.0218	-0.5261	-0.2945	0.2485	-0.2428	0.6293	0.0081	0.2086
0.50	-0.0388	-0.5986	-0.3038	0.6033	-0.0430	0.8332	0.0106	0.1336
0.55	-0.0347	-0.4764	-0.2361	0.8726	0.4219	0.8990	0.0096	-0.2272
0.60	-0.0361	0.0037	-0.2960	0.9661	0.6123	0.7534	0.0100	-0.3352
0.65	0.0008	0.3728	-0.3667	1.3957	1.0343	0.3230	0.0072	-0.4632
0.70	0.0108	-0.1238	-0.2026	1.1282	1.1836	0.4973	0.0038	-0.4477
0.75	0.1023	0.7726	0.5040	1.7867	2.1934	-1.5479	-0.0115	-0.0977

Table.App 4: DSYHS regression constants 2008

Residuary Resistance of Keel

Regression formula

$$\frac{R_{Rk}}{\nabla_k \cdot \rho \cdot g} = a_0 + a_1 \cdot \frac{T}{B_{WL}} + a_2 \cdot \frac{T_c + Z_{cbk}}{\nabla_k^{\frac{1}{3}}} + a_4 \cdot \frac{\nabla_c}{\nabla_k} \quad [\text{APP 3}]$$

The constants for this regression can be found in the corresponding publication of Keuning [Keuning, 1997].

C.2 NPL-Molland Regression

Residuary Resistance

$$C_R = \left(a_1 + a_2 \cdot \frac{LCB}{L_{WL}} + a_3 \cdot \frac{B}{L_{WL}} + a_4 \cdot \frac{B}{T} + a_5 \cdot \frac{s}{L_{WL}} \right) \cdot \frac{\nabla^{\frac{1}{3}}}{L_{WL}} \quad [\text{APP 4}]$$

Trim Angle

$$\tau = \left(a_1 + a_2 \cdot \frac{LCB}{L_{WL}} + a_3 \cdot \frac{B}{L_{WL}} + a_4 \cdot \frac{B}{T} + a_5 \cdot \frac{s}{L_{WL}} \right) \cdot \frac{\nabla^{\frac{1}{3}}}{L_{WL}} \quad [\text{APP 5}]$$

Parameter range

NPL-Molland Regression					
0.2	<	Froude number	<	1.0	
7.00	<	$\frac{L_{WL}}{B_{WL}}$	<	15.10	
0.436	<	$\frac{LCB}{L_{WL}}$	<	0.455	
6.3	<	$\frac{L_{WL}}{\nabla^{1/3}}$	<	9.5	
0.653	<	C_P	<	0.733	
0.2	<	$\frac{s}{L_{WL}}$	<	0.5	

Table.App 5: Parameter range of the NPL-Molland Series [Molland, 1994]

Regression Constants

Froude No.	a_1	a_2	a_3	a_4	a_5
0.20	2.3641E-02	2.0787E-03	-9.8015E-02	3.6743E-03	-7.4475E-04
0.25	8.1048E-02	-1.1406E-01	-8.1117E-02	2.4880E-03	-3.9869E-03
0.30	9.2027E-02	-1.2002E-01	-4.7304E-02	-3.1825E-04	-9.6156E-03
0.35	9.8716E-02	-1.4088E-01	5.0868E-02	-1.1934E-03	-1.7528E-02
0.40	1.1462E-01	-1.8198E-01	1.5454E-01	-3.4479E-03	-8.5972E-03
0.45	1.9912E-01	-3.6887E-01	4.7748E-01	-1.1716E-02	-3.5066E-02
0.50	2.5341E-01	-5.1243E-01	6.6013E-01	-1.4911E-02	-4.7457E-02
0.55	2.3065E-01	-4.7458E-01	6.3852E-01	-1.4060E-02	-4.4239E-02
0.60	1.8009E-01	-3.7030E-01	5.2675E-01	-1.1451E-02	-3.0653E-02
0.65	1.5325E-01	-3.1598E-01	3.5717E-01	-7.3416E-03	-1.2307E-02
0.70	1.4200E-01	-2.9540E-01	2.8432E-01	-5.6984E-03	-4.5523E-03
0.75	1.1903E-01	-2.4491E-01	2.2942E-01	-4.3175E-03	-1.1435E-03
0.80	1.1354E-01	-2.3332E-01	1.8725E-01	-3.3135E-03	1.0368E-03
0.85	1.0354E-01	-2.1127E-01	1.5102E-01	-2.2520E-03	2.4931E-03
0.90	8.3301E-02	-1.6378E-01	1.1757E-01	-1.2941E-03	2.4787E-03
0.95	9.0597E-02	-1.7985E-01	9.0385E-02	-5.3003E-04	3.0756E-03

Table.App 6: Catamaran residuary resistance regression constants

Froude No.	a_1	a_2	a_3	a_4	a_5
0.20	-9.9377E-02	2.5345E-01	1.6643E-02	2.0913E-03	0.0000E+00
0.25	-8.1579E-02	2.3076E-01	-1.2320E-02	1.4749E-03	0.0000E+00
0.30	-4.4522E-02	1.6099E-01	-3.5904E-03	-4.9807E-04	0.0000E+00
0.35	6.6701E-03	3.9240E-02	7.1732E-02	-2.1545E-03	0.0000E+00
0.40	3.0908E-02	-1.8982E-02	1.2094E-01	-1.9727E-03	0.0000E+00
0.45	7.6832E-02	-1.3510E-01	3.4982E-01	-8.4474E-03	0.0000E+00
0.50	9.9772E-02	-1.9758E-01	4.7130E-01	-1.2418E-02	0.0000E+00
0.55	1.2632E-01	-2.6338E-01	4.5563E-01	-1.2066E-02	0.0000E+00
0.60	1.0822E-01	-2.2698E-01	3.9848E-01	-9.8652E-03	0.0000E+00
0.65	7.7686E-02	-1.5676E-01	3.4063E-01	-8.5415E-03	0.0000E+00
0.70	7.8086E-02	-1.6000E-01	2.9209E-01	-6.9376E-03	0.0000E+00
0.75	8.4982E-02	-1.7698E-01	2.5593E-01	-5.8298E-03	0.0000E+00
0.80	6.0642E-02	-1.2194E-01	2.2584E-01	-4.9288E-03	0.0000E+00
0.85	6.4661E-02	-1.3021E-01	1.9633E-01	-4.3032E-03	0.0000E+00
0.90	4.5345E-02	-8.5320E-02	1.6637E-01	-3.4366E-03	0.0000E+00
0.95	3.8848E-02	-6.9524E-02	1.3322E-01	-2.2769E-03	0.0000E+00

Table.App 7: Monohull residuary resistance regression constants

Froude No.	a_1	a_2	a_3	a_4	a_5
0.20	8.6081E+00	-1.8620E+01	1.0417E+01	-5.0534E-01	-2.0518E-01
0.25	1.3179E+01	-2.7895E+01	9.4403E+00	-5.0136E-01	-6.3251E-01
0.30	1.1164E+01	-2.3236E+01	1.2856E+01	-4.8311E-01	-8.4645E-01
0.35	7.9308E+00	-1.8553E+01	1.8140E+01	-5.4882E-01	2.7961E+00
0.40	1.9814E+01	-4.2501E+01	7.9986E+01	-2.1731E+00	1.1887E+00
0.45	4.1685E+01	-7.8477E+01	1.6120E+02	-4.3895E+00	-1.0797E+01
0.50	5.7819E+01	-1.0975E+02	2.3093E+02	-5.7429E+00	-2.0474E+01
0.55	7.7387E+01	-1.5809E+02	2.6616E+02	-5.9406E+00	-2.1893E+01
0.60	7.4971E+01	-1.5637E+02	2.6982E+02	-5.9316E+00	-1.8737E+01
0.65	6.0440E+01	-1.2809E+02	2.4549E+02	-5.2975E+00	-1.1221E+01
0.70	5.4965E+01	-1.1819E+02	2.3346E+02	-5.2251E+00	-6.2242E+00
0.75	6.1068E+01	-1.3451E+02	2.2179E+02	-4.9759E+00	-2.0995E+00
0.80	7.2468E+01	-1.6188E+02	2.1121E+02	-4.6704E+00	6.4284E-01
0.85	5.3372E+01	-1.1814E+02	1.9867E+02	-4.2694E+00	2.2760E+00
0.90	5.2172E+01	-1.1393E+02	1.7975E+02	-3.7984E+00	3.7175E+00
0.95	5.3171E+01	-1.1406E+02	1.6469E+02	-3.5910E+00	4.6062E+00

Table.App 8: Catamaran trim regression constants

Froude No.	a_1	a_2	a_3	a_4	a_5
0.20	-3.2516E-01	1.1016E+00	1.2336E+01	-6.4715E-01	0.0000E+00
0.25	1.8166E+00	-2.7978E+00	1.0892E+01	-6.6622E-01	0.0000E+00
0.30	-1.7612E+01	4.4017E+01	2.3569E+01	-1.8263E+00	0.0000E+00
0.35	-2.4960E+01	5.8679E+01	7.7591E+00	-1.9095E-01	0.0000E+00
0.40	-1.2871E+01	3.4097E+01	3.9749E+01	-1.3247E+00	0.0000E+00
0.45	1.7745E+01	-3.4534E+01	1.0836E+02	-3.3087E+00	0.0000E+00
0.50	1.8547E+01	-3.9653E+01	1.6809E+02	-4.2987E+00	0.0000E+00
0.55	1.9795E+01	-4.3821E+01	2.1298E+02	-5.5387E+00	0.0000E+00
0.60	2.6386E+01	-6.0977E+01	2.3708E+02	-5.9404E+00	0.0000E+00
0.65	2.7100E+01	-6.3779E+01	2.4910E+02	-6.0674E+00	0.0000E+00
0.70	2.6036E+01	-6.0262E+01	2.5006E+02	-6.2341E+00	0.0000E+00
0.75	2.7801E+01	-6.3908E+01	2.4681E+02	-6.0561E+00	0.0000E+00
0.80	3.1032E+01	-6.9935E+01	2.3931E+02	-5.8478E+00	0.0000E+00
0.85	3.4831E+01	-7.5081E+01	2.2431E+02	-5.6767E+00	0.0000E+00
0.90	3.0764E+01	-6.2081E+01	2.0779E+02	-5.4574E+00	0.0000E+00
0.95	3.1610E+01	-6.2989E+01	1.9447E+02	-4.9189E+00	0.0000E+00

Table.App 9: Monohull trim regression constants

C.3 Schwetz-Sahoo Resistance Regression

Regression formula

$$C_{W_{mon}} = C_1 \cdot \left(\frac{L_{WL}}{\nabla^{1/3}} \right)^{C_2} \cdot \left(\frac{LCB}{LCF} \right)^{C_3} \cdot \left(\frac{B}{T} \right)^{C_4} \cdot C_B^{C_5} \quad [\text{APP 6}]$$

$$C_{W_{cat}} = C_1 \cdot \left(\frac{L_{WL}}{\nabla^{1/3}} \right)^{C_2} \cdot \left(\frac{s}{L_{WL}} \right)^{C_3} \cdot \left(\frac{LCB}{LCF} \right)^{C_4} \cdot i_E^{C_5} \cdot C_B^{C_6} \cdot \left(\frac{B}{T} \right)^{C_7} \quad [\text{APP 7}]$$

Where: i_E is the half waterline entry angle

Parameter range

NPL-Molland Regression				
0.4	<	Froude number	<	1.4
0.92	<	$\frac{LCB}{LCF}$	<	1.2
6.3	<	$\frac{L_{WL}}{\nabla^{1/3}}$	<	9.6
0.46	<	C_B	<	0.68
1.47	<	$\frac{B}{T}$	<	2.3

Table.App 10: Parameter range of the Schwetz-Sahoo regression [Schwetz, 2002]

Regression Constants

F_n	C_1	C_2	C_3	C_4	C_5
0.50	0.30	-1.2168	-2.2795	-2.5075	1.4337
0.60	0.41	-1.4599	-1.9655	-2.4304	1.5754
0.70	0.68	-2.1421	-1.6111	-1.6934	1.1637
0.80	0.78	-2.4272	-1.5211	-1.4089	1.0263
0.90	0.87	-2.6947	-1.5148	-1.1202	0.8731
1.00	0.93	-2.9213	-1.5536	-0.8650	0.7080
1.10	1.00	-3.1409	-1.5821	-0.6142	0.5526
1.20	1.16	-3.3948	-1.5593	-0.3228	0.4110
1.30	1.38	-3.6728	-1.5278	0.0000	0.2509
1.40	1.65	-3.9787	-1.5547	0.3523	0.0000

Table.App 11: Monohull wave resistance regression constants

F_n	C_1	C_2	C_3	C_4	C_5	C_6	C_7
0.50	1.501	-2.632	-0.201	-1.554	-0.132	1.070	-1.460
0.60	1.122	-2.817	-0.305	-1.265	-0.090	0.971	-1.259
0.70	0.613	-2.734	-0.278	-1.290	-0.064	0.988	-1.317
0.80	0.282	-2.652	-0.195	-1.472	-0.052	0.996	-1.395
0.90	0.209	-2.668	-0.111	-1.645	-0.048	1.002	-1.422
1.00	0.356	-2.820	-0.056	-1.756	-0.052	0.964	-1.339
1.10	0.878	-3.129	0.000	-1.640	-0.068	0.974	-1.171
1.20	1.455	-3.476	0.000	-1.365	-0.092	1.051	-0.962
1.30	1.594	-3.615	0.000	-1.105	-0.069	1.179	-0.873
1.40	2.337	-4.056	-0.032	-0.658	-0.072	1.338	-0.614

Table.App 12: Catamaran wave resistance regression constants

C.4 Sahoo Resistance Regression

Regression formula

$$C_{W_{mon}} = e^{C_1} \cdot \left(\frac{L_{WL}}{B}\right)^{C_2} \cdot C_B^{C_3} \cdot \left(\frac{L_{WL}}{\nabla^{1/3}}\right)^{C_4} \cdot (i_E)^{C_5} \cdot (\beta)^{C_6} \quad [\text{APP 8}]$$

Where: β is the half waterline entry angle

$$C_{W_{cat}} = e^{C_1} \cdot \left(\frac{L_{WL}}{B}\right)^{C_2} \cdot \left(\frac{B}{T}\right)^{C_3} \cdot C_B^{C_4} \cdot \left(\frac{L_{WL}}{\nabla^{1/3}}\right)^{C_5} \cdot (i_E)^{C_6} \cdot (\beta)^{C_7} \cdot \left(\frac{s}{L_{WL}}\right)^{C_8} \quad [\text{APP 9}]$$

Parameter range

NPL-Molland Regression					
0.2	<	Froude number	<	1.0	
8.22	<	$\frac{L_{WL}}{\nabla^{1/3}}$	<	11.20	
0.40	<	C_B	<	0.50	
1.5	<	$\frac{B}{T}$	<	2.5	
0.2	<	$\frac{s}{L_{WL}}$	<	0.4	

Table.App 13: Parameter range of the Sahoo Regression [Sahoo, 2004]

Regression Constants

<i>Fn</i>	C_1	C_2	C_3	C_4	C_5	C_6
0.20	3.001	-0.159	0.515	-3.666	-0.194	0.000
0.30	1.221	0.000	0.815	-3.445	0.218	0.000
0.40	3.180	-0.702	0.377	-3.114	-0.390	0.000
0.50	2.519	0.396	-0.775	-4.175	0.000	-0.410
0.60	2.031	-0.239	0.000	-3.402	-0.138	-0.091
0.70	1.130	-0.220	0.000	-3.221	-0.043	-0.081
0.80	0.600	-0.272	0.000	-3.079	0.000	-0.063
0.90	-0.216	0.000	-0.228	-3.158	0.173	-0.178
1.00	-1.086	0.000	-0.396	-2.965	0.300	-0.203

Table.App 14: Monohull wave resistance regression constants

<i>Fn</i>	C_1	C_2	C_3	C_4	C_5	C_6	C_7	C_8
0.20	2.571	0.436	0.000	0.000	-4.124	-0.039	-0.199	0.037
0.30	0.585	0.000	0.000	0.945	-3.282	0.246	0.087	-0.089
0.40	3.324	0.000	-0.471	-0.963	-3.523	0.000	-0.688	-0.035
0.50	2.439	0.379	0.000	-0.600	-4.262	0.000	-0.337	-0.368
0.60	1.809	-0.110	0.000	0.000	-3.625	-0.061	-0.095	-0.314
0.70	1.055	0.000	0.082	-0.025	-3.617	0.000	-0.064	-0.181
0.80	0.603	0.222	0.266	0.000	-3.869	0.000	0.000	-0.069
0.90	-0.466	0.049	0.162	0.000	-3.322	0.128	0.000	-0.006
1.00	-1.221	0.000	0.117	0.000	-3.046	0.264	0.000	0.075

Table.App 15: Catamaran wave resistance regression constants

C.5 Doctors Transom Wetted Surface Area

$$\eta_{dry} = C_1 \cdot Fn_{TR}^{C_2} \cdot \frac{B^{C_3}}{T} \cdot Re_{TR}^{C_4} \quad [\text{APP 10}]$$

Type of Analysis	Number of Coefficients	Regression Constants			
	N_{fit}	C_1	C_2	C_3	C_4
Moving Probe	2	0.1570	1.835		
	3	0.1559	1.830	0.01580	
	4	0.002472	1.862	0.2859	0.3588
Transom Probe	2	0.08057	2.831		
	3	0.07340	2.835	0.1247	
	4	0.06296	2.834	0.1352	0.01338

C.6 VPLP Transom Wetted Surface Area

$$Fn_T = a_1 \cdot \eta_{dry} + a_2 \cdot \frac{B_{WL}}{T_c} + a_3 \cdot \frac{LCB}{L_{WL}} + a_4 \cdot \frac{A_{TA}}{A_X} \quad [\text{APP 11}]$$

The constants found below are preliminary, as the VPLP catamaran series still needs to be extended further, but it gives an indication of the form of the regression formula and the trends found in the constants.

Transom Froude No.	a_1	a_2	a_3	a_4
0.000	0.0000	0.0000	0.0000	0.0000
0.020	75.0540	-0.1154	-1.6354	-0.0872
0.075	54.9810	-0.3782	-4.8285	-0.7149
0.150	33.6640	-0.4642	-5.8084	-0.8704
0.275	21.2440	-0.4781	-6.6872	-1.0395
0.400	16.3160	-0.5028	-7.5123	-1.1377
0.550	12.7850	-0.5018	-8.1210	-1.1897
0.700	10.6420	-0.4979	-8.6478	-1.2166
0.850	9.1647	-0.4902	-9.0902	-1.2211
1.000	8.0815	-0.4808	-9.4675	-1.2251

Table.App 16: Monohull transom wetted surface area regression constants

Appendix D Design of the VPLP Hull Form

A short description of the design process of the VPLP parent hull form will be given in this appendix. The process can be divided into three steps. First of all, four different hull concepts were designed, after which a trade of was made and the final hull form was chosen. This hull form is optimized further in order to comply with a general design brief such that it is representative for the kind of hull forms used at VPLP Yacht Design.

D.1 Hull Form Concepts

The fore body of all hull concepts, with their small entrance angle and vertical sections, is kept constant in order to find the influence of the different aft body shapes on the resistance. Values like the longitudinal centre of buoyancy, beam and length are determined by the design brief and therefore kept constant too. The four design concepts will be elaborated and are shown in Fig.App 4.

Torpedo

This shape is commonly applied for container ships. It consists of a horizontal propeller shaft with can the propeller hub and hull aligned to decrease resistance. This hull shape as extra volume placed aft, which moves the LCB aft. When using a fixed LCB for the different concepts, this means that the aft shape of the torpedo has sleeker lines than the other concepts, which would most likely decrease the resistance due to from effects and the pressure resistance. Furthermore, the trim angle at higher speeds may be smaller than for the rounded canoe body. This shape however will introduce construction difficulties, but none that can't be solved.

Canoe

The canoe body hull is used as a reference shape, as this shape is widely applied and has proven to be efficient in low resistance and low trimming angles at higher speeds. The canoe body can be applied in a very extreme form by keeping the sides vertical and the bottom horizontal. This increases the wetted surface area but also increases the internal volume, so less beam is required for the same displacement. In this research, the canoe body is designed with round edges in order to decrease strange flow effects at the sharp corners.

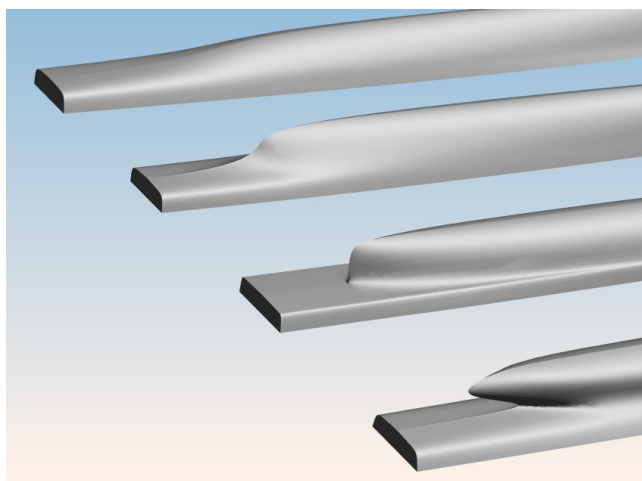


Fig.App 4: The 4 hull concepts

Smooth canoe

A more rounded version of the canoe hull described above, which decreases the wetted surface area to a minimum. The decrease in displacement is counteracted by a larger draft and wider beam, as this wider beam would also be beneficial for internal arrangement. This hull shape will require an inclined propeller shaft and will most likely has a higher trim angle at elevated speeds.

V-shape

This is a hull with flat planning stern with sharp bow, which results in a V-shaped bow section. This shape will have a decreased resistance at higher speeds, but will experience a higher trim angle at these speeds. This shape requires a larger transom depth with respect to the other designs if a fixed LCB position is applied for the different concepts. This shape has less sleek streamlines at lower speeds before hydrodynamic lift will start to play a role which will, together with the larger transom depth, deliver a higher resistance at low speeds.

D.2 Choice of VPLP Hull Form

For this research the decision was taken to study only two of these concepts. A trade of between the pros and cons of each concept was made and is shown in the table below.

Concepts:	Torpedo	Canoe	Smooth Canoe	V-Shape
Production	Difficult	Normal	Normal	Normal
Propulsion	Horizontal shaft	Horizontal shaft	Inclined shaft	Inclined shaft
Transom	Small	Small	Normal	Large
Angle of Entrance	Fine	Fine	Larger	Larger
Wetted Surface Area	Large	Large	Normal	Normal
Trim at high speed	Low	Low	Medium	High

Table.App 17: Overview of hull concepts

D.3 Final Design VPLP Hull Form

The length of the parent hull form is chosen to be 21 meters, as it is expected to be somewhere in the middle of the range of yachts lengths demanded by the different clients. At the moment, projects are running for motor catamarans of 18.2, 21.0, 23.3 and 26.8 meters.

At the forward part of the hull, U-shaped sections are used instead of V-shaped sections. This results in more vertical sides of the hull. This is done to decrease the accelerations due to this shape and decrease dynamic trim at higher speeds. At the same time, this allows a better determination of the form factor using a bow down trim to make the transom stern to run clear.

The beam could be smaller for less wave resistance due to the smaller angle of entrance at the bow, but the beam is limited due to the required luxurious interior in the hulls. A waterline beam of 1900 mm is applied. With respect to the aft body of the hull, a tunnel is added to suit a large diameter propeller as this increases its efficiency.

The longitudinal centre of buoyancy is placed at 45% as often for cruising catamarans the engines are not placed optimal for weight distribution. Often engine rooms are too small and placed too far back, moving the centre of gravity aft, resulting in "fat" aft sections.

As the hull form is designed as a generic form that can be applied to different designs and projects, features as spray rails and aft swimming platforms are excluded from the parent hull form.

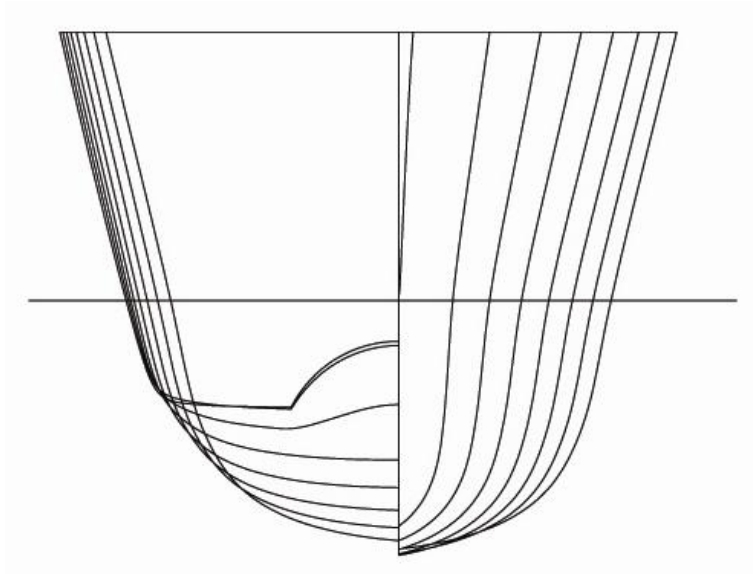


Fig.App 5: VPLP V-shape parent hull form sections

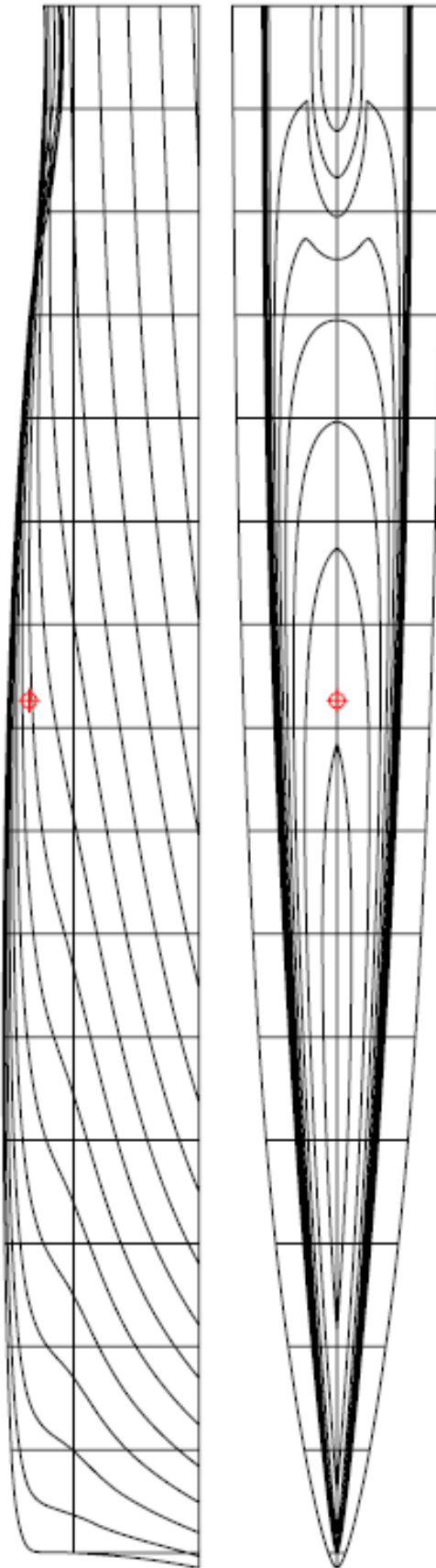


Fig.App 6: VPLP V-shape parent hull form lines

Appendix E Test Matrices

E.1 Form Factor Test Matrix

The test matrix for the form factor tests is applied to the towing tank tests that are performed to determine the form factor of the VPLP hull form with and without the presence of the tunnel. The trim angle of 2.60 degrees that is used here, result in the transom to run clear, with the waterline at the bottom of the transom. The second trim angle corresponds with half of the transom wetted and is an angle of 1.34 degrees. This matrix is used for the slow speed towing tank test, where 9 speeds between Froude number 0.1 and 0.3 are used.

		Tunnel Cases	
		With Tunnel	Without Tunnel
Trim Cases	WL at Bottom Transom	Mono Cata 0.3 Cata 0.5	Mono Cata 0.3
	WL at Half of Transom	Mono Cata 0.3 Cata 0.5	---
	WL at Zero Trim	Mono Cata 0.3 Cata 0.5	Mono Cata 0.3

Table.App 18: Form factor test matrix

E.2 Validation Resistance Matrix

For the comparison of the different CFD packages and the towing tank tests, different configurations are tested with these three methods. All CFD calculations are performed on the test matrix shown below. The catamaran cases are tested with a separation ratio of 0.3. This matrix results in 6 configurations that are tested with the use of the CFD packages.

		Trim Cases		
		Bow Up (0.77 degrees)	Normal (0 degrees)	Dow Down (-0.77 degrees)
Displacement Cases	Light $\left(\frac{L}{\nabla^{1/3}}=8.5\right)$	---	Mono	---
	Design $\left(\frac{L}{\nabla^{1/3}}=8.0\right)$	Mono	Mono Cata	Mono
	Heavy $\left(\frac{L}{\nabla^{1/3}}=7.5\right)$	---	Mono	---

Table.App 19: Test matrix of CFD tests for the validation

The test matrix for the towing tank tests is based on the one for the CFD calculations, but has several configurations added to it, as can be seen in Table.App 20. The catamaran configurations mentioned in this test matrix are towed at three different separations ratios: 0.25, 0.30 and 0.40. This results in a total of 18 configurations tested over the entire speed range.

		Trim Cases		
		Bow Up (0.77 degrees)	Normal (0 degrees)	Dow Down (-0.77 degrees)
Displacement Cases	Light $\left(\frac{L}{\nabla^{1/3}}=8.5\right)$	Mono	Mono Cata	Mono
	Design $\left(\frac{L}{\nabla^{1/3}}=8.0\right)$	Mono	Mono Cata	Mono
	Heavy $\left(\frac{L}{\nabla^{1/3}}=7.5\right)$	Mono	Mono Cata	Mono

Table.App 20: Test matrix for towing tank tests for validation CFD

E.3 Proposed Total Resistance Matrix

The final matrix explained here is the proposed test matrix that is required to extend the database in order to build an accurate and robust regression in the following stage of the project at VPLP. The middle column of Table.App 21, which is shown in black, is the matrix that is already tested as shown in Table.App 20. The new cases that are required are written in red.

		Design Cases		
		Design at $\frac{L}{\nabla^{1/3}}=7$	Design at $\frac{L}{\nabla^{1/3}}=8$	Design at $\frac{L}{\nabla^{1/3}}=9$
Displacement Cases	Light $\left(\frac{L}{\nabla^{1/3}}=X+0.5\right)$	Mono Cata	Mono Cata	---
	Design $\left(\frac{L}{\nabla^{1/3}}=X\right)$	Mono Cata	Mono Cata	Mono Cata
	Heavy $\left(\frac{L}{\nabla^{1/3}}=X-0.5\right)$	Mono Cata	Mono Cata	Mono Cata

Table.App 21: Total proposed matrix

Appendix F *Van Peteghem Lauriot Prévost Yacht Design*

VPLP, which is short for Van Peteghem Lauriot Prévost Yacht Design, is a yacht design office created in 1983 by Marc Van Peteghem and Vincent Lauriot Prévost. Both studied naval architecture at the Southampton Institute and started their company in Marseilles with the eye on racing trimarans. Very soon, they moved their office to Paris for mobility reasons, as well as to organise the new demand for cruising catamarans. This alliance between cruising multihull and racing multihulls has been the signature of VPLP.

Since 1966, the company is based in two different locations, one in Paris and one in Vannes. This facilitates the connection to the teams, skippers and shipyards of the ocean racing seen in Brittany. Together with some special projects, the cruising multihulls are designed in the Paris office.



Fig.App 7: VPLP's first realisation: The foiling trimaran Gerard Lambert (1984)

After 25 years, VPLP is the world largest yacht design office with more than 20 employees and a continuous average of 5 interns and VPLP is the world leading multihull design office covering all fields of multihull design, like:

- Conception of the cruising catamarans built by CNB Lagoon, the catamaran department of Groupe Bénéteau, the world leader in production cruising catamarans.
- Conception of one-off cruising multihulls like Douce France, currently the largest sailing catamaran in the world.
- Conception of ocean race multihulls, holding the majority of podium places and records in ocean racing.
- Conception of "working" multihulls like ambulance boats and fishing boats.
- Conception of special projects like racing monohulls, foiling trimarans and catamarans



Fig.App 8: Noah 86' trawler catamaran